Thalamocortical Oscillations in Sleep and Anaesthesia

by

Thomas Clifford Gent

A thesis submitted in fulfilment of the requirements for the degree of Doctor of Philosophy of
Imperial College London

June 2011

Anaesthesia Mechanism Research Group
Biophysics Section
Blackett Laboratory
Imperial College London
SW7 2AZ

Abstract

The last 20 years have seen a substantial advancement in the understanding of the molecular targets of general anaesthetics however the neural mechanisms involved in causing loss of consciousness remain poorly understood. Thalamocortical oscillations are present in natural sleep and are induced by many general anaesthetics suggesting that modulation of this reciprocal system may be involved in the regulation of consciousness.

Dynamic changes of thalamocortical oscillations in natural sleep and anaesthesia were investigated in rats chronically implanted with skull screw and depth electrodes in the cortex and thalamus. The hypothesis that discrete areas within the thalamus are responsible for regulation of arousal was tested. The anaesthetics propofol and dexmedetomidine but not midazolam produced switches in delta frequency at loss of righting reflex (LORR). This switch in frequency mirrored that seen within non-rapid eye movement sleep (NREM), whereas the onset of NREM was characterized by a switch from theta to delta in the EEG.

Depth recordings during NREM indicated that the switch into a NREM state occurred in the central medial thalamus (CMT) significantly before the cingulate, barrel cortex and ventrobasal nucleus (VB), and that the CMT switch corresponded to the switch seen in the global EEG. Dexmedetomidine hypnosis showed a delta frequency shift that occurred simultaneously within the thalamus and cortex, and furthermore that the thalamus exhibited phase advancement over the cortex at the point of LORR.

In conclusion, globalised changes within the thalamocortical system occur for propofol and dexmedetomidine LORR in the rat. This change represents a transition within drug free NREM and may implicate a common pathway responsible for a decrease in arousal. Furthermore, the phase advancement of the intralaminar thalamus over the cortex at LORR suggests a crucial role for this part of the thalamocortical system for regulating consciousness.

I declare that the contents of this thesis are entirely my own work and have not been submitted in any form for another degree. All information derived from the work of others has been acknowledged in the text and a list of references given.

Acknowledgments

Contents

List of Figures

List of Tables

1 Introduction

Anaesthesia /annisstheeziə/ *noun* insensitivity to pain, especially as induced by an anaesthetic before a surgical operation

The ability to render patients unconscious and insensible to pain has revolutionised medicine and surgery. Since the birth of modern anaesthesia 170 years ago, numerous pharmacological agents have been employed ranging from Morton's ether demonstration in 1846 to today's complex poly-pharmacy. This has comprised of a highly heterogeneous group of chemicals, all sharing a common endpoint. Yet despite a plethora of intrigue and investigation into such drugs, the answer to one question remains elusive: How do anaesthetics produce unconsciousness?

1.1 Historical Perspectives

The 16th October 1846 will forever be synonymous with arguably the biggest turning point in modern medicine. On this day, a young dentist from Charlton, Massachusetts, William T.G. Morton gave the first public demonstration of ether anaesthesia allowing a tumour on the neck of a patient to be removed without apparent pain at the Massachusetts General Hospital. The report of surgeon John C. Warren makes fascinating yet familiar reading:

"On October 17th [i.e., 16th]*, the patient being prepared for the operation, the apparatus was applied to his mouth by Dr. Morton for about three minutes, at the end of which time he sank into a state of insensibility."*

Morton had only weeks earlier satisfied himself that the use of ether could ameliorate the pain from tooth extraction in his own practice. The report of this in The Boston Journal quickly attracted attention that lead to the now infamous 16th October events.

What is less widely known is that a similar yet unpublished procedure had taken place four years previously by physician Crawford Long. Following public demonstrations of the exhilarating effects of nitrous oxide Long considered using ether to allow surgical operations without causing pain. Long knew little of nitrous oxide, but had been witness to numerous "ether frolics" whilst a medical student. Ether and nitrous oxide were widely considered to cause similar effects. Interestingly the patient James Venable had previously participated in ether frolics and may have been more familiar with the effects of ether than was Long. With the use of ether Long removed a small tumour from

Venable's neck, without pain or even a sensation of the knife. This is now generally accepted as the first instance of ether being used for surgical anaesthesia other than for dental procedures. Long's demotion in the story of anaesthesia was due to his timidity in making his findings widely known. Despite numerous further applications for amputation and obstetric procedures, Long did not publish his findings until 1849, by which time Morton's work had been well reported and he had become established as the pioneer of the field.

The next important development in the history of anaesthesia came in 1844 in Hartford, Connecticut during a public exhibition on the exhilarating effects of nitrous oxide. One of the volunteers, Samuel Cooley became so excited that he struck out with his leg striking it on a wooden settee, bruising it badly yet feeling no pain. Sat next to Cooley was another dentist Horace Wells who pondered on using nitrous oxide for alleviating the pain of tooth extraction. Wells had one of his own teeth extracted the following day whilst under the influence of nitrous oxide and later exclaimed:

"It is the greatest discovery ever made! I didn't feel it so much as the prick of a pin!"

This might have been far more revolutionary had it not been for a calamitous turn of events at Harvard Medical School. In 1845 Wells was granted permission to address the surgery class at Harvard, administering nitrous oxide to a boy prior to tooth extraction. However the boy cried out when his tooth was pulled and Wells, disgraced, left the theatre to the chants of *"Humbug! Humbug!"*. The boy in question later admitted that the cry was made in shock and not because of pain, yet the damage was done and nitrous oxide was abandoned for several years. Following the successful demonstration of ether by Wells' former partner Morton, Wells abandoned all medical practice and became addicted to chloroform. He committed suicide in prison after throwing sulphuric acid over a prostitute in his drug induced delirium. He sliced through an artery in his leg, using chloroform to dull the pain. History, it seems, is not without a sense of irony.

The phenomenon of ether anaesthesia spread rapidly following Morton's demonstration of ether. Oliver Holmes proposed the name anaesthesia to denote the *"insensibility… to objects of touch"* in a letter to Morton.

The first qualified physician to dedicate all of his time to anaesthesia was John Snow. He made significant advances in administration and correct dosing rates of both ether and chloroform, anaesthetising Queen Victoria for the birth of her son Leopold.

Long before these revolutionary years which gave birth to modern anaesthesia, the concept of pain relief was well known. Wine had been used for centuries to alleviate the pain of surgical operations, as well as for its antiseptic properties. In the middle ages, monks were reported to administer alcohol fumes before and after surgery.

Similarly the concept of artificially inducing sleep dates back to ancient times, most commonly employing henbane, poppy, mandagora and hemp. Homer's Odyssey describes Helen, daughter of Zeus, preparing a poppy like drug dissolved in wine to sleep off grief and forget pain. Indeed this was most likely a crude opium tincture, more commonly known as laudanum, a mainstay of many medical remedies during the 18th and 19th centuries.

1.2 Molecular Targets of General Anaesthetics

1.1.1 Meyer-Overton Hypothesis

The earliest proposed mechanisms for the action of the sedative and hypnotic effects of general anaesthetics revolved around the premise of Meyer and Overton who independently discovered that potency of a general anaesthetic is directly proportional to its oil/water partition coefficient (Meyer, 1899; Overton, 1901). This was interpreted as anaesthetics disrupting the lipid bilayer portions of nerve membranes. The major dilemma that this theory had were that at clinically relevant concentrations of anaesthetic, the lipid perturbation was comparable to that brought about by modest increases in temperature. Indeed temperature increases were predicted to increase anaesthetic potency when in fact the converse is generally true. Furthermore, long chain alcohols cease to have anaesthetic action above a certain length despite their solubility predicting potency as anaesthetics. This phenomenon became known as the cut-off point to account for the discrepancy.

1.1.1 Protein Theory

The first demonstration that anaesthetics interacted with proteins was confirmed by Franks and Lieb (1984), who demonstrated that the potency of an anaesthetic was directly proportional to the potency for inhibition of the water soluble protein firefly luciferase, at concentrations close to those required for mammalian anaesthesia. Furthermore, optical isomers of certain anaesthetics such as barbiturates (Andrews *et al.*, 1982; Richter *et al.*, 1982), ketamine (Ryder *et al.*, 1978; White *et al.*, 1985) and isoflurane (Dickinson *et al.*, 1994) have a differing potency which is not explained by a non-selective mechanism. Since these findings, many receptors have been found to have sensitivity to anaesthetic agents, and the regional distribution of these receptors within the brain has led to the proposal of discrete neural pathways which may regulate anaesthetic induced loss of consciousness.

$GABA_A$ receptors are pentameric molecules that are found throughout the CNS in a variety of configurations, though the majority are α1β2γ2, α2β3γ2 and α3βnγ2 (McKernan *et al.*, 1996). Their importance as anaesthetic targets has long been appreciated (Macdonald *et al.*, 1978) and indeed nearly all anaesthetic agents have been found to potentiate postsynaptic $GABA_A$ currents at varying concentrations, with a few exceptions notably xenon (de Sousa *et al.*, 2000) and cyclopropane (Raines *et al.*, 2001). The majority of research into determining the roles various receptors in recent years has focused on transgenic animals (Rudolph *et al.*, 2004a). Such experiments are not without flaws since compensatory mechanisms are likely to occur in order to produce a viable animal, particularly if the mutation is critically involved in an endogenous pathway. Indeed some knock-out mutations have proved to be fatal preventing investigation, therefore point mutation knock-in models are becoming more commonly employed (Rudolph *et al.*, 2004b). This approach is currently

the best method of assessing the importance of target receptors in producing a behavioural endpoint. Perhaps one of the most prominent of these studies involved a N265M point mutation in the β_3 subunit, rendering mice insensitive to etomidate and propofol LORR (Jurd *et al.*, 2003), however this did not alter sensitivity to alphaxalone, halothane or enflurane. This data confirms earlier *in vitro* experiments which demonstrated that oocytes containing the β_3 subunit were insensitive to alphaxalone (Wooltorton *et al.*, 1997). The sedative effects of diazepam have been shown to be dependent on the α1 subunit as demonstrated by knock in mice (Rudolph *et al.*, 1999). Interestingly, an α1 knock out mouse model had an increased sensitivity to diazepam compared to wild types (Reynolds *et al.*, 2003), highlighting the potential for compensation.

The α_2 adrenergic receptors are becoming a more commonly studied receptor type for mechanisms of drug induced unconsciousness. These receptors are G-protein linked receptors that exist as dimers (Ruffolo *et al.*, 1994). Of these, the α_{2a} receptor has been shown to modulate the sedative properties of dexmedetomidine (Lakhlani *et al.*, 1997), the other receptor subtypes being important for the vasoactive effects of these drugs. The α_{2a} adrenoreceptor has a limited distribution throughout the CNS (Nicholas *et al.*, 1993) making it an ideal tool to investigate the neuronal mechanisms of anaesthetics. Areas with high expression include the locus coeruleus (LC), the reticular thalamus, raphe nucleus and layer VI of the cortex. The α_2 adrenoreceptor characterised *in vivo* by dexmedetomidine has been shown to be presynaptic causing inhibition of adrenergic neurones (Correa-Sales *et al.*, 1992) however a postsynaptic effect in layer VI of the cortex remains a plausible possibility, since stimulation of this region produces a strong inhibitory effect on the thalamus via the GABAergic reticular nucleus (Zhang *et al.*, 2004).

Anaesthetic activated K+ currents were first identified in snails (Franks *et al.*, 1988) and subsequently in mammals (Goldstein *et al.*, 2001; Patel *et al.*, 2001). These currents have been identified as coming from the two-pore domain potassium channels (K2P), largely responsible for a leak conductance, analogous to extrasynaptic GABA receptors. They have since been identified as being important targets of volatile anaesthetics both *in vitro* (Liu *et al.*, 2004) and *in vivo* (Pang *et al.*, 2009). The K2P channels are now known to consist of many subtypes, all of which have a varying sensitivity to each volatile anaesthetic, although most are activated by halothane (Patel *et al.*, 2001), of which TASK-3 is now known to have an effect on *in vivo* sensitivity to halothane (Pang *et al.*, 2009).

NMDA receptors consist of two NR1 subunits and two other subunits. These may consist of NR2(A-C) subunits or NR3 subunits that have been identified as well as numerous splice variants. They are found presynaptically and extrasynaptically as well as postsynaptically and mediate the slow

component of synaptic transmission (Cull-Candy *et al.*, 2001). The related AMPA receptors mediate the fast component of synaptic transmission and have little anaesthetic sensitivity (Plested *et al.*, 2004). Whilst most volatile anaesthetics have some inhibition of NMDA receptors, the majority of research has focused on xenon, ketamine and nitrous oxide. Isoflurane and xenon have both been demonstrated to competitively bind at the obligatory glycine binding site (Dickinson *et al.*, 2007). One potential argument against NMDA receptors being a major mediator of consciousness is that selective drugs produce aberrant behavioural effects prior to LORR and LOC (Carter, 1995). Indeed ketamine LOC in humans is characterised by EEG activity unlike other anaesthetics and is reported to be more like a cataleptic stupor and may recruit other receptors as targets at higher concentrations (Lingenhohl *et al.*, 1998).

1.3 Neural Substrates of General Anaesthetics

The mechanisms by which anaesthetics induce loss of consciousness (LOC) are not fully understood, however there is evidence to suggest that many anaesthetics involve the thalamocortical system in some form. Most intravenous anaesthetics including propofol (Dutta *et al.*, 1997; Ferenets *et al.*, 2006), dexmedetomidine (Huupponen *et al.*, 2008; Mason *et al.*, 2009), midazolam (Judge *et al.*, 2009) and barbiturates (Dossi *et al.*, 1992; Steriade, 1997) produce delta oscillations (1-4Hz) and spindles (waxing and waning 7-14Hz events), both of which are generated by the thalamocortical system (Steriade *et al.*, 1993c). These are also common features of natural sleep, leading to the hypothesis that anaesthetic LOC and sleep share common pathways. There are subtle differences in the fine structure of these oscillations when comparing different anaesthetics and sleep, these will be considered later. Investigations of thalamocortical oscillations in sleep and anaesthesia have traditionally been investigated in animals at steady state and often deep anaesthesia (Huupponen *et al.*, 2008; Steriade *et al.*, 1993b) and only a handful of recent studies have started to address the question of how these oscillations relate to the onset of LOC (Gervasoni *et al.*, 2004; Hwang *et al.*, 2010; Magnin *et al.*, 2010; Velly *et al.*, 2007). These studies radically conflict in their conclusions as to the relevance of the thalamus in LOC of anaesthesia and natural sleep. There is *in vitro* evidence for a direct action of anaesthetics on thalamic relay neurones, in that they express K2P channels and are sensitive to volatile anaesthetics (Meuth *et al.*, 2003). Furthermore TC neurones express extrasynaptic $GABA_A$ receptors making them sensitive to the general anaesthetic etomidate and the sleep promoting drug gaboxadol (Belelli *et al.*, 2005). Pharmacological excitation of the central medial thalamus has been shown to reverse sevoflurane anaesthesia (Alkire *et al.*, 2009; Alkire *et al.*, 2007) and depression to reduce arousal (Miller *et al.*, 1990). Stroke patients with widespread damage to the thalamus may be left in a minimally conscious state (Brown *et al.*, 2010; Schiff, 2008) resembling anaesthesia. However this conflicts with a recent report in rats showing that extensive thalamic lesioning did not alter behaviour or EEG, yet destruction of the basal forebrain resulted in animals being unresponsive with a continuous <1Hz EEG rhythm (Fuller *et al.*, 2011).

The principle counter argument to the thalamus being a putative target for anaesthetics is for a direct action in the neocortex. Several recent reports have concluded that anaesthetics have their major depressant effects within the cortex. Velly et al. (2007) concluded that during propofol and sevoflurane induction of anaesthesia the cortex reached an electrophysiological state of anaesthesia 10 minutes before the subthalamic nucleus, used as a surrogate for the thalamus. Additional to this, ablation of primary sensory ventromedial basal nucleus (VB) in rats did not alter cortical arousal from anaesthesia (Constantinople *et al.*, 2011). Instead intracortical connections were responsible for wide ranging cortical arousal. Many of the molecular anaesthetic targets are found within the

cortex making it a reasonable candidate for direct anaesthetic action. Furthermore, the hyperpolarization activated current (I_h) responsible for setting thalamocortical neurones in the required state for spindles and delta oscillations (McCormick *et al.*, 1990) is inhibited by propofol (Ying *et al.*, 2006) and therefore disputes a direct action of propofol on the thalamus.

There still remains a large body of investigation required to establish whether either the thalamus or cortex are putative anaesthetic targets, which leads to a third possibility, the hypothalamus. The hypothalamus contains a number of arousal and sleep active nuclei which exist in mutual inhibition within the sleep regulating "flip-flop" switch (Saper *et al.*, 2010). Their role in natural sleep will be considered in the next section. The arousal nuclei of the hypothalamus form the ascending reticular activation system, which passes via the thalamus and terminates in the cortex. There are several nuclei within the hypothalamus and pons providing excitatory cholinergic input to the thalamus (Jones, 2005) either directly or by indirectly inhibiting GABAergic reticular neurones and causing increased cortical arousal (Steriade *et al.*, 1988b). Microinjection of GABAergic agents into these nuclei result in LORR and EEG similarities with sleep (Devor *et al.*, 2001; Sukhotinsky *et al.*, 2007). The adrenergic locus coeruleus (LC) is considered to be the site of action of α_{2a} adrenergic receptors such as dexmedetomidine (Chiu *et al.*, 1995; Correa-Sales *et al.*, 1992; Jorm *et al.*, 1993). LC neurones are sensitive to halothane due to expression of TASK channels (Sirois *et al.*, 2000) however they are excited by sevoflurane (Yasui *et al.*, 2007) and is presumably the source of paradoxical excitation seen in sevoflurane anaesthesia. The orexinergic perifornical hypothalamus and histaminergic tuberomammillary nucleus are important sources of ascending arousal to the cortex (Lee *et al.*, 2005; Panula *et al.*, 1984) and have been recently demonstrated as potential direct targets for the actions of propofol (Jurd *et al.*, 2003; Zecharia *et al.*, 2009).

There is no complete mechanism for anaesthetic induced LOC at present. Investigation of the thalamus and cortex has evidence to suggest direct and indirect action by anaesthetics. Clearly a greater understanding of the mechanisms of arousal and the functional connectivity of the hypothalamus, thalamus and cortex are required to ascertain how anaesthetics exert their effects.

1.4 Mechanisms of Sleep

The majority of research into sleep mechanisms in recent years has focused on hypothalamic sleep and arousal pathways, with the leading hypothesis of sleep controlling being the "flip-flop" switch (Saper *et al.*, 2001). This mechanism allows for the possibility that anaesthetics recruit the endogenous sleep pathways to exert their effects (Correa-Sales *et al.*, 1992; Nelson *et al.*, 2002) and indeed sleep arousal nuclei have been demonstrated to be anaesthetic sensitive (Jorm *et al.*, 1993; Zecharia *et al.*, 2009).

Sleep is characterised in the EEG by a slowing of frequency and an increase in amplitude, inferring an increase in cortical synchrony compared to wakefulness (Franks, 2008). These changes in the EEG can take several seconds to up to a minute to occur in humans (Wright *et al.*, 1995) but in rodents takes place in less than a couple of seconds (Takahashi *et al.*, 2010). Thus the principle of a sleep regulating switch seems plausible (Saper *et al.*, 2010).

Moruzzi and Magoun (1949) first demonstrated that midbrain reticular formation stimulation could cause arousal and EEG patterns of wakefulness. Much of the work on sleep since has been based on these findings and has identified monoaminergic and cholinergic cell groups as providing the important projections to the forebrain (Saper *et al.*, 2010). The cholinergic innervation is derived from the pedunculopontine (PPT) and laterodorsal tegmental (LDT) nuclei which provide extensive innervations of the hypothalamus, thalamus, basal forebrain and frontal cortex (Hallanger *et al.*, 1987). The projections of these nuclei coupled with their behavioural state dependant firing suggest a role for cortical arousal (Steriade *et al.*, 1993a). LDT neurones increase firing rates just prior to wakefulness transitions in the cortex (Boucetta *et al.*, 2009).

The monoaminergic nuclei consist of the noradrenergic LC, the histaminergic tuberomammillary nucleus (TMN) and the serotinergic dorsal raphe nucleus (DRN). Most of the projections from these nuclei are to within the hypothalamus to the GABAergic sleep promoting ventrolateral preoptic nucleus (VLPO) (Saper *et al.*, 2001). The other major projections are the basal forebrain and cortex (Aston-Jones *et al.*, 1981; Panula *et al.*, 1984) however a small number of projections are sent to the intralaminar nuclei of the thalamus, forming an important part of the ascending reticular formation (Schiff, 2008). In addition to the monoaminergic nuclei, the orexinergic perifornical nucleus (PeF) in the lateral hypothalamus was more recently identified as being important in arousal (Adamantidis *et al.*, 2007; Lin *et al.*, 1999) and has been considered to modulate the "flip flop" switch (Saper *et al.*, 2001).

The basal forebrain is a prominent arousal system located rostrally in the brain, and consists primarily of either GABAergic or cholinergic neurones, though a few are glutamatergic (Manns *et al.*, 2001). Most of the basal forebrain cells are wake active and the glutamatergic cells contribute to cortical arousal (Jones, 2004). Lesioning experiments of the basal forebrain have had mixed results in alter states of arousal and EEG oscillations (Fuller *et al.*, 2011; Kaur *et al.*, 2008) and there is a requirement for transgenic studies to selectively investigate the role of the GABAergic cell population (Saper *et al.*, 2010).

 The thalamus is the largest source of glutamatergic input to the cortex (Jones *et al.*, 1974). The nature of the connectivity between the thalamus and cortex will be discussed in more detail in the next section, however the midline and intralaminar nuclei provide diffuse cortical projections and the role of the central medial thalamus (CMT) has recently been investigated in sevoflurane anaesthesia. (Alkire *et al.*, 2009; Alkire *et al.*, 2007). Furthermore, the thalamus is considered to be the origin of the delta oscillation, prominent in sleep and anaesthesia (Dossi *et al.*, 1992; Leresche *et al.*, 1990), and the GABAergic reticular thalamus the pacemaker for sleep spindles (Steriade *et al.*, 1987). Despite this initially compelling indication of the thalamus, there is relatively little evidence for its role in sleep regulation. Investigations of thalamic lesions are contradictory at present. Experimental lesions in animals seem to provide little alteration in wakefulness and EEG (Fuller *et al.*, 2011) (Moruzzi *et al.*, 1949; Steriade, 1995) however patients with bilateral thalamic lesions are frequently rendered unresponsive in a minimally conscious state (Schiff, 2008). Indeed such patients may have intact functional long range cortical networks (Schiff *et al.*, 2005) and thalamic stimulation has been demonstrated to provide increased arousal in cases of severe traumatic brain injury (Schiff *et al.*, 2007).

1.5 The Thalamus

The thalamus has classically been considered in its role as a relay of sensory information to the cortex. However more recently it is being increasingly recognised as playing a fundamental role in regulating wakefulness (Steriade *et al.*, 1988a). Indeed lesions to the thalamus may result in states of permanent coma (Brown *et al.*, 2010). The thalamus is the major structure in the diencephalon, existing as a bilaterally lobed region and largely consisting of symmetrically paired nuclei. These nuclei are categorised into four main types which will be considered in turn. There are fundamental differences in the connectivity of these types of nuclei and the inputs to the thalamus coined "drivers" and "modulators" (Sherman *et al.*, 1998), which may have important connotations when considering the discrete areas of the thalamus in terms of arousal.

1.5.1 First Order Nuclei

Primary or first order nuclei relay primary information from all sensory inputs, with the exception of olfaction, to a corresponding primary sensory region of the parietal cortex (see figure 1.1). The best studied of these nuclei in rodents is the ventrobasal nucleus (VB). The driver of VB is ascending projection from the colliculus carrying sensory information about the contralateral vibrissae. The projection from VB is to layer IV of the barrel cortex, part of the primary somatosensory cortex. The barrel cortex then sends a projection from layer VI back to VB as a modulator and driver projection from layer V to the higher order posterior nucleus (Po; see figure 1.1) (Reichova *et al.*, 2004). Destruction of VB has recently been found not to impact on arousal in the barrel cortex in rats, suggesting that other ascending pathways or intracortical networks are more important for excitation of the somatosensory cortex (Constantinople *et al.*, 2011). The depolarisation phase of thalamocortical relay cells (TC) in delta and slow oscillations is stereotypical (McCormick *et al.*, 1990) and this is thought to prevent the transmission of primary sensory information (Crunelli *et al.*, 2006). The failure to respond to external stimuli is one of the cardinal features of sleep and anaesthesia, but whether or not blockade of primary sensory information through the first order thalamic nuclei is sufficient to cause LOC is yet to be confirmed. Minimally conscious state that follows thalamic lesions is rarely specific for the first order nuclei (Brown *et al.*, 2010) so this phenotype may be attributable to loss of either first or higher order nuclei.

1.5.2 Higher Order Nuclei

Secondary or higher order nuclei do not receive any primary sensory inputs, but receive the corticothalamic projections from layer V of the parietal cortex as driver (see figure 1.1), such as the barrel cortex to Po (Reichova *et al.*, 2004) and from layer VI as a modulator (Guillery *et al.*, 2002). The projection of these thalamic nuclei is to layer IV cortical neurones in diffuse areas of the cortex.

The projections are varied to both primary sensory cortex and also associational areas in the cortex involved in cross modality sensory processing. The higher order nuclei can thus be said to have a role in contextual processing of sensory information. There is little evidence for or against the role of higher order nuclei in arousal and anaesthesia. However many investigations on somatosensory evoked potentials are conducted in anaesthetised rodents using for example vibrissal stimulation (Jacob *et al.*, 2008) and peripheral nerve stimulation (Li *et al.*, 2003). This suggests the preservation of a degree of primary somatosensory transmission, so higher order nuclei may represent an alternative regulator of higher order arousal to the cortex. Layer VI of the cortex is one of the few brain regions with high expressions of the adrenergic α_{2a} receptor (Nicholas *et al.*, 1993) suggesting that dexmedetomidine may produce some of its effects by altering the modulatory effect of the cortex on the thalamus.
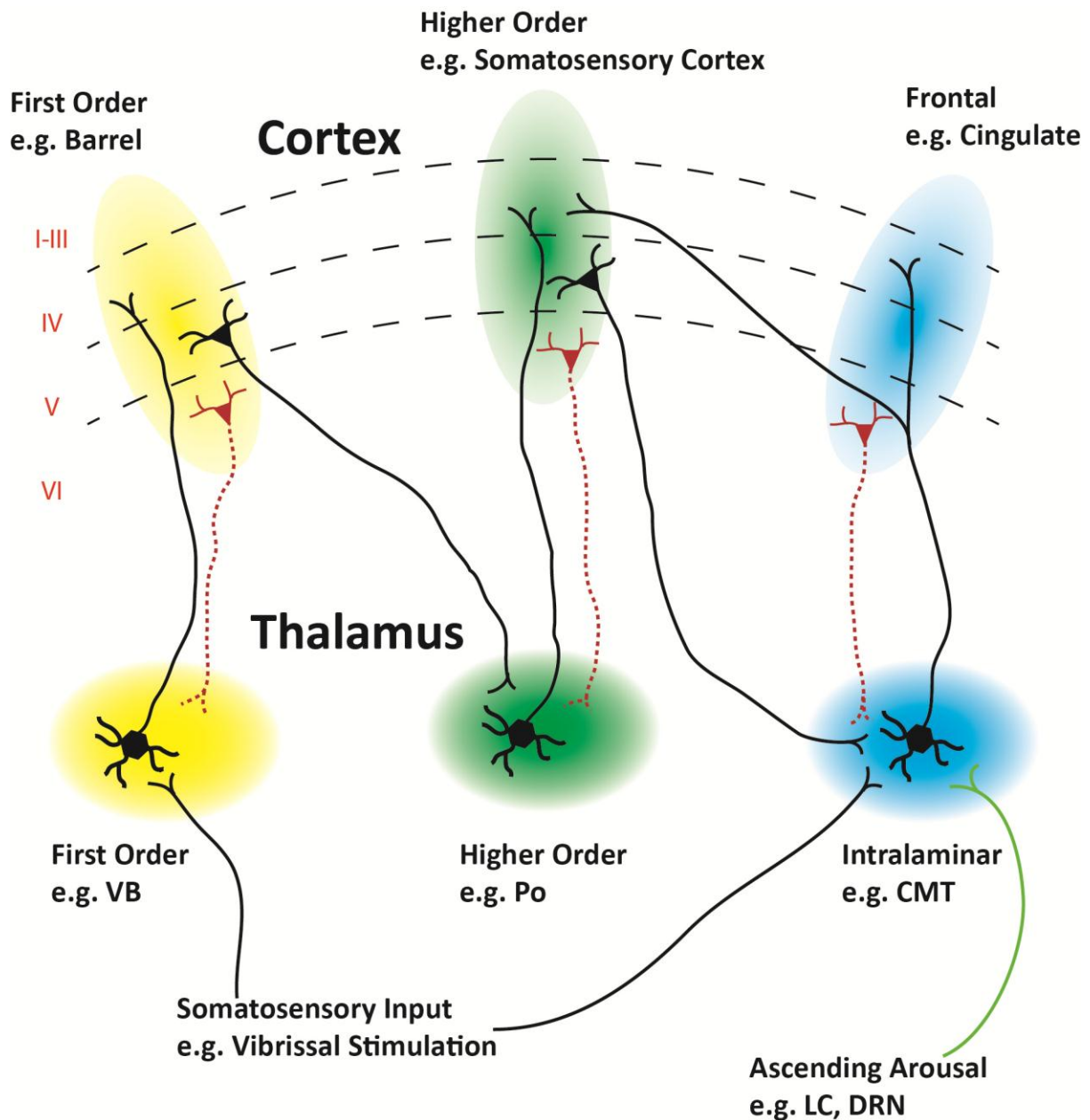
Figure 1.1 Functional connectivity of the thalamus and cortex
The thalamus is composed of first order, higher order, intralaminar/midline and the reticular nucleus (not shown). All areas project to cortical layer IV and receive modulatory input from layer VI. Cortical drive comes from layer V projections. The first order nuclei receive inputs from primary sensory information such as whisker stimulation via the colliculus and trigeminal nucleus of the brainstem. They project to layer IV of discrete brain regions, such as the barrel cortex in the case if vibrissae sensation. The corticofugal projection from layer V primary sensory areas projects back to a higher order part of the thalamus such as Po for somatosensory information. The higher order nuclei may receive projections from numerous primary sensory cortical areas. They in turn project to higher order areas of the cortex such as the secondary somatosensory cortex. The intralaminar nuclei have properties of both first and higher order nuclei as well as important projections to the striatum. They receive some sensory input as well as ascending arousal forming part of the reticular activating system as well as projections from higher cortical areas and project to multiple cortical areas including frontal cortex. The intracortical network projections are diffuse and between layers I-III and VI (not shown).

1.5.3 Midline and Intralaminar Nuclei

The midline and intralaminar nuclei are an enigmatic group of nuclei that have received little attention as anaesthetic targets until recently (Alkire *et al.*, 2009; Alkire *et al.*, 2007). However they have been well documented for their role in arousal as part of the ascending reticular formation (Moruzzi *et al.*, 1949; Schiff, 2008).

These nuclei have properties of both first and higher order nuclei, as they receive sensory input from the brainstem (Krout *et al.*, 2002) and project to widespread cortical areas as well as the striatum (Steriade *et al.*, 1982a). Indeed they receive more brainstem and basal forebrain projections than any other area of the thalamus (Kolmac *et al.*, 1999) as summarised in table 1.1. They receive heavy innervations from the adrenergic LC and serotinergic DRN (Oke *et al.*, 1997).

Imaging studies of the human brain have demonstrated an increase in midline thalamus activation during periods of increased alertness (Kinomura *et al.*, 1996). Blood flow in the brain has been used frequently in imaging studies as a surrogate for neuronal activity. One particular study in humans demonstrated a high correlation of midline thalamic blood flow with that of the anterior cingulate cortex (Hofle *et al.*, 1997). The cingulate has reciprocal connections with the midline thalamus and projects throughout the frontal cortex (Schiff, 2008), suggesting a higher order of the thalamocortical system which is likely involved in arousal. There are several studies indicating covariance power in the gamma frequency range between the midline thalamus and the cortex (Schiff, 2008) but little evidence of electrophysiological behaviour in the delta range during sleep or anaesthesia. However there is limited *c-fos* data to indicate that the central medial thalamus and paraventricular nucleus in the midline thalamus of rats follows a circadian cycle, being most active during wakefulness and opposite to the sleep active VLPO (Novak *et al.*, 1998).

Nucleus	TMN	Pef	LC	DRN	ACh	DPMe
Paraventricular	++	+++	+	+++		+++
Paratenial	++	-		+++		
Intermediodorsal		+		+++		
Reuniens	+/++	++			+++	+++
Rhomboid	+/++	++		+/++		+++
Posterior central medial	++	+++	++		+++	+++
Paracentral		-	++			+++
Central lateral		++	++		+++	+++
Anterior central medial	++	+			+++	+++
Centre median		-			+++	
Parafasicular		-	+++			+++

Table 1.1 Table of the modulatory inputs to the midline and intralaminar nuclei.

Direct pharmacological evidence of the role of these nuclei in arousal is sparse for a number of reasons. The nuclei are midline and sit directly below the third ventricle, making any direct injection likely to diffuse back into the CSF and diffuse to other brain areas. Additionally, *in vitro* electrophysiology is difficult because of the surrounding lamina. However there is interesting data to implicate the role of the central medial thalamus (CMT) in arousal. Miller and Ferrendelli (1990) found that infusion of the GABA$_A$ agonists piperidine-4-sulphonic acid or the GABA$_B$ agonist baclofen into the CMT produced a reduced *in vivo* arousal in a dose dependant manner resulting in LORR at higher doses. The authors controlled for drug diffusion into the CSF in these experiments. Following on from this work, Alkire et al. (Alkire *et al.*, 2009; 2007) found that activation of the CMT using nicotine and potassium channel antibodies could reverse sevoflurane anaesthesia, suggesting an important role of the cholinergic transmission from the brainstem or basal forebrain.

The CMT has projections to a wide range of cortical regions, including the somatosensory and prefrontal cortex as well as the striatum (Van der Werf *et al.*, 2002), areas involved in decision making. Primary somatosensory transmission is maintained through increasing depths of anaesthesia, however the effects within the cortex become less spatially specific as depth increases (Erchova *et al.*, 2002). Whilst this could be due to a reduction in long range cortical network activity,

it would also be explained by a decrease in transmission from the intralaminar nuclei to widespread cortical areas.

1.5.4 The Reticular Thalamus

The reticular thalamus (RT) is a GABAergic sheet that wraps around the rostral ventral and lateral thalamus and has been demonstrated to be the source of 7-14Hz spindles in sleep and anaesthesia (Steriade *et al.*, 1987). RT neurones form reciprocating projections with TC neurones, though their major source of excitation is the neocortex (Jones, 2002), and they are inhibited by the cholinergic projections of the brainstem and basal forebrain (Steriade *et al.*, 1993a). An important feature of RT neurones is their mutual connectivity by spikelets (Landisman *et al.*, 2002), electrical equivalents of gap junctions, which are fast decaying events that differ from excitatory postsynaptic potentials (EPSPs) (Fuentealba *et al.*, 2004a). These spikelets are unable to initiate action potentials unlike EPSPs at certain levels of membrane depolarisation. They have been shown capable of synchronising the RT neurones at spindle frequencies and may be responsible for co-ordinating spindles throughout the thalamus by ensuring that GABAergic bursts occur simultaneously from the whole of the RT (Fuentealba *et al.*, 2004b). This GABAergic transmission hyperpolarises large numbers of thalamic relay neurones which then paradoxically burst fire. There is little evidence to support the RT as a putative anaesthetic target, however *in situ* hybridisation has suggested a high presence of the adrenergic α_{2a} receptor (Nicholas *et al.*, 1993), suggesting a possible role in dexmedetomidine anaesthesia, which produces spindle oscillations very similar to that of NREM (Huupponen *et al.*, 2008). Input from layer VI of the cortex (also rich in α_{2a}) results in suppression of the thalamus, by a reticular mediated pathway (Zhang *et al.*, 2004).

1.6 The Thalamocortical System

The thalamocortical system consists of a feedforward/feedback loop between the cerebral cortex and the thalamus. Additionally the reticular thalamus provides a strong GABAergic input to thalamic relay neurones and receives glutamatergic inputs from the cortex and relay neurones. The thalamocortical system gives rise to three key oscillations that are seen during various stages of sleep and anaesthesia, the slow oscillation (<1Hz), delta (1-4Hz) and spindles (7-14Hz). These will be considered in terms of their genesis within the thalamocortical loop and what this may tell us about how anaesthetics may be acting within the thalamocortical oscillation to produce anaesthesia.

1.6.1 Spindles

Spindles are 7-14Hz waxing and waning oscillations (See Figure 1.2) seen during the early stages of NREM sleep (Molle et al., 2002) and some forms of anaesthesia, namely propofol, barbiturate and dexmedetomidine (Andersen *et al.*, 1967; Huupponen *et al.*, 2008; Leslie *et al.*, 2009). Spindles were first described by Berger (1929), although the nomenclature was introduced by Loomis et al. (1935b). The generation of spindles was first ascribed to the thalamus by Morison and Bassett (1945) who observed stable spindles within the intralaminar thalamus in cats following bilateral decortication and high brainstem transection.

Spindles are considered to originate from the reticular thalamus (Steriade et al., 1987), a thin GABAergic sheet that covers the rostral, lateral and ventral parts of the thalamus. Isolated reticular neurones oscillate at 7-14Hz and thalamic ablation *in vivo* abolishes spindles in the EEG (Bazhenov *et al.*, 1999; Steriade *et al.*, 1987) as well as other thalamic nuclei (Steriade et al., 1985). The importance of the reticular thalamus in production of spindles is augmented by the observation that anterior thalamic nuclei which do not receive afferents from the reticular thalamus (Steriade *et al.*, 1984b), do not exhibit spontaneous or evoked spindles *in vivo* (Mulle et al., 1985).

Spindles are preceded by a lengthy (200-300ms) hyperpolarization of reticular neurones (Fuentealba et al., 2004b) with a reversal potential of -100mV, suggestive of a slow K^+ conductance. Interestingly, there was also significant decrease in the input resistance to these cells during this hyperpolarisation, suggestive of an active inhibitory process rather than passive inactivation (Steriade, 2005). The hyperpolarisation is likely to have a dendritic origin since current injection to depolarise the soma abolished the hyperpolarising potentials rather than augmenting them. The cortex sends projections to the reticular thalamus and is capable of producing hyperpolarisation in these cells (Contreras *et al.*, 1996b; Zhang *et al.*, 2004). It is likely that an excitatory volley from the cortex could cause a spike burst in a small population of reticular neurones, producing a prolonged hyperpolarisation in the reticular thalamus by GABAergic dendrodendritic projections (Deschenes et

al., 1985) and electrical connections (Fuentealba *et al.*, 2004a; Landisman *et al.*, 2002). Indeed, this intra-reticular connectivity is likely to be the reason for the failure to observe spindles in isolated reticular cells in certain studies (von Krosigk et al., 1993), since transection of the long dendrites of the reticular thalamus ablates spindles (Steriade et al., 1993c).

When reticular neurones become sufficiently hyperpolarised, they become capable of rapid (100-300Hz) firing due in part to a low threshold calcium current (I_T) from T-type calcium channels that are inactivated at more depolarised potentials. This bursting induces a series of slow (6-10Hz) IPSPs in thalamic relay neurones (Bal *et al.*, 1995b; von Krosigk *et al.*, 1993). Successive incoming IPSPs activate a hyperpolarisation activated current (I_h) which results in a calcium conductance (I_T) which depolarises the relay neurone (McCormick *et al.*, 1990). When this calcium current becomes sufficiently large (paradoxically from a sufficiently large hyperpolarisation) to activate an action potential, the relay neurone burst fires resulting in spindles at the thalamic level. These paradoxical rebound spike bursts in the thalamus are responsible for the transfer of spindles to the cortex where they are measured in the EEG (Steriade et al., 1993c). Projections from thalamic relay neurones to layer IV of the cortex result in complimentary firing in the cortex which produces the extracellular ion flux measured globally as the EEG. The importance of this projection was demonstrated by Steriade (1985) who demonstrated the abolition of spindles within the EEG when the cortex is deafferented from the thalamus.

The waxing and waning nature of spindles is the result of interaction between GABAergic reticular neurones and glutamatergic thalamic relay neurones (Bal et al., 1995a). The waxing is due to progressive recruitment of reticular neurones to burst in synchrony and a corresponding number of thalamic relay neurones to perform paradoxical burst firing with generalized spread to large portions of the thalamocortical network (Kim et al., 1995). The waning however is the result of progressive Ca^{2+} induced-AMP activation of I_h and therefore inactivation of I_T, which results in a 1-4mV after depolarisation within thalamic relay neurones (Bal *et al.*, 1996). This leaves the relay neurones refractory to IPSP formation from the GABAergic input from reticular neurones. This represents a desynchronisation of the thalamic input to the cortex (Bazhenov et al., 2000).

In the *in vitro* thalamic slice preparation, spindles appear to move as a travelling wave (Kim et al., 1995), however, spindles occur uniformly across the thalamus and cortex *in vivo*. This requires corticothalamic feedback (Contreras *et al.*, 1996a) as layer VI cortical neurones send projections to the reticular thalamus. Interestingly, intracortical connectivity is not a prerequisite for this synchrony.

Spindles found during sleep are very similar in frequency and duration to those during some anaesthetic states (Huupponen et al., 2008). However, between anaesthetic states, differences in spindle structure within the waveform do exist (Crunelli et al., 2006). For example, during natural sleep, spindles are intimately associated with K-complexes (Loomis et al., 1935a), yet during barbiturate anaesthesia, a commonly used method to induce spindle oscillations for experimental investigation (Steriade *et al.*, 1984a), K-complexes appear to be absent (von Krosigk et al., 1993). In xylazine/ketamine anaesthesia, spindles occur as part of a K complex (Contreras *et al.*, 1996b). Since the K-complex is actually an EEG reflection of the cortical slow oscillation (Amzica *et al.*, 1997), it is possible that spindles seen during these three states may have a different genesis (Crunelli et al., 2006).
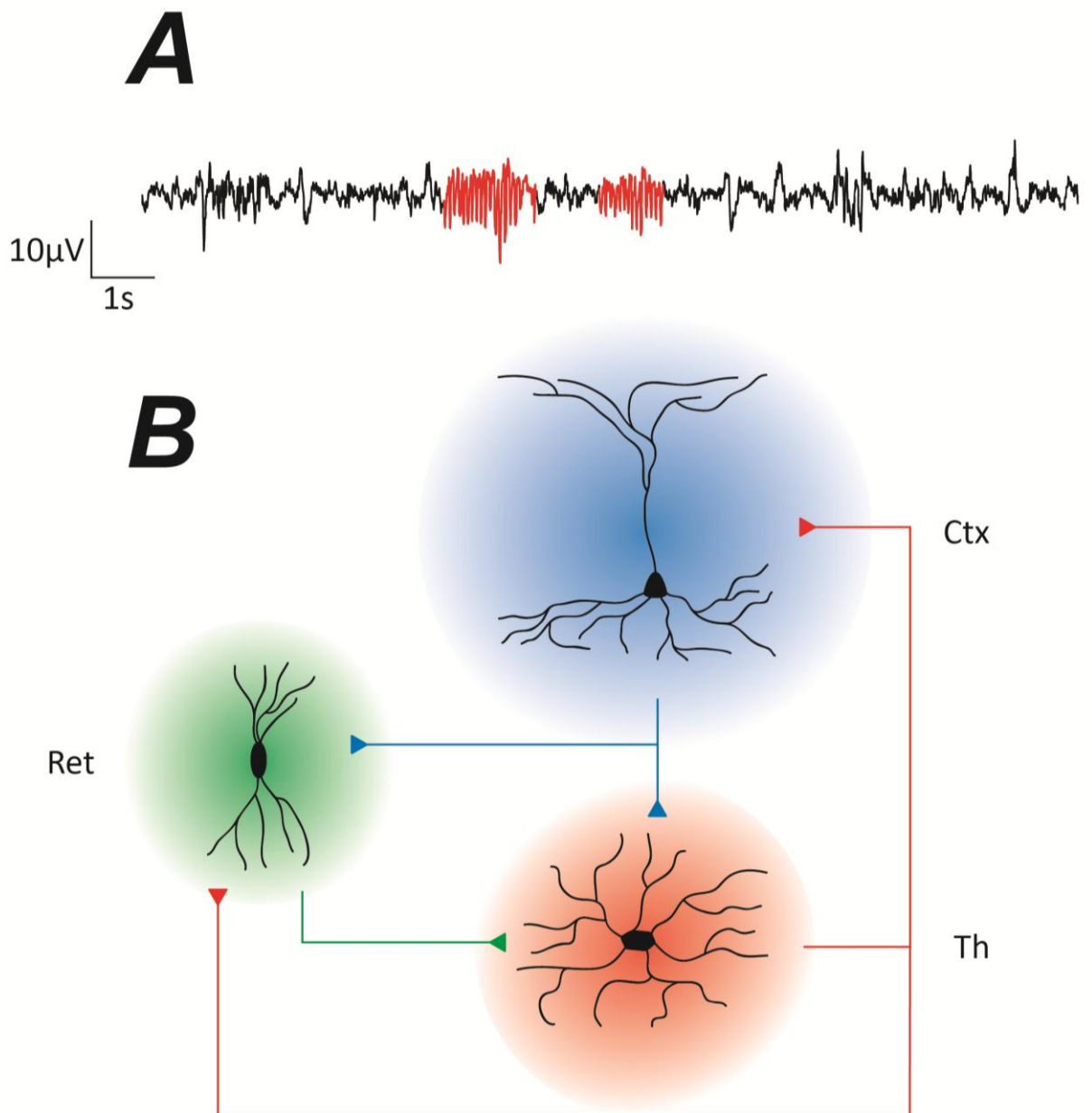
Figure 1.2 Spindles are 7-14Hz transient rhythms originating from the thalamocortical system.
A. Spindle events recorded from the barrel cortex of a dexmedetomidine sedated rat. Spindles are waxing and waning events that last typically for 1-1.5s and are found in natural sleep and some forms of anaesthesia. Note the increased frequency of the oscillations of 12Hz compared to the delta oscillation of 4Hz in the rest of the recording. **B**. Spindles result from rebound burst firing of thalamic relay neurones following hyperpolarisation by GABAergic input from the reticular thalamus. A prolonged GABAergic IPSP from the reticular thalamus inactivates an inhibitory low threshold calcium current (IT). When the IPSP decays, a hyperpolarisation activated current is activated and starts to depolarise the relay neuron, riding on the back of I_T resulting in burst firing. Thus the inhibitory GABAergic input from the reticular thalamus results in paradoxical excitatory responses in thalamic relay neurons.

1.6.2 Delta (1-4Hz) Oscillations

The delta oscillation is the principal EEG rhythm seen during advanced stages of NREM sleep and many forms of anaesthesia. Delta oscillations have been recorded *in vivo* from decorticated thalamic cells (Dossi et al., 1992) and in thalamic slice preparations *in vitro* (Leresche *et al.*, 1990; Leresche *et al.*, 1991). These "pacemaker" potentials were insensitive to tetrodotoxin, indicating the oscillation was due to intrinsic properties of the thalamocortical cell.

Thalamic relay neurones are required to be hyperpolarized to initiate delta oscillations (Hughes *et al.*, 1998; McCormick *et al.*, 1990). In a similar manner to spindle production, the hyperpolarisation of relay neurones activates I_h, which starts to depolarise the cell. A low threshold calcium spike (I_T) rides on the back of I_h to create a single action potential. During the depolarisation, I_h becomes inactivated and as the low threshold spike ends, the cell hyperpolarises to reactivate I_h and the cycle restarts. Hughes et al., (1998) showed that I_h is crucial for the genesis of intrinsic delta oscillations. Pharmacological block of the I_h current abolishes delta, yet delta can be reinitiated by a synthetic dynamic current injection of I_h.

The more intricate cellular mechanisms of the delta oscillation have received much less attention than the slow oscillation and spindles, largely because the metronomic timing of thalamic relay neurones is not reflected in the EEG. In contrast to the slow oscillation and spindles, delta is irregular in the EEG with waxing and waning frequency and amplitude (Steriade, 2005). This ultimately suggests that other cortical inputs are disrupting the rhythm produced in a thalamocortical manner. The delta oscillation is grouped by the slow oscillation during the DOWN state. This is thought to be by cortical excitation of a few reticular neurones during the UP state that will hyperpolarise large numbers of thalamic relay neurones allowing a rebound delta oscillation (Crunelli *et al.*, 2010).

Many anaesthetics such as dexmedetomidine, barbiturates, propofol and fentanyl increase power within the delta range in the EEG. However most of these studies compare oscillations in static states either side of the transition into consciousness (Bol *et al.*, 1997; Jugovac *et al.*, 2006). One recent study (Velly et al., 2007) investigated dynamic changes of EEG during the onset of unconsciousness, but largely ignored the cardinal indicators of thalamocortical activity and instead looked at dimensional activation (Da) of the waveform. Da is measure of the chaos within in a system and a low Da score is interpreted as a network having a high degree of synchrony, such as in the delta oscillation. This study showed that the activity of the thalamus did not decrease until several minutes after propofol LOC in humans, unlike the cortex which deactivated at LOC. A similar study in sleep in humans suggests a sharp decrease in Da of the thalamus at the onset of natural sleep of humans, occurring before the cortex (Magnin et al., 2010). Clearly further investigation is

required to determine the relative importance of the delta oscillation mechanism in the transition into unconsciousness.

1.6.3 Slow (<1Hz) Oscillation

The slow oscillation is the most recently discovered rhythm of the thalamocortical system (Steriade et al., 1993e) and was previously considered to be part of the delta range of frequencies seen in the EEG. It was found to be present in the EEG of natural sleep in both cats and humans although has since been identified in numerous mammalian species (Cunningham *et al.*, 2006; Hughes *et al.*, 2002; Sanchez-Vives *et al.*, 2000).

The slow oscillation was first described as an oscillation of the membrane potential of neocortical cells consisting of depolarisation with cell firing and quiescent periods of hyperpolarisation (Steriade et al., 1993e) now more commonly referred to as UP and DOWN states. The depolarising windows were seen regardless of resting membrane potential and cell firing was dependant on reaching threshold. Additionally to this, the UP and DOWN states of individual cortical cells were shown to have an excellent temporal correlation to the slow oscillation seen in the EEG and also appeared to temporally synchronise spindles and delta oscillations to the DOWN state (Steriade et al., 1993d). The UP state consists of a barrage of intracortical inhibitory and excitatory synaptic drive, whereas the DOWN state is a period of quiescence dominated by a slow K^+ current (Rudolph et al., 2007) although the exact mechanisms of this are currently poorly appreciated.

In anaesthetised animals, cells of the thalamus and reticular thalamus participate in the slow oscillation with synchrony to cortical regions (Contreras *et al.*, 1997; Steriade, 1997). This is thought to be by activation of metabotropic glutamate receptors (mGluR) by the corticofugal afferents (Blethyn et al., 2006). In thalamocortical neurones, the DOWN to UP transition involves a low threshold Ca^{2+} spike and high frequency burst spiking (Contreras *et al.*, 1996b). Interestingly, the start of this UP state in thalamocortical neurones precedes that of cortical neurones by 20-50ms (Contreras *et al.*, 1995), suggesting that the spike bursts from thalamocortical neurones might trigger the depolarisation phases in the cortex. However, the slow oscillation was shown in the isolated forebrain and the intact brain following destruction of thalamocortical cells by kainic acid or electrolytic lesioning and decortication leads to abolition of the slow oscillation in the thalamus (Steriade *et al.*, 1993d; Timofeev *et al.*, 1996). Additionally, the slow oscillation persists in cortical slab preparations *in vitro* (Timofeev et al., 2000) thus concluding that the oscillation is generated in the cortex and imposed in the thalamus (Steriade et al., 1993b). However, these experiments have not compared the slow oscillation before and after isolation and lesioning. This is highlighted by two important observations. Firstly, local cortical network disruption by lidocaine infusion does not alter

long range cortical coherence in the slow oscillation band. Secondly muscimol injection in the thalamus may abolish slow oscillations in individual cortical neurones (Doi et al., 2007). These findings are compounded by an additional observation; sectioning thalamocortical and corticothalamic afferents *in vitro* reduces the occurrence of UP states by 60% (Rigas *et al.*, 2007).

The slow oscillation has been demonstrated in numerous types of cortical neuron and is considered to be a feature of all neurones of the neocortex (Contreras *et al.*, 1995). Synchrony between relatively distant neurones has been demonstrated in urethane anaesthetised cats (Volgushev et al., 2006). However, studies in anaesthetised rats and naturally sleeping humans show that the slow oscillation behaves as a travelling wave (Luczak *et al.*, 2007; Massimini *et al.*, 2004) in a posterior direction from the frontal cortex. Interestingly, the firing characteristics of individual neurones are highly stereotypical and independent of wave direction, indicating a localised network interaction (Luczak et al., 2007). As sleep progresses from stage II to IV, the frequency of the slow oscillation increases from 0.3 to 1Hz (Amzica *et al.*, 1997) and contains clear periods of delta oscillations in the down state. The hastening of the slow oscillation as sleep deepens is due to the reduction in firing of neurones in the midbrain reticular formation and the mesopontine cholinergic nuclei (Steriade *et al.*, 1990; Steriade *et al.*, 1982b). This removes the excitatory drive to the cortex, resulting in progressive increase in hyperpolarisation and a shortening of the depolarisation window, thus decreasing the time until the next UP state.

The slow oscillation permeates all stages of NREM sleep in humans (Achermann *et al.*, 1997; Cash *et al.*, 2009) although EEG representation in the form of the K-complex is seen particularly during stage II. The slow oscillation also occurs in anaesthesia, although different anaesthetics appear to clamp the oscillation at differing frequencies. The combination of ketamine/xylazine sets the oscillation much higher (0.6-1Hz) than urethane (0.3-0.4Hz) (Steriade et al., 1993e). Isoflurane markedly reduces the frequency of the oscillation with increasing percentage of inspired gas (Doi et al., 2007). It appears that anaesthetics also alter the cellular dynamics of the oscillation since ketamine/xylazine shortens that UP state (Luczak et al., 2007) and barbiturates attenuate the characteristic UP-DOWN fluctuations (Steriade et al., 1993e). This clamping of the slow oscillation, as with spindles, by anaesthetics results in an oscillation that lacks the dynamic properties of the natural sleep rhythm (Destexhe et al., 1999).

1.6.4   K-Complexes

The K-complex is the EEG reflection of the slow oscillation seen during the early stages of NREM sleep (Amzica *et al.*, 1997). Despite the relatively recent description of the slow oscillation, the K-complex has long been recognised in the human sleep EEG (Loomis et al., 1938).

The K complex has two components corresponding to the depolarising and hyperpolarising stages of the slow oscillation (Amzica *et al.*, 2002). The depolarisation phase is associated with a surface positive transient spike in the EEG (Amzica *et al.*, 1997). This is followed by a surface negative prolonged deflection in the EEG corresponding to the global hyperpolarisation of cortical neurones (Contreras *et al.*, 1995).

Functionally, the slow rhythm K-complex provides a regular synchronous input to the thalamus and trigger spindles and delta oscillations. This is important for preventing the transmission of sensory information from the thalamus to cortex, a prerequisite for sleep (Amzica *et al.*, 2002). This is because the resulting hyperpolarisation of thalamic cells results in depolarisation by the low threshold calcium current (I_T) (McCormick *et al.*, 1990) which is stereotypical and non-adaptable and therefore incongruent with sensory transmission. Some believe the K-complex reflects periods of arousal within sleep (Halasz, 1998; Niiyama *et al.*, 1996) because of the dynamic state of the UP state is similar to wakefulness (Destexhe et al., 2007). This seems reasonable since UP states are required to augment memories gained during consciousness. However K-complexes are not present in the EEG during wakefulness, even though UP-DOWN states persist (Luczak et al., 2007) but with reduced trans-cortical synchrony, due to cholinergic and noradrenergic activation (Steriade et al., 1993a). Thus K-complexes are unlikely to represent arousal in the classical sense. Despite the fact that the slow oscillation can be measured in many different preparations of cortical slabs (Timofeev *et al.*, 2000), recent *in vivo* data from humans suggest that the complexes arise from the cingulate and some temporal regions, suggest a role for the frontal cortex for initiating the slow oscillation as a pacemaker.

1.7 The Electroencephalogram

The electroencephalogram (EEG) is a non-invasive measurement of electrical activity derived from the pyramidal cells of the cerebral cortex. Activity is recorded from macroelectrodes on the scalp and gives a differential voltage from two electrodes.

The first brain derived electrical activity was measured by Caton (1875) using a galvanometer on rabbits and monkeys. This seminal work demonstrated a small fluctuating current in the conscious animal which increased in amplitude during sleep and disappeared after death. This work went largely unappreciated until Berger's experiments on humans in 1929 (Berger, 1929) which recognised Caton's important discoveries. Berger demonstrated the alpha (8-12Hz) rhythm in quiet conscious subjects using a galvanometer similar to Caton's and also demonstrated alpha blockade with higher frequency beta oscillations which occur when the subject blinks their eyes. Berger would go on to work on important alterations in the EEG pattern in disease states such as epilepsy.

Whilst Caton and Berger's early EEG recordings consisted of silver unipolar electrodes, modern EEG recording devices used in clinical practice consist of multiple serial bipolar electrodes. The primary uses are for localising focal brain disorders such as epilepsy or stroke, investigating sleep disorders and monitoring anaesthetic depth.

The earliest explanation for the genesis of EEG rhythms came from Rotheberger in 1931 and stated that the oscillations were due to action potentials travelling along chains of interconnected neurones. He proposed that the frequency of the oscillation was determined by the time taken for a series of action potentials to complete a loop of these interconnected neurones and became known as the circus movement theory. A further refinement was made to this by Bishop (1936) who proposed that the reverberation of action potentials between the thalamus and the cortex were responsible for the generation of oscillations. Subsequent experiments showed that the cortical electrical components contributing to the overall oscillation are too slow for action potentials (Adrian *et al.*, 1934; Renshaw *et al.*, 1940) and therefore fundamentally invalidated Bishops model. Later Bremer (1958) would propose an alternative theory that the EEG oscillation was derived from non-propagated potentials of cortical neurones and that these neurones had intrinsic properties that participated in the generation of oscillations, rather than the cortex being driven by pacemakers. He further stipulated that oscillation formation was the result of synchronization of oscillatory activity in a large number of neurones and that the synchronization was a result of intracortical excitatory connections. Additional experiment on spinal motor neurones lead to the hypothesis that the slow nature of EEG oscillations was the result of slow propagation of electrical potentials to the soma from distal dendrites (Eccles, 1951). This was later confirmed by intracellular experiments showing a

close correlation of synaptic potentials to the EEG (Creutzfeldt *et al.*, 1966a; Creutzfeldt *et al.*, 1966b).

It is now considered that the EEG arrives from inhibitory and excitatory postsynaptic potentials in the cortex which are able to summate in the extracellular field. The resulting EEG deflection is determined by whether the postsynaptic potential is positive or negative and how far it is from the recording site. Whereas intracellular recording of depolarisation will give a positive deflection, extracellular recording will vary depending on the distance as the electrical field has a source and sink. Close to the recording site, the extracellular recording deflection will also be positive as it represents the sink of the current. However at more distant recording sites the deflection is reversed since it is closer to the source. For inhibitory potentials the converse is true. The resulting field potential is the summation of these post synaptic events in thousands of cells, and clearly requires a degree of cellular synchrony to produce a slow oscillation such as delta (1-4Hz) and theta (5-12Hz).

2   General Methods

2.1 Animals and Surgery

All animals were adult male Sprague-Dawley rats weighing 320-360g. All procedures were carried out under UK Home Office Licensing. Animals were kept under a strict twelve hours light, twelve hours dark cycle (lights on at 19:30, lights off at 07:30). A minimum of four days acclimatization to the new holding facility was allowed before commencing experimental procedures. All animals were a minimum of 8 weeks old and 320g before surgery was performed. All experiments and recordings were performed on animals under 6 months of age.

2.1.1   Venous Catheter Insertion

Induction of anaesthesia was achieved by intraperitoneal injection of ketamine, 70mg/kg (Ketaset, Fort Dodge Animal Health) and xylazine, 10mg/kg (Rompun, Pfizer). Suitable depth of anaesthesia was determined by failure of the withdrawal reflex following a noxious stimulus (pinching) to digits of both hind limbs. Hair was clipped from an area measuring 3cm×3cm on the dorsum between the scapulae and an area measuring 2cm×3cm of the right axilla. The skin was aseptically prepared by the application of 10% povidone-iodine (Betadine, Purdue Pharma) followed by 70% ethanol solution. A 2cm longitudinal incision was made in the surgical site on the dorsum and the subcutaneous connective tissue broken down by blunt dissection. A 1.5cm longitudinal incision was made 0.5cm axial to the right axilla and the right jugular vein was exposed by blunt dissection and undermined (Figure 2.1b-c). All excessive connective tissue was removed from around the dissected portion of the vein. A single ligation of the vein was made with 5 metric polyamide suture at the cranial extent of the dissection. A second loose ligation was made at the caudal extent of the dissection and the vein exteriorised. Venopuncture was made using a 25g hypodermic needle. A 30g stainless steel wire was inserted into the vein via the puncture and the catheter (figure 2.1a) run over the wire into the vein by 3cm in the caudal direction. Adequate catheter placement was assessed by the ability to aspirate blood from the access port. The caudal ligation was tied permanently to fix the catheter. A narrow tunnel of subcutaneous tissue was undermined from the port to the surgically prepared site in the axilla by blunt dissection and the catheter fed through to the dorsal surgical site. The vascular access port consisted of a silicon septum (Infusion Concepts, UK) connected to a blunted 25g needle with a Luer lock (Figure 2.1a). The port was flushed with sterile 0.9% NaCl solution containing 2% heparin and connected to the catheter tubing. The port was sutured to the underlying rhomboideus muscle with 5 metric polyamide suture (4-0 Ethilon, Ethicon). Skin sutures were closed with polyglactin sutures (Vicryl, Ethicon). Following closure, bactericidal treatment of surgical sites was achieved with a single application of 10% povidone-

iodine. Post-operative analgesia was achieved with a single subcutaneous dose of buprenorphine, 0.02mg/kg (Vetergesic, Alstoe Animal Health, UK). Intraoperative fluid therapy was provided by 0.9% NaCl given at 10ml/kg/hr.
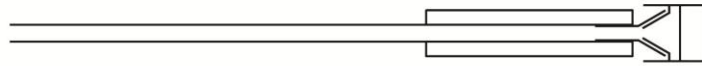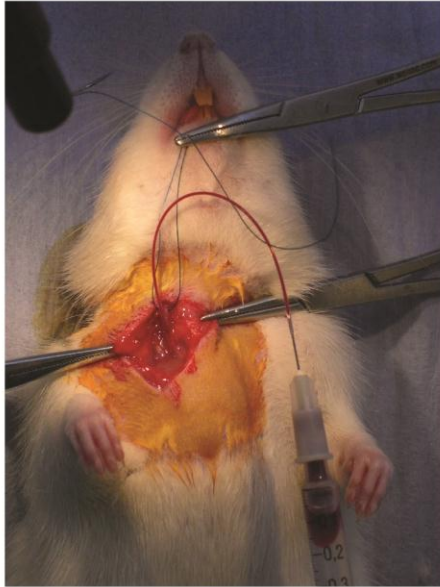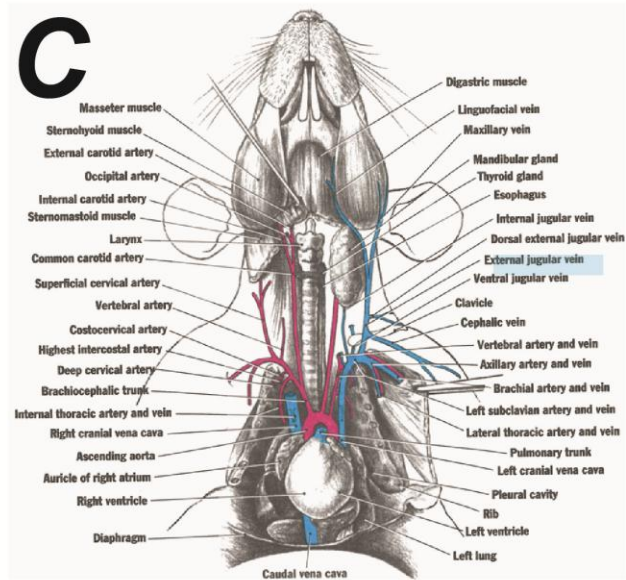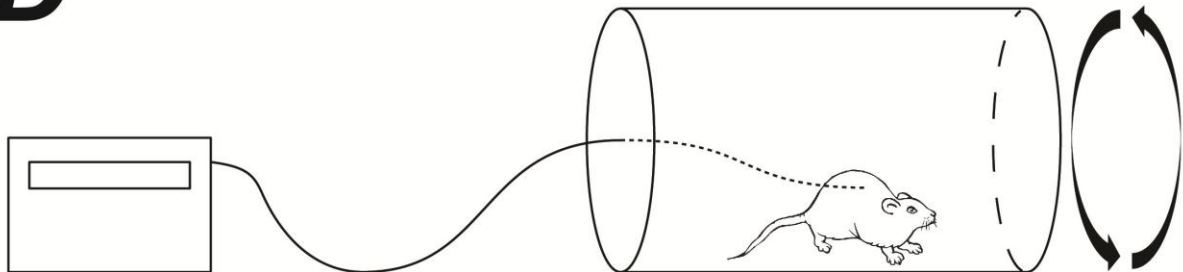
Figure 2.1 Loss of righting reflex experiments by intravenous drug administration
A. Schematic of a jugular catheter. The catheter consists of a 9.5cm length of 25g PTFE tubing connected to a blunted 25g needle. A silicone injection cap is connected by a Luer lock to the needle and is buried under the skin between the shoulder blades. PPE tubing over the junction of the blunted needle and the PTFE tubing prevents tube kinking whilst under the skin. **B**. Photograph showing the placement of PTFE tubing in the external jugular vein and aspiration of venous blood from the right atrium of the heart. **C**. Anatomical rendering showing the location of the external jugular vein (label highlighted in blue), the point of insertion of the jugular catheter (Copied from (Walker *et al.*, 1997)) **D**. Schematic of the LORR experiments. Anaesthetic agents are pumped from a syringe driver through a lead line. A hypodermic needle passes through the skin into the injection port in the rats back. The rat is in a cylinder continually revolving at 5rpm allowing precise timing of LORR.

2.1.2 Placement of Recording Electrodes

Induction of anaesthesia was achieved by intraperitoneal injection of ketamine, 70mg/kg (Ketaset, Fort Dodge Animal Health) and xylazine, 10mg/kg (Rompun, Pfizer). Maintenance was achieved by inhalation of halothane at 0.8%. Depth of anaesthesia was assessed as above. Hair was clipped from an area measuring 1.5×2cm on the top of the head and the skin aseptically prepared by the application of 10% povidone-iodine. The rat was placed in a stereotactic frame and was secured by ear bolts. A 1.5cm longitudinal incision was made in the skin exposing the underlying periosteum. The surrounding connective tissue was undermined by blunt dissection. Bregma and lambda were located and the skull realigned such that bregma and lambda had the same dorsoventral and mediolateral coordinates. The tungsten bipolar electrodes (Microprobes, USA) were placed according to the co-ordinates of Paxinos and Watson (1986) (see Table 2.1) with all measurements taken using Bregma as the reference point. Electrodes were secured in a stereotactic arm and lowered into the brain perpendicular to the bregma-lambda plane and secured to the skull using cyanoacrylate glue. Anchor screws and screw electrodes were placed in the skull over the parietal cortex. The free ends of the electrodes were soldered to a seven pin connecting plug (Figure 2.2c). The remainder of exposed wires and electrodes were secured with methyl-methacrylate cement. Post-operative analgesia was achieved with a single subcutaneous dose of buprenorphine, 0.02mg/kg (Vetergesic, Alstoe Animal Health, UK). Intraoperative fluid therapy was provided by 0.9% NaCl given at 10ml/kg/hr.

Structure	Co-ordinates WRT Bregma (mm)		
	Anterior-Posterior	Medio-Lateral	Dorso-Ventral
Cingulate Cortex	3.0	-0.8	-2.3
Barrel Cortex	-2.5	-5.0	-3.0
Central Medial Thalamus	-3.2	0.0	-6.5
Ventrobasal Nucleus	-3.4	-3.0	-6.0

Table 2.1 Co-ordinates used for recording from various nuclei
Co-ordinates taken from (Paxinos *et al.*, 1986)

2.2 Loss of Righting Reflex Experiments

All LORR experiments were performed during the dark period (7:30-19:30) to minimise the likely effects of natural sleep. Drugs were delivered as a constant rate infusion (CRI) by an infusion pump (Harvard 22, Harvard Apparatus). The purpose of using an infusion to affect LORR rather than a bolus, was to investigate the dynamic changes in the EEG over time. A bolus is likely to produce large EEG changes over too short a time period to allow in-depth analysis. The syringe was connected to a lead line which in turn connected to the vascular access port via a 23g needle. Electrophysiological data was collected on a miniature recording device (Neurologger 2, courtesy of Dr A. Vyssotski, University of Zurich) (Figure 2.2) and downloaded at the end of the experiment. Animals were placed in a transparent tube with an internal diameter of 15cm rotating at 5 revolutions per minute (Figure 2.1d). A five minute baseline recording was made before starting drug infusion. Drug infusion was stopped at the point of loss of righting reflex.

Drug	Infusion Rate (mg/kg/min)
Propofol (10mg/ml)	10
Midazolam(5mg/ml)	10
Dexmedetomidine (20µg/ml)	0.02

Table 2.2 Infusion rates for intravenous anaesthetic drugs used in LORR experiments

2.3 Sleep experiments

Natural sleep was recorded in the home cage using Neurologgers during the light period (19:30-7:30) only.
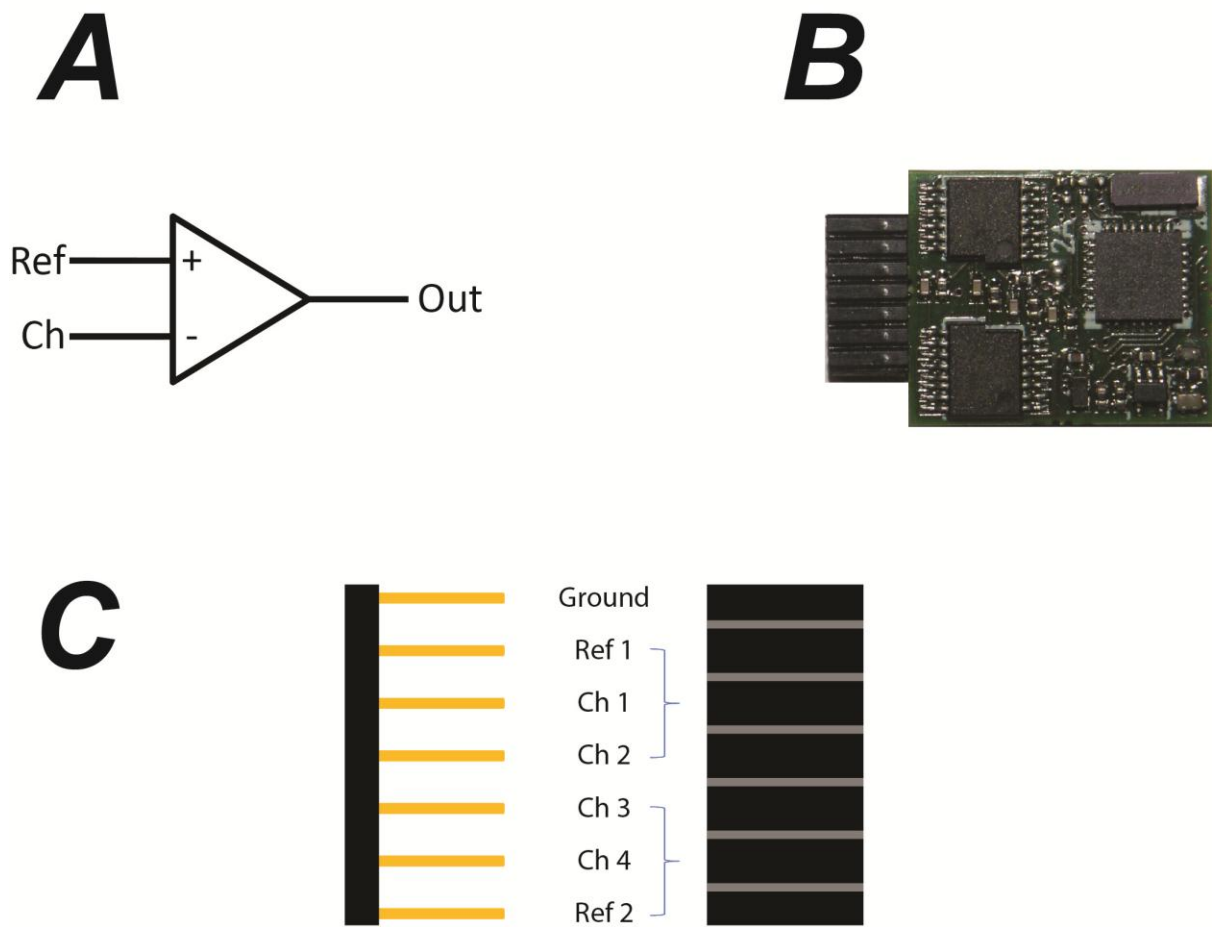
Figure 2.2 Neurologger device used for recording EEG and depth field potentials in anaesthetic and sleep experiments.
A. Schematic diagram of a differential amplifier, the basis of the signal acquisition of the Neurologger. Both inputs Ref and Ch oscillate with respect to a distant ground (screw over the nasal bone of the animal). Out is the difference of the two signals. **B**. Photograph of a single Neurologger showing the pin connector and the PCB. Each device measures 14.5 x 22.5mm and weighs 3.2g complete with battery. **C**. Schematic diagram of the connectivity of the Neurologger to electrodes implanted in the brain. Note each reference acts as a differential for two recording channels, hence each device is capable of two independent differential recordings.

2.4 Data Analysis

Data was downloaded in binary format and converted to .txt. Waveforms were visualised in Spike 2 software (CED, UK). Relevant segments of the waveform were exported for individual analysis.

2.4.1 Sleep scoring

Sleep was scored using EEG and EMG using a previously defined algorithm (Costa-Miserachs *et al.*, 2003). The algorithm works on *if-then-else* logic to discriminate signals that are consistent with Wake, NREM and REM. The EEG waveform is first band passed into delta (1-4.5Hz) and theta (5-12Hz) and rectified waveforms made from these. The algorithm then assesses the theta:delta ratio of the rectified EEG and the rectified EMG amplitude to assign one of four scores to each epoch of data:

1. Wake (W) – moderate theta:delta and high EMG
2. NREM (N) – low theta:delta and low EMG
3. REM (R) – high theta:delta and low EMG
4. Doubt (D) – for any data inconsistent with the above 1-3 as defined by pre-set thresholds

Recordings were scored in 4s epochs and four subsequent epochs put together to give an overall score for a 16s epoch:

WWWW, WWWN, WWWR, WWWD, WWNR and WWWDD scored as Wake.

NNNN, NNNW, NNNR, NNND, NNDW, NNDD and NNWR scored as NREM.

RRRR, RRRW, RRRN, RRRD and RRDD scored as REM.

All other combinations scored as Doubt.

2.4.2 Morlet Wavelet Analysis

Classically *in vivo* oscillations such as the EEG were analysed by Fast Fourier Transform (FFT) to produce a power spectrum with respect to oscillation frequency for a given segment of data. Whilst this has accuracy in the frequency domain, it lacks resolution in the time domain. In order to investigate the precise changes occurring around LORR, the Morlet Wavelet analysis was used to give much higher time resolution to a dynamically changing waveform, using software written for Matlab by Torrence and Compo (1998).

The continuous wavelet transform is given by the equation:

$$W(s, \tau) = x(t) * \psi(s, \tau)$$

Where s is a given scale, τ is the time shift, x(t) is the waveform, * is the complex convolution, and ψ is the wavelet, in this case the Morlet wavelet defined as:

$$\psi_0 = \pi^{-1/4} e^{i\omega_0 t/s} e^{-\left(\frac{t}{s}\right)^2/2}$$

Where ω_0 is the number of cycles within the Gaussian envelope.

The Morlet power spectrum is calculated as a matrix as the square of W for each defined value of s and τ.

The output from this analysis is a matrix with scale on the y-axis, time on the x-axis and power on the z-axis. The spectrograms are all normalized to the maximum power within that spectrum, shown in red. Therefore z-axis' of different spectra cannot not be compared for power. Each scale corresponds to a given frequency. The matrix thus shows changes in power for each frequency with respect to time.

The Morlet power spectrum has good frequency but poor time resolution at low frequencies and poor frequency but good time resolution at higher frequencies. Since the frequency is shown on a harmonic axis, power cannot be inferred from the intensity on the z-axis alone. The total power is given by integrating the intensity of the z-axis over the frequency range. Thus power at a low frequency will have a high intensity over a small frequency range, whereas power at a high frequency will have low intensity over a high frequency range.

2.4.3   Cross Wavelet Transform

The cross wavelet transform has previously been used in meteorology for ascertaining coherence and inferring causality from two signals. It has recently been used in neuroscience to investigate coherence between different brain regions (Gervasoni *et al.*, 2004; Li *et al.*, 2007) and calculates covariance in power from the continuous wavelet transform. For this analysis, software written by Grinsted et al. (2004) was used to calculate power covariance and phase coherence from paired recordings. Covariance assesses where two signals each have high power in both the time and frequency domains. It is calculated by multiplying the cross wavelet transform of one signal, x, by the complex conjugate of the wavelet transform of a second signal, y. Thus:

$$W_{xy}(s,\tau) = W_x(s,\tau) \cdot W_y^*(s,\tau)$$

Where W_{xy} is the covariant power for a particular scale, s, and time window, τ.

The output is a matrix with scale on the y-axis, time on the x-axis and covariant power on the z-axis. The matrix therefore shows changes in covariant power for each frequency with respect to time. The analysis delineates areas of covariant power which are significantly increased over the background noise of the spectrum. These regions of significance were used for calculating the average phase spectrograms as described in the next section.

2.4.4 Wavelet Phase Correlation

Phase correlation gives an angle of phase between two signals, determining whether one signal leads or lags behind the other. It is calculated by the following equation:

$$\phi(s,\tau) = tan^{-1}\left(\frac{\Im\big(W_{xy}(s,\tau)\big)}{\Re\big(W_{xy}(s,\tau)\big)}\right)$$

Where ϕ is the phase angle at scale s and time τ. $\Im$ and $\Re$ are the imaginary and real parts of the cross wavelet transform phase W_{xy} respectively.

The output from this is a matrix with scale on the y-axis, time on the x-axis and phase difference of W_x with respect to W_y on the z-axis. The phase was calculated between +π to −π, with 0 being exactly in phase, ±π being exactly antiphase, π/2 when W_x is leading W_y by 90° and −π/2 when W_x is lagging W_y by 90°. The matrix therefore shows the change in phase difference of the two signals for each scale with respect to time.

Averaged phase spectra were generated by averaging phases from each contributing spectrum on an element by element basis. Only phases corresponding to areas of significant covariant power for that particular spectrum were included. Phase averages were generated by averaging all phases within a particular frequency band.

2.5 Brain Slice Preparation

Following completion of all recordings, animals were deeply anaesthetised with intraperitoneal xylazine (15mg/kg) and ketamine (100mg/kg). The left ventricle of the heart was then punctured using a blunted 16g needle and a small puncture made in the right ventricle. The heart was perfused with 60ml of ice cold PBS at 10ml/min followed by 60ml of 4% paraformaldehyde at 10ml/min. The brain was then removed and post fixed in 4% paraformaldehyde for 24 hours followed by 24-48 hours in 30% sucrose until the brain sank. Brains were frozen in dry ice and slices were cut at a thickness of 50µm on a microtome, mounted on glass slides and stained with Cresyl violet. Electrode placement was verified by following the tract of the electrode in the histological slices.

3 EEG Measurements of Sleep and Anaesthesia

3.1 Determining a suitable method of data analysis

Classically, EEG data has been analysed by fast Fourier transform (FFT). The inherent problem with this form of analysis is that it requires a shifting window function. To increase sensitivity in the frequency domain requires an increase in the window function size, therefore decreasing the sensitivity in the time domain. Figure 3.1a shows a typical 60s EEG recording from a conscious active rat. FFT power spectra composed of 1024 bins have a frequency resolution of 0.09766 Hz, but a time resolution of only 10.24s when with a data sampling frequency of 100Hz (Figure 3.1b). Note how the FFT power gives poor detail about the fine structure of the waveform in the time domain. This detail is restricted to changes between power spectra, since an individual power spectrum has no time domain detail. Transitions from wakefulness into unconsciousness are likely to occur over a much shorter timescale, and therefore make this an unsuitable method for data analysis for investigating changes in the waveform for very short time periods. Morlet wavelet analysis was used to analyse the same data recording (Figure 3.1c). The distinct advantage of this form of analysis is that it gives a much higher resolution in the time domain and allows investigation of the fine structure of the waveform. The limitation to the Morlet wavelet analysis is that low frequency events have good frequency but poor time resolution, whereas high frequency events have poor frequency but good time resolution. The principal frequency in the recording is a theta rhythm of 8Hz. However the Morlet power spectrum reveals that this is not a continuous oscillation, but interspersed with bursts of delta power.
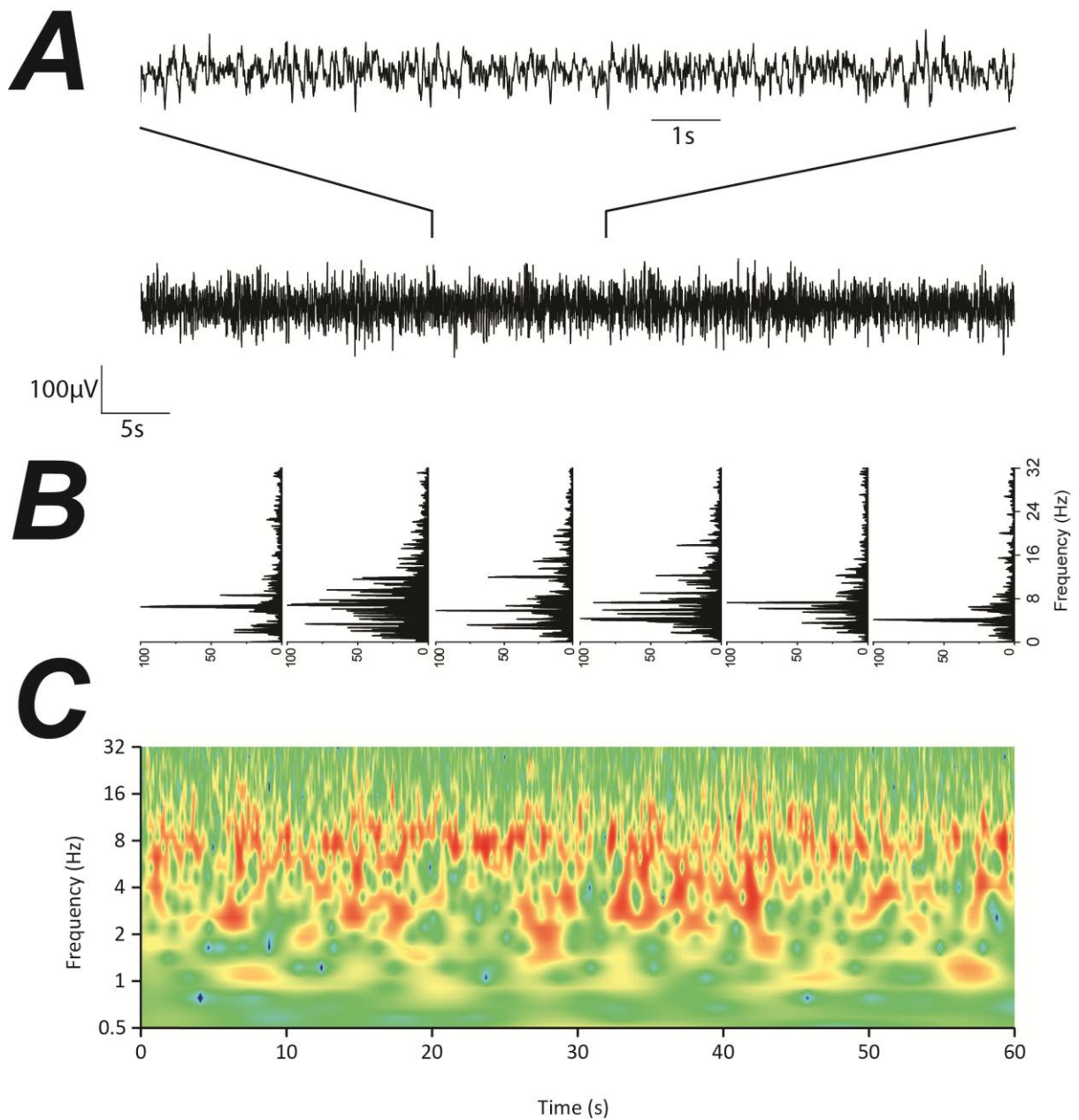
Figure 3.1 Morlet wavelet analysis provides much greater time resolution compared to fast fourier transform.

A. A sixty second EEG recording from a conscious active rat (lower pane) with a 12s segment highlighted to show the detail (upper pane). The waveform consists of fairly uniform amplitude waves that are at a fast frequency **B**. FFT power spectra displayed in 1024 bins giving a resolution of 0.09766Hz in the frequency domain and 10.24s in the time domain. The peak power frequency is consistently within the theta frequency range although the exact frequency changes between spectra. **C**. A morlet wavelet power spectrum of the same 60s EEG recording. The theta rhythm is still the predominant frequency within the waveform, however note that it is not continuous within the time domain, but fragmented. Note also that the fragmentation of the rhythm is shown in better time resolution than for the FFT power spectra.

3.2 Recording EEG during transitions into anaesthesia

Recent studies in humans and rodents arrive at different conclusions regarding the relative importance of the thalamus and cortex for the transition into unconsciousness (Gervasoni *et al.*, 2004; Hwang *et al.*, 2010; Magnin *et al.*, 2010; Velly *et al.*, 2007). Furthermore, many investigations into the EEG effects of anaesthetics use steady state rather than dynamic measurements (Bol *et al.*, 1997; Jugovac *et al.*, 2006). To address the question of how brain dynamics change during transitions into anaesthetic induced unconsciousness, EEG measurements were made from adult male rats during loss of righting reflex (LORR) induced by propofol, dexmedetomidine and midazolam.

Classically, the simplest way to record the electrical activity in the rodent brain is from extradural screws placed on the skull. This gives a global measure of cortical activity. In order to measure transitions from wakefulness into unconsciousness during natural sleep and anaesthesia, screws were placed in the skull and EMG electrode wires imbedded in the trapezius muscles of the neck.

Animals were maintained on a 12:12hr light:dark cycle with the light period starting at 19:30. Anaesthetic experiments were conducted in a continuously rotating cylinder to determine the exact time point of LORR (Figure 2.2c Anaesthetic drugs were delivered intravenously via a subcutaneous implanted venous access port. Propofol and midazolam were delivered at 10 mg/kg/min until the point of LORR, dexmedetomidine was delivered at 20 µg/kg over 60s. All LORR experiments were conducted during the dark period.

3.2.1 Characterising conscious activity in the EEG

In order to determine the effects of various anaesthetics and natural sleep on the EEG, it was first necessary to determine the EEG signature for conscious activity. At the start of each LORR experiment, a conscious baseline was recorded from each animal before starting drug infusion. This was done in the cylinder whilst rotating at 5rpm. Figure 3.2a shows a typical EEG trace from a conscious unrestrained rat (upper trace) and the corresponding EMG lower trace. The EEG and EMG waveforms are fairly regular in amplitude and frequency. Figure 3.2b shows a normalised average of conscious EEG recordings from 15 animals over 60s. The predominant frequency in the EEG is a theta rhythm of 7 Hz with some lower power delta oscillations at 3-4Hz. Figure 3.2c shows an averaged Morlet power spectrum for the same conscious EEG recordings (n=15). This shows the peak power to be a theta rhythm with bursts delta oscillations. Given that type I theta occurs during conscious movement (Kramis *et al.*, 1975), it is possible that these delta bursts are from momentary lapses in movement within the cylinder. This behaviour was observed, but could not be accurately correlated to the frequency changes.
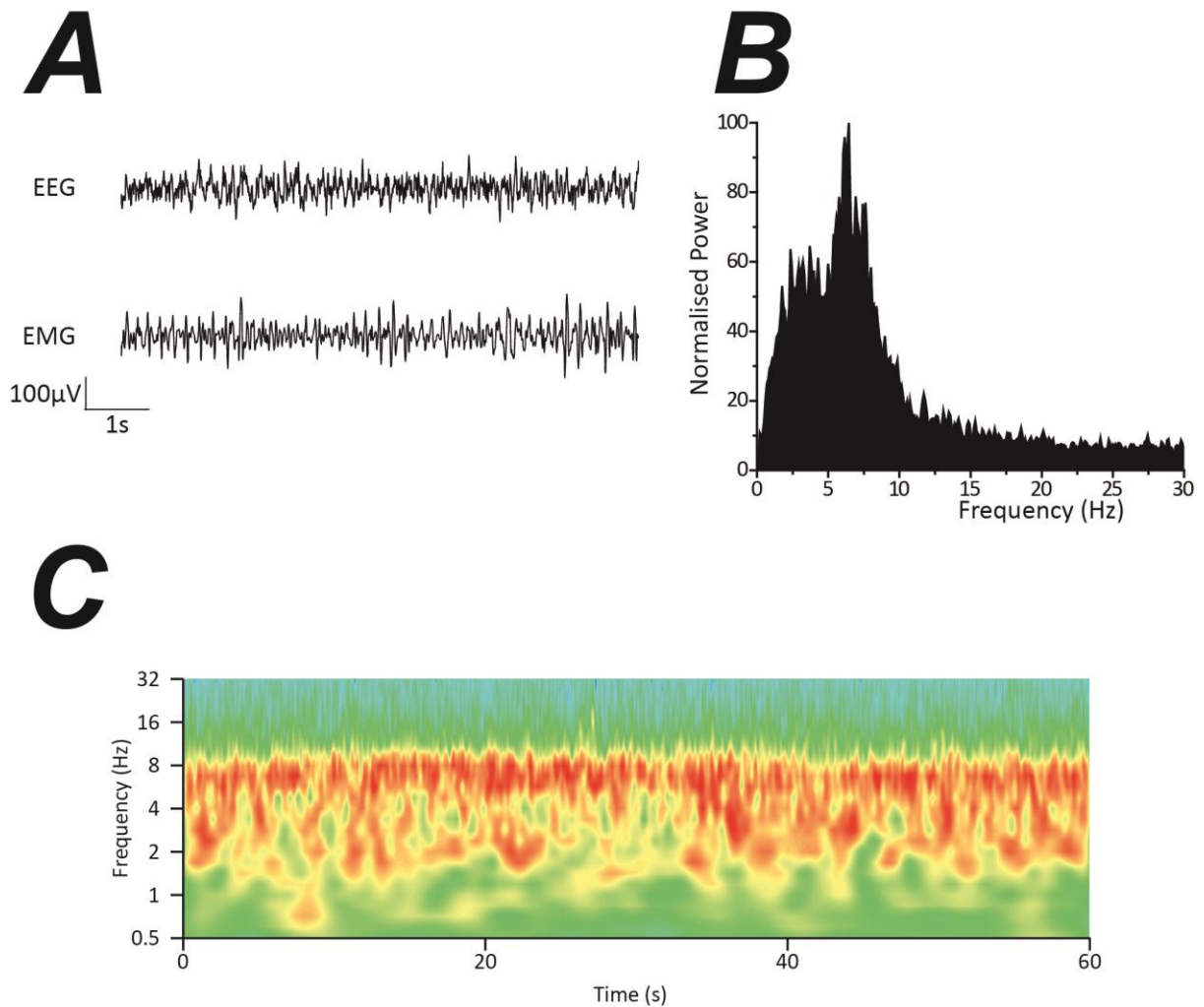
Figure 3.2 Conscious EEG recording taken during active wakefulness in the rotating cylinder
A. Conscious recordings in the rat are characterised by a theta rhythm of low amplitude fast frequency in the EEG and high amplitude in the EMG. The EEG has a regular appearance in frequency and amplitude. **B**. Normalised power spectrum of 15 recordings of conscious EEG. The power spectrum shows that peak power of the theta rhythm is 6-7Hz. This is consistent with a type I exploratory theta rythym as the rat is constantly moving within the rotating cylinder. **C**. The Morlet power spectrum of averaged data demonstrates that theta is the predominant rhythm during wakefulness, although paroxysms of delta (2-5Hz) occur (n=15).

3.2.2   Dexmedetomidine LORR

The α_2 adrenoreceptor agonist dexmedetomidine is well documented for producing delta oscillations and spindles in man and rodents (Bol *et al.*, 1997; Huupponen *et al.*, 2008). It produces LORR via the α_{2a} adrenoreceptor (Lakhlani et al., 1997) which has limited expression within the brain (Nicholas et al., 1993) and was therefore employed as a site-selective drug to investigate drug-induced loss of consciousness. LORR was conducted in a continuously rotating cylinder and dexmedetomidine infused intravenously at 20µg/kg over 60s. The time taken to LORR from the start of the infusion was 87.8 ± 24.7s (mean ± s.e.m., n=9) and in all cases LORR occurred after the infusion was finished. Figure 3.3a shows a typical EEG trace from a rat during dexmedetomidine LORR. Prior to LORR the EEG amplitude is small and LORR is associated with a sustained increase in EEG waveform amplitude. Note the transient increase in amplitude of the EEG at 11s which is commonly found just prior to LORR. Figure 3.3b shows the averaged Morlet power spectrum of EEG data recorded during dexmedetomidine LORR (n=9). Drug infusion was completed before the 0 time point for all animals, thus the entire spectrogram shows data recorded in the presence of dexmedetomidine. Compared to the conscious data in Figure 3.2, there appears to be greater high power across the whole spectrum. This is largely due to the peak power being at lower frequency as the frequency scale is harmonic, not linear. A prominent delta oscillation is established prior to LORR and at the point of LORR, the frequency shifts to a lower value. Note the brief events in the spindle frequency range which start prior to LORR and reach a maximum in event frequency at the point of LORR. Figure 3.3c shows the paired results of the frequencies from each recording immediately before and after LORR (n=9). Power spectra were generated by FFT from with a bin size of 512 for 2.56s either side of the determined LORR point. This was the greatest time resolution possible for a bin size of 512 given the data sampling frequency of 200Hz. The frequencies with the highest power in each case were compared. The frequencies of peak power before and after LORR were in the delta (1-5Hz) band for all cases. The average frequency prior to LORR (3.0 ± 0.7Hz) was significantly greater than for after LORR (1.9 ± 0.4Hz) ($p<0.01$ paired Student's t-test) and in all cases, there was a reduction of frequency following LORR. No significant changes in delta oscillation were seen during the 30s prior to or 30s after LORR, only frequency change within delta was observed at the point of LORR.
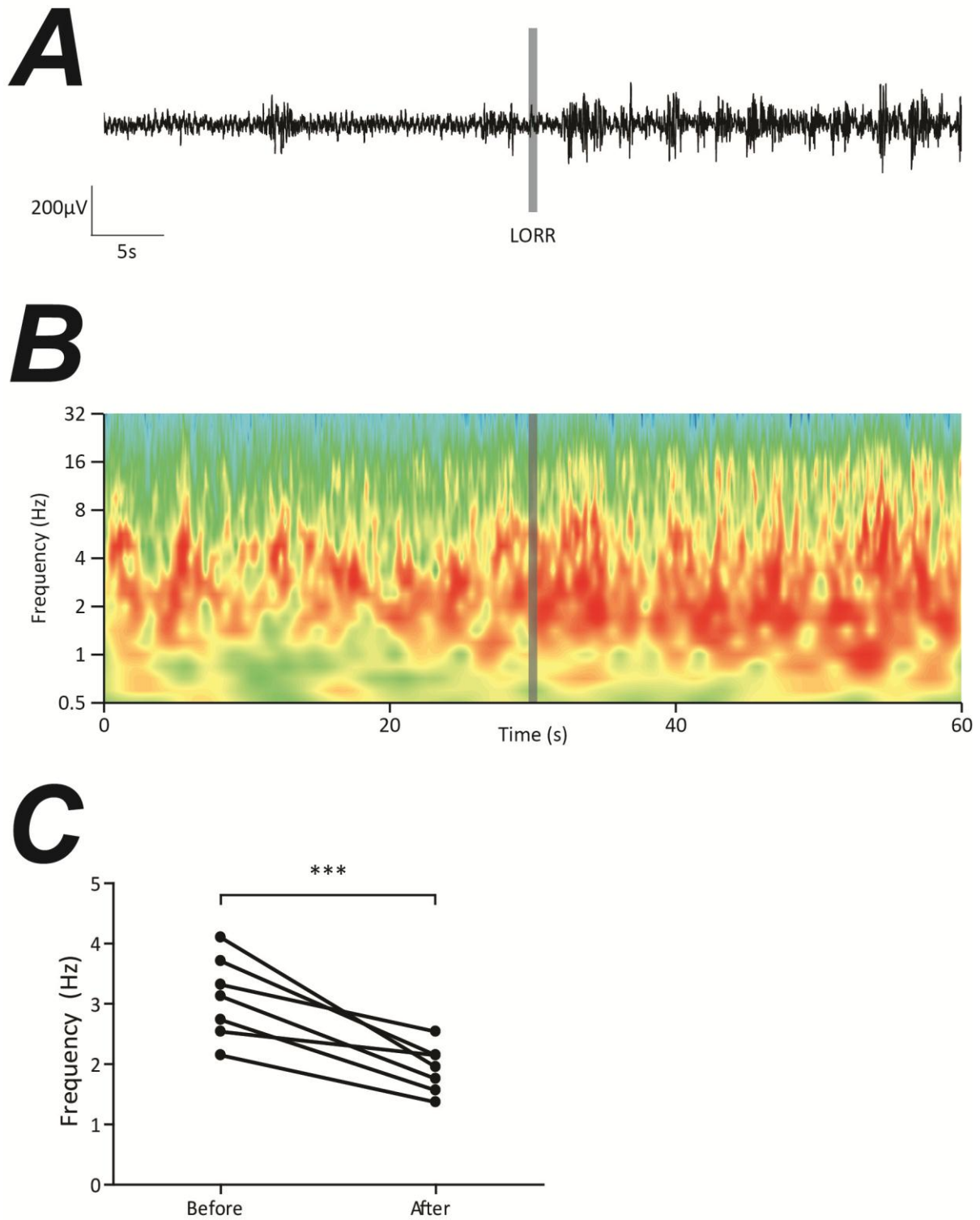
Figure 3.3 Dexmedetomidine LORR is associated with a delta frequency shift at LORR.
A. A typical EEG trace from a rat during dexmedetomidine LORR. At the point of LORR there is a large increase in amplitude of the waveform. **B**. A Morlet power spectrum of an average of 9 dexmedetomidine LORR recordings. Intravenous infusion of dexmedetomidine results in delta oscillations dominating the EEG prior to LORR. At the point of LORR there is a shift in the delta frequency and an increase in power. **C**. The frequencies of the peak delta power immediately (2.56s) prior to LORR (3.0 ± 0.7Hz) are significantly higher than immediately following LORR (1.9 ± 0.4Hz) (p<0.01 paired t-test). No significant changes in peak power frequency were found from 0 to 28s or 32-60s, thus the significant frequency changes occurred at LORR.

3.2.3 Propofol LORR

The GABA$_A$ modulator propofol has been shown to increase delta power in the EEG of rats (Jugovac *et al.*, 2006; Kuizenga *et al.*, 2001) and has been postulated to have a preferential effect on the cortex in humans (Velly et al., 2007). Moreover propofol has also been shown to produce spindles and have both NREM and REM-like EEG characteristics (Leslie et al., 2009). LORR was conducted in a continuously rotating chamber with intravenous infusions of propofol at 10 mg/kg/min until LORR was achieved. The mean dose required to achieve LORR was 11.1 ± 2.2 mg/kg (n=5). Figure 3.4a shows a typical EEG recording for 60s around propofol LORR. There is a moderate increase in the waveform amplitude immediately following LORR which is sustained for around 15s before reducing again. Note the increased amplitude of the waveform prior to LORR compared to the same period in dexmedetomidine recordings (Figure 3.3a). Figure 3.4b shows the averaged Morlet power spectrum for EEG data recording during LORR with propofol (n=5). The mean time to LORR from the start of infusion was 66s, thus the whole spectrogram shows recordings in the presence of propofol. In contrast with dexmedetomidine, propofol does not produce a substantial delta oscillation prior to LORR. At the beginning of the power spectrum, a theta rhythm of 7-8Hz can be seen. Continuous infusion of propofol reduces the frequency of this oscillation so that it becomes continuous and indistinct from the delta oscillation. At the point of LORR there is a moderate reduction in the delta frequency and an increase in delta power immediately following LORR. Note that prior to LORR events start occurring in the spindle range which increase in event frequency and decrease in waveform frequency to stabilise at LORR. Whilst the event frequency is similar to that seen with dexmedetomidine, the frequency of individual spindles mirrors the theta to delta ramp. Figure 3.4c demonstrates the delta frequency shift and is calculated in the same manner as for dexmedetomidine. There is a significant change in delta frequency across the point of LORR from 3.9 ± 0.4Hz prior to LORR to 2.5 ± 0.9Hz after LORR ($p<0.05$ Student's paired t-test). In all cases there was a reduction in frequency following LORR.
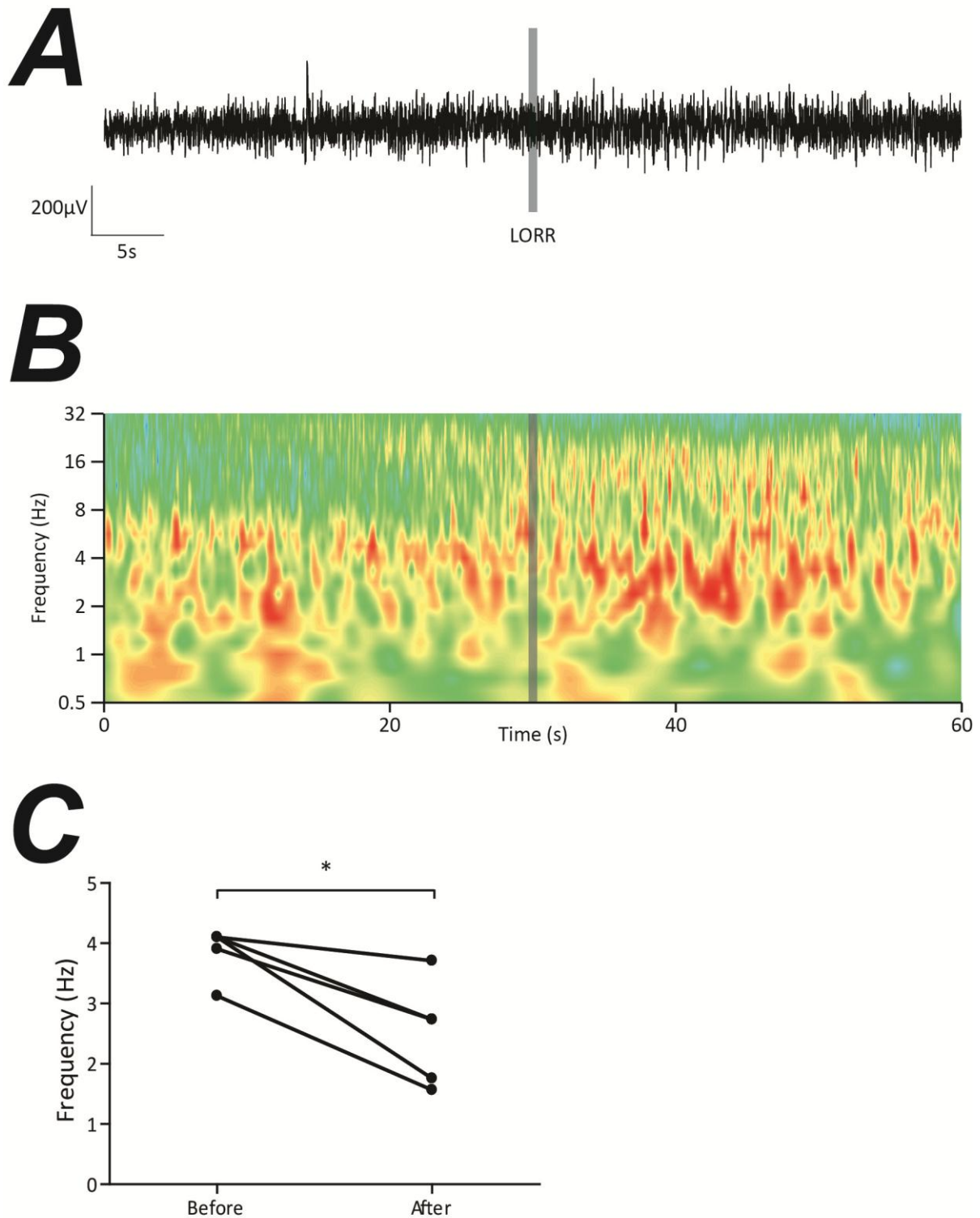
Figure 3.4 Propofol LORR is associated with a delta frequency shift at LORR.
A. A typical EEG trace from a rat during propofol LORR. At the point of LORR there is a small increase in amplitude of the waveform. **B**. A Morlet power spectrum of an average of 5 propofol LORR recordings. Intravenous infusion of propofol results in the theta oscillation of wakefulness reducing in frequency to the delta range. At the point of LORR the delta frequency plateaus. Note also how oscillations in the gamma range follow a similar pattern to result in a spindle frequency. **C**. The frequencies of the peak delta power immediately prior to LORR (3.9 ± 0.4Hz) are significantly higher than immediately following LORR (2.5 ± 0.9Hz) (p<0.05 paired t-test). No significant changes in peak power frequency were found from 32-60s.

3.2.4   Midazolam LORR

Midazolam is also a $GABA_A$ modulator which has been shown not to increase delta power in the EEG of rats but instead increases alpha and beta power and produces spindles (Feshchenko *et al.*, 1997; Jugovac *et al.*, 2006). Given the lack of delta power increase produced by midazolam, it was used as a comparison to dexmedetomidine and propofol as an anaesthetic which may not be recruiting the thalamocortical system to induce unconsciousness. LORR was conducted in a continuously rotating chamber with midazolam infused at 10 mg/kg/min until LORR was achieved. The average dose required to induce LORR was 9.7 ± 1.9 mg/kg (n=6). Figure 3.5a shows a typical EEG recording for a 60s EEG recording around midazolam LORR. There is an increase in the waveform amplitude although this does not occur in a sustained manner until 10-15s after LORR. Note that the amplitude of the conscious part of the waveform is similar to propofol and in contrast to dexmedetomidine. Figure 3.5b shows the averaged Morlet power spectrum for EEG data recording during LORR with midazolam (n=6). As with dexmedetomidine, midazolam produces a dominant delta oscillation prior to LORR. At LORR there are no discernible frequency shifts as with dexmedetomidine and an increase in power in the delta band do not occur until 10-15s after LORR. Note the events in the spindle frequency range which occur predominantly after LORR and reach a maximal event frequency at the same time as the increase in delta power. Figure 3.5c shows the peak power delta frequencies immediately before and after LORR. The mean frequency before LORR was 2.3 ± 0.6Hz and 2.3 ± 1.5Hz immediately after LORR (p>0.1 Student's paired t-test).
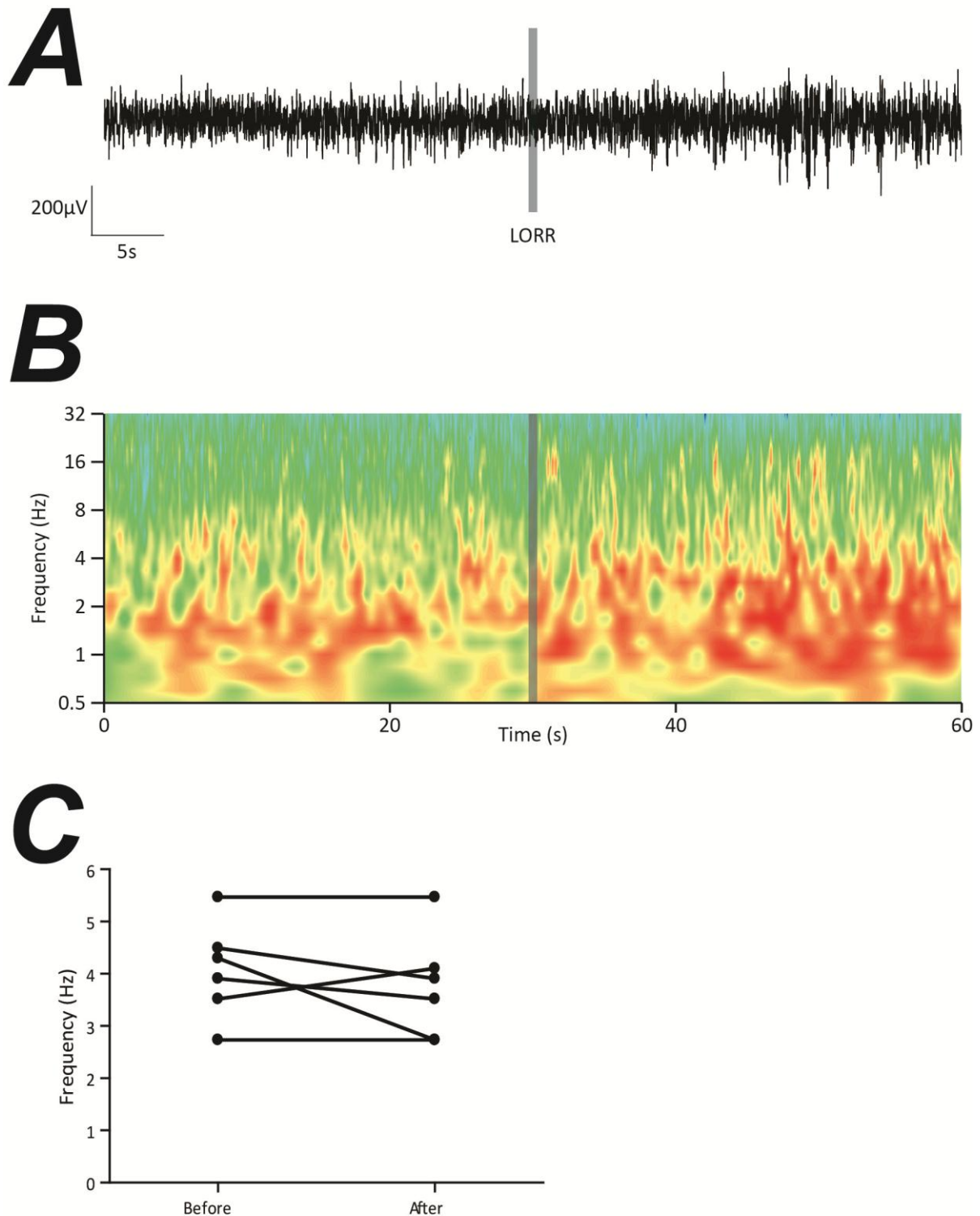
Figure 3.5 Midazolam LORR is not associated with a delta frequency shift at LORR.
A. A typical EEG trace from a rat during midazolam LORR. There is an increase in amplitude of the waveform 15 seconds after LORR. **B**. A Morlet power spectrum of an average of 6 midazolam LORR recordings. Intravenous infusion of midazolam results in delta oscillations dominating the EEG prior to LORR. No discernible spindles are observed in the EEG at the point of LORR. The change in power and peak power frequency can be seen 10-15s after LORR**. C**. The frequencies of the peak delta power immediately prior to LORR (2.3 ± 0.6Hz) are not significantly different than immediately following LORR (2.3 ± 1.5Hz) (p>0.1 paired t-test).

3.3 Recording EEG during transitions into natural sleep

Numerous previous studies have investigated EEG correlates of sleep although few have investigated dynamic transitions from wakefulness into natural sleep (Magnin et al., 2010). This study in humans showed that changes in the EEG occurred slowly and for a variable amount of time after subjects were deemed to have fallen asleep. Natural sleep shares many of electrophysiological characteristics of anaesthesia and there is evidence that it may also share some of the neural pathways (Franks, 2008; Nelson *et al.*, 2003). Wake-to-sleep transitions were investigated to see how similar the electrophysiological processes were to anaesthesia.

3.3.1 Characterisation of natural sleep

In order to investigate transitions from wakefulness into sleep it was first necessary to characterise REM and NREM in the EEG. Active wakefulness has already been characterised in figure 3.2. Rats were chronically instrumented with skull screw electrodes. Natural sleep was recorded in the home cage during the light period (19:30 to 7:30).

Figure 3.6a shows a typical EEG and EMG trace from a rat in NREM sleep. The EEG has a marked increase in amplitude compared to wakefulness and the EMG has very small amplitude. Closer inspection of the EEG reveals that the waveform is composed of two main oscillations. Spindles are shown in red and occur at regular intervals, the rest of the waveform in black has a delta frequency. Figure 3.6b shows the normalised averaged FFT power spectrum of 15 separate recordings of NREM sleep. NREM is dominated by delta oscillations with peak power at 3-4Hz. A smaller peak at 12Hz can be seen and represents spindles. Figure 3.6c shows the averaged Morlet power spectrum for the same 15 NREM recordings. Delta is the dominant frequency although theta and spindles are also evident. Note how k-complexes of the slow oscillation are not represented on the power spectrum in the <1Hz range.

Figure 3.7a shows a typical EEG and EMG trace from a rat during REM sleep. The EEG has a very uniform frequency and amplitude in comparison to NREM and wakefulness and the EMG is quiescent. The amplitude of the EEG is comparable to the waveform produced during wakefulness. Figure 3.7b shows the normalised averaged FFT power spectrum of 15 REM recordings. The power spectrum has a sharply tuned theta peak at 7-8Hz with little other frequency contribution to the power spectrum. The theta frequency of REM sleep is higher than during wakefulness. Figure 3.7c shows the averaged Morlet wavelet power spectrum for the same 15 REM recordings. There is only one band of high power which is continuous and there are no bursts of delta in contrast with wakeful theta.

Figure 3.6 NREM sleep EEG recording

Recordings taken from animals during natural sleep in the home cage during the light period (19:30-7:30) **A.** NREM sleep recordings in the rat are by delta oscillation (2-5Hz) dominated in the EEG and low amplitude in the EMG. Spindles are highlighted in red. Note the relative heterogeneity of the waveform when compared to conscious and REM recordings. **B**. Normalised power spectrum for 15 recordings of NREM EEG. The power spectrum shows that peak power of the delta rhythm is 3-4Hz. **C**. The Morlet power spectrum of averaged data demonstrates that delta is the predominant rhythm during NREM sleep although theta does occur and higher frequency oscillations are consistent with spindles (10-16Hz) (n=15).

Figure 3.7 REM sleep EEG recording
Recordings taken from animals during natural sleep in the home cage during the light period (19:30-7:30) **A.** REM sleep recordings in the rat are characterised by a theta rhythm in the EEG and an atonal EMG. Note how the waveforme for REM is highly uniform in both frequency and amplitude when compared to NREM and conscious recordings. **B.** Normalised power spectrum of 15 EEG recordings during REM sleep. The power spectrum shows that peak power of the theta rhythm is 7-8Hz consistent with a type I theta rythym. **C**. The Morlet power spectrum of averaged data demonstrates that theta is the only rhythm found during REM sleep (n=15), the theta rhythm is also continuous unlike the fragmented theta rhythm of consciousness.

3.3.2 Wake to NREM transitions

The only previous study to investigate dynamic transitions into natural sleep investigated entropic changes over prolonged periods in humans (Magnin et al., 2010). To investigate the fine detail of wake to sleep transitions, the sleep recordings were scored by a predefined algorithm based on work by Costa-Miserachs et al (2003) (see Methods). Sixty second segments of recordings were analysed by Morlet wavelet analysis, to show changes from wakefulness into NREM sleep. Figure 3.8a shows typical EEG and EMG recordings for Wake-to-NREM transitions. The EEG has a low amplitude as shown previously (Figure 3.2a) for active consciousness prior to the onset of sleep. The EMG has corresponding large amplitude. Prior to the onset of NREM, the amplitude of the EMG decreases to reach basal amplitude at the onset of sleep. The EEG however shows no significant changes in amplitude until the onset of sleep whereupon there is a sharp sustained increase in waveform amplitude. Figure 3.8b shows the averaged Morlet power spectrum of 9 wake-to-NREM transitions. The wake phase shows a fragmented theta rhythm with paroxysms of low powered delta as seen in active wakefulness. At the onset of sleep there is a sudden change in the frequency component to a mixed frequency range dominated by delta but containing theta and spindle frequencies.
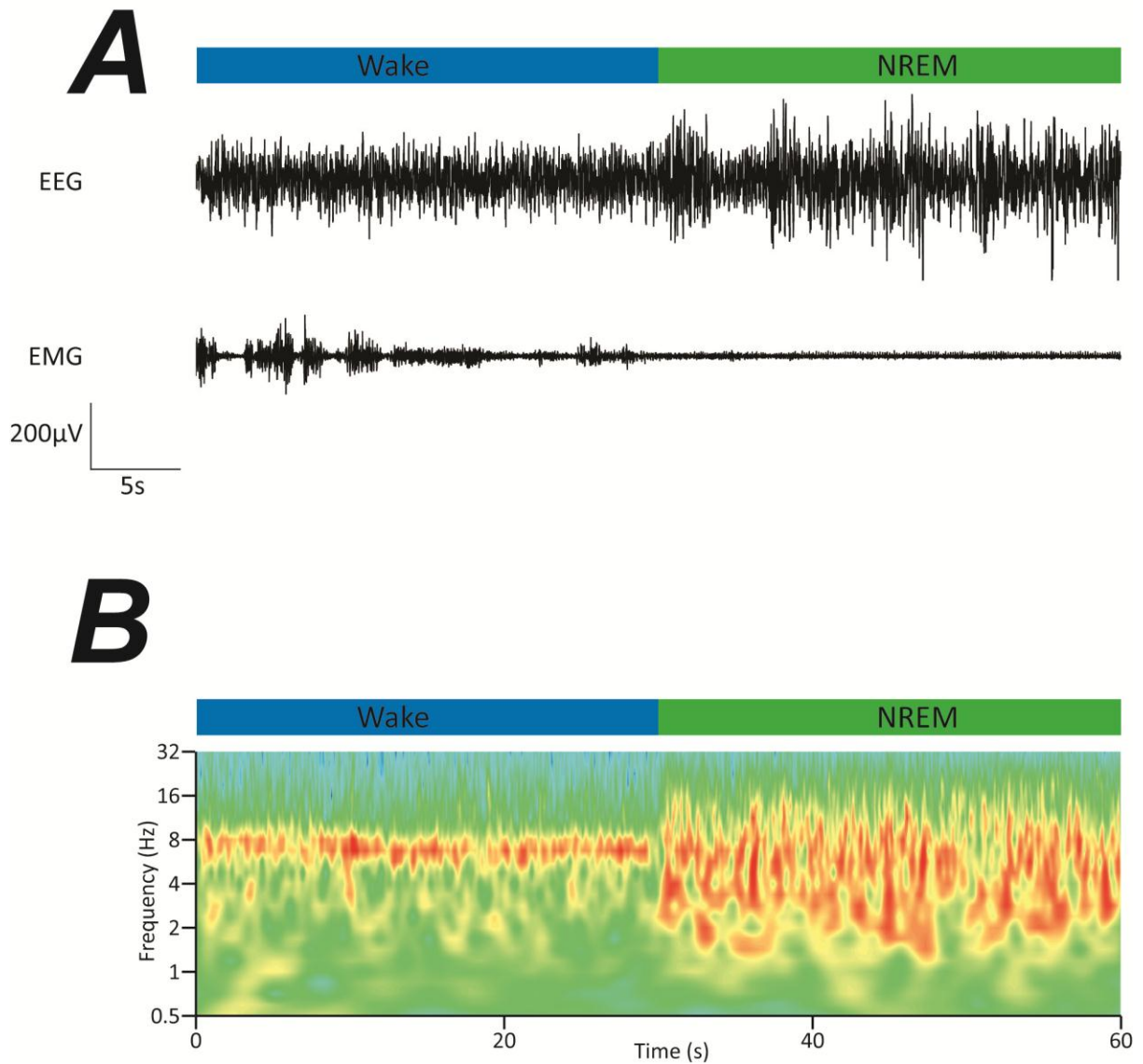
Figure 3.8 Transitions from wakefulnuss into NREM sleep are characterised by abrupt EEG changes from theta to delta

Recordings taken from animals during natural sleep in the home cage during the light period (19:30-7:30) **A.** The EEG waveform changes from a low amplitude theta rhythm to high amplitude mixed oscillation domintated by delta wave at a sudden transition point. The EMG tone tapers to a low amplitude several seconds before the onset of the high amplitude EEG waves. **B**. Morlet power spectrum of the average of 9 wake to NREM transitions. In the 30 seconds prior to NREM onset, the EEG is dominated by a theta oscillation with paroxysmal delta as seen during active wakefulness. At the onset of NREM sleep there is a rapid transition to a delta dominated oscillation with some theta and spindles also seen.

3.3.3 NREM to Wake transitions

Whilst there are still no encompassing mechanisms proposed for loss of consciousness in natural sleep, some theories are based on the premise of a hypothalamic "flip-flop switch" (Saper et al., 2001). Given that the EEG in wake-to-NREM transitions appears to behave as an instantaneous switch, the reverse transition from NREM to Wake was investigated. Figure 3.9a shows typical EEG and EMG recordings for NREM to Wake transitions. Prior to waking, the EEG has a variable but large amplitude compared with the awake phase which follows. The EMG has low amplitude prior to waking then slowly increases in amplitude afterwards. The EEG however shows a sharp change in amplitude at waking and thereafter the amplitude is stable. Figure 3.9b shows the averaged Morlet spectrum for 9 NREM to Wake transitions. In the 30s prior to waking, the frequency pattern is the same as for the onset of NREM. Similarly, at the onset of wakefulness there is an abrupt transition to a conscious theta rhythm with paroxysmal delta oscillations, as seen during active wakefulness.
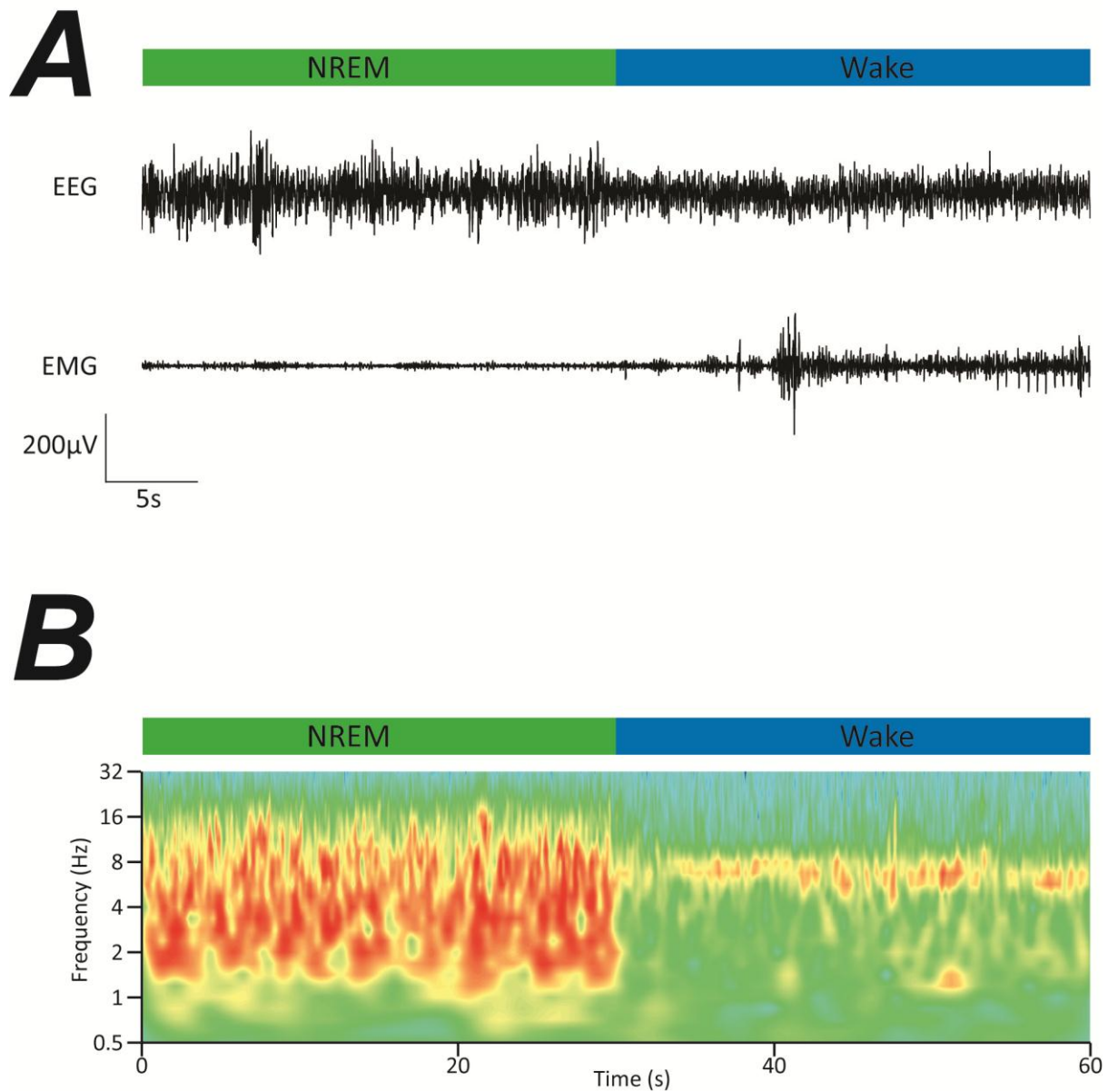
Figure 3.9 Transitions from NREM to wakefuleness are characterised by and abrupt EEG changes from delta to theta.
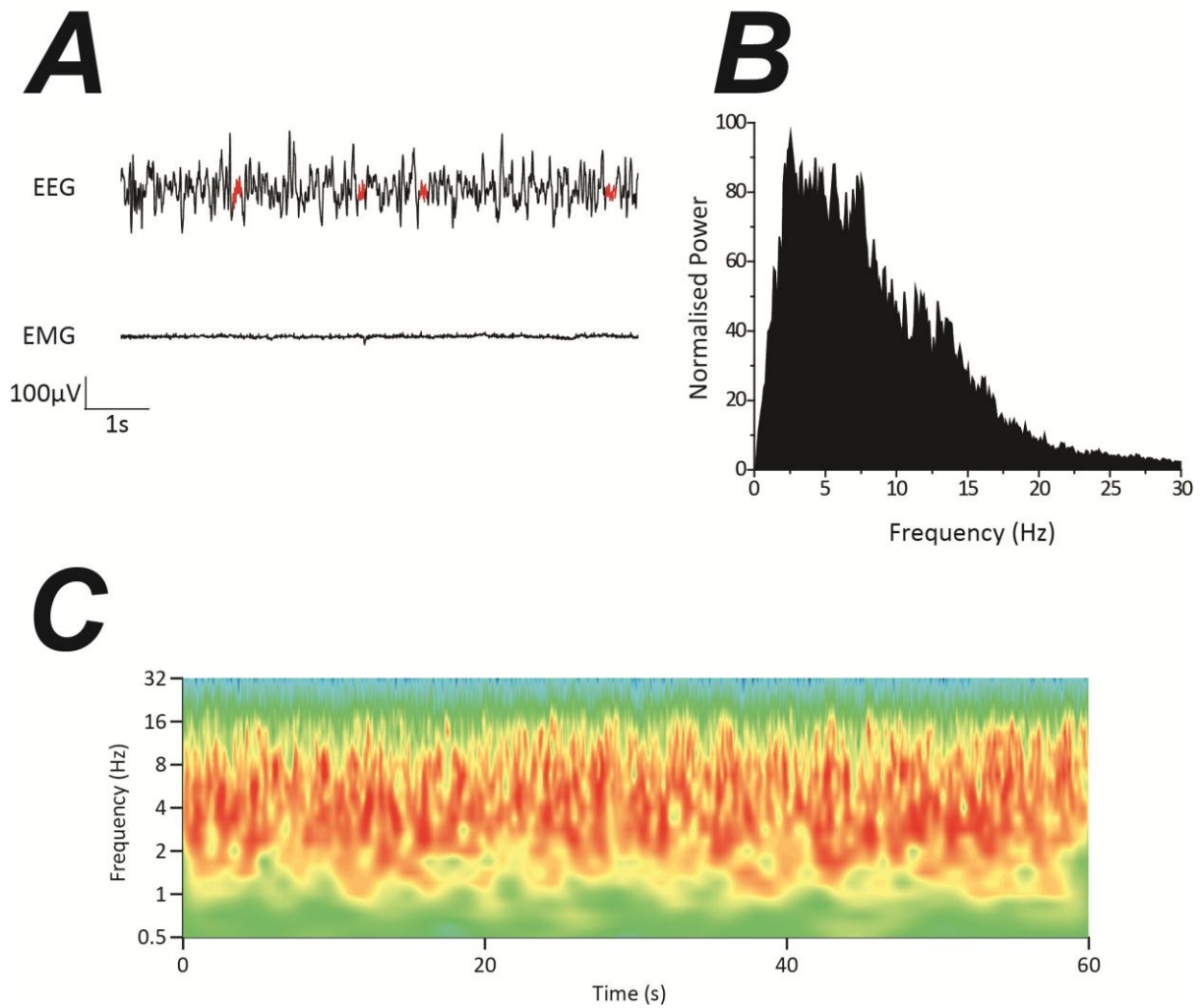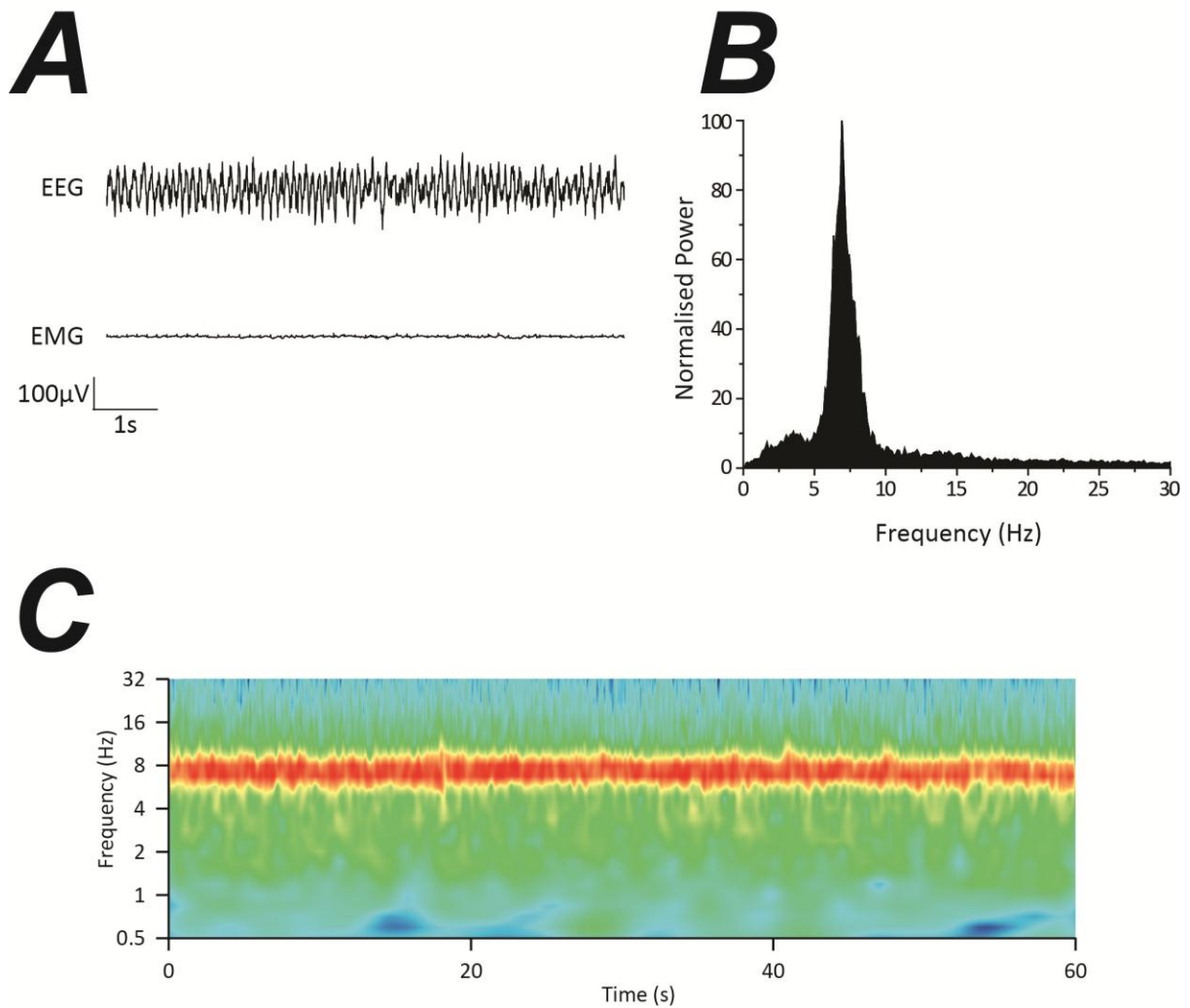Recordings taken from animals during natural sleep in the home cage during the light period (19:30-7:30) **A.** The EEG waveform changes from a slow frequency high ampitude rhythm to a lower amplitude, faster rhthym at a sudden transition point. The increase in EMG tone does not occur until several seconds after the transition and tapers from low amplitude to a maximum. **B**. Morlet power spectrum of the average of 9 NREM to wake transitions. In the 30 seconds prior to wakefulness, the EEG is dominated by a mixed freqency oscillation dominated by delta. At the onset of wakefulness, there is a rapid transtition to a theta rhythm indistinguishable to that seen during active wakefulness. The theta is of the same 6-7Hz in frequency and is fragmented with bursts of delta.

3.4 Thalamic activity during anaesthetic LORR

Given that LORR by propofol and dexmedetomidine and also transitions from Wake to NREM resulted in abrupt alterations in delta at the point of LORR, the electrical activity of the thalamus was investigated. Isolated sections of thalamus *in vitro* have been shown to exhibit delta oscillations (Leresche *et al.*, 1990) as have decorticated thalamic cells *in vivo* (Dossi *et al.*, 1992) and are considered to be the source of the delta oscillation. Several recent studies of thalamic activity around loss of consciousness have given conflicting theories about the timing of thalamic deactivation in sleep and anaesthesia (Gervasoni *et al.*, 2004; Hwang *et al.*, 2010; Magnin *et al.*, 2010; Velly *et al.*, 2007). Rats were chronically instrumented with EEG skull electrodes and depth electrodes in the thalamus. Recent evidence suggests that the central medial thalamus (CMT) may have an important role in regulating consciousness (Alkire *et al.*, 2009; Alkire *et al.*, 2007). To this end, electrodes were implanted in the CMT with a reference electrode in the ventral portion of the medial geniculate nucleus of the thalamus (GMv) and the resulting field potential from the thalamus (EThG) recorded.

3.4.1 Dexmedetomidine LORR

Dexmedetomidine LORR was performed as described in section 3.1.3. The mean time to LORR following the start of infusion was 91 ± 11.4s (n=3). Figure 3.10a shows the averaged Morlet power spectra for the EEG and EthG (n=3 each). The EEG follows the same pattern as previously described for dexmedetomidine LORR, of a delta dominated oscillation with a shift in frequency at the point of LORR. The thalamus shows a similar pattern in frequency shift. Note also that the thalamus has a concurrent theta rhythm which also switches frequency at LORR in harmony with delta. Figure 3.10b shows the averaged cross wavelet transform of the EEG and the EThG. The highest correlation between the signals is in the delta region before and after LORR. Note that there is only correlation in the theta band prior to LORR but there is positive correlation in the spindle frequency range following LORR. Figure 3.10c shows the phase coherence spectrum of the EEG in relation to the EThG. Prior to LORR, the EThG waveform is $\pi/2$ ahead of the EEG in the theta and delta bands. Following LORR this phase coherence shifts to become antiphase.
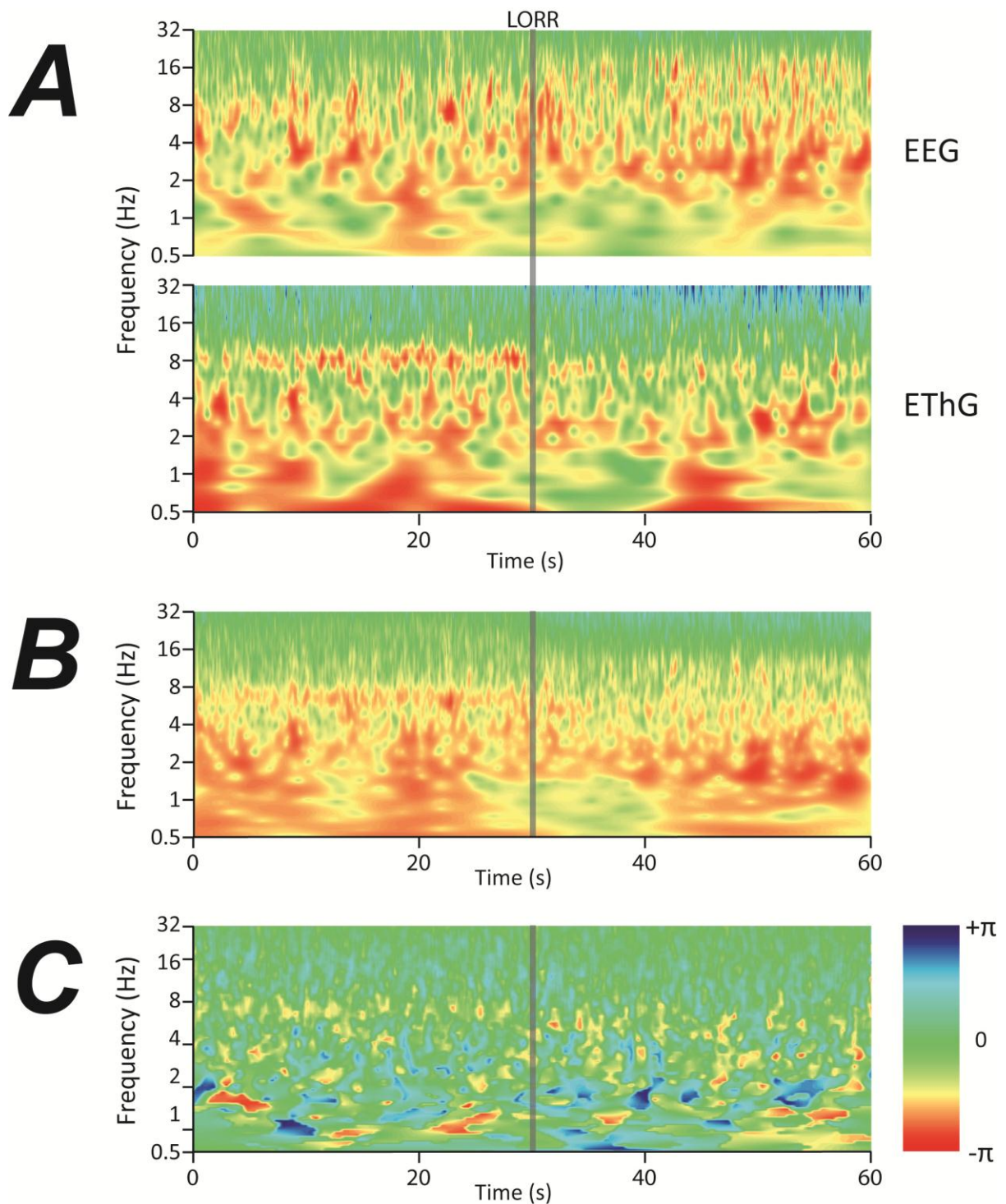
Figure 3.10 Loss of righting reflex induced by dexmedetomidine is associated with a delta frequency transition in the thalamus.

A. Averaged morlet power spectra (n=4) for both EEG and EthG. In both cases there is a prominent delta rhythm prior to LORR which switches to a lower frequency at LORR. Note the increase of events in the spindle frequency range increasing to a maximum at LORR. LORR is marked by the grey line at 30s. **B**. Averaged cross wavelet transform for the same data as in A. The frequency domains sharing high power are in the delta range before and after LORR. **C.** Averaged phase coherence spectrum for the same data as in A. Before LORR the phase is –π/2, i.e.: the thalamus waveform is 90° in front of the cortex as indicated by the yellow sections to the left of the spectrogram. After LORR there is a predominance of phase shift towards –π, i.e.: the thalamus and EEG are in antiphase where there is an increase in the red components on the right of the spectrogram.

3.4.2 Propofol LORR

Propofol LORR was performed as described in section 3.1.4. The mean dose required for LORR was 10.5 ± 1.9 mg/kg (n=4). Figure 3.11a shows the averaged Morlet power spectra for the EEG and EThG. The EEG follows the pattern previously described. Interestingly the EThG closely mirrors the EEG pattern of a conscious theta rhythm that reduces in frequency to become continuous with delta. At LORR there is a noticeable switch in the delta frequency and the delta frequency remains stable thereafter. Spindles are also observed in the EthG and like the EEG reduce in frequency prior to LORR and then stabilise in frequency after LORR. Note that in the frequency range of less than 2Hz, the EThG has significantly less high power than the EEG. This may represent increased noise on the EEG recording as the electrodes are more superficial and liable to mechanical artefacts. Figure 3.11b shows the averaged cross wavelet transform for the EEG and EThG. The EEG and EThG correlate highly in the theta to delta ramp and the delta following LORR. There is also positive correlation in the spindle frequency range. Figure 3.11c shows the phase coherence spectrum of the EEG when compared to the EThG. Prior to LORR, in the theta-delta ramp, the EThG waveform is $\pi/2$ radians ahead of the EEG. Following LORR, this phase relationship shifts to antiphase, as with dexmedetomidine.
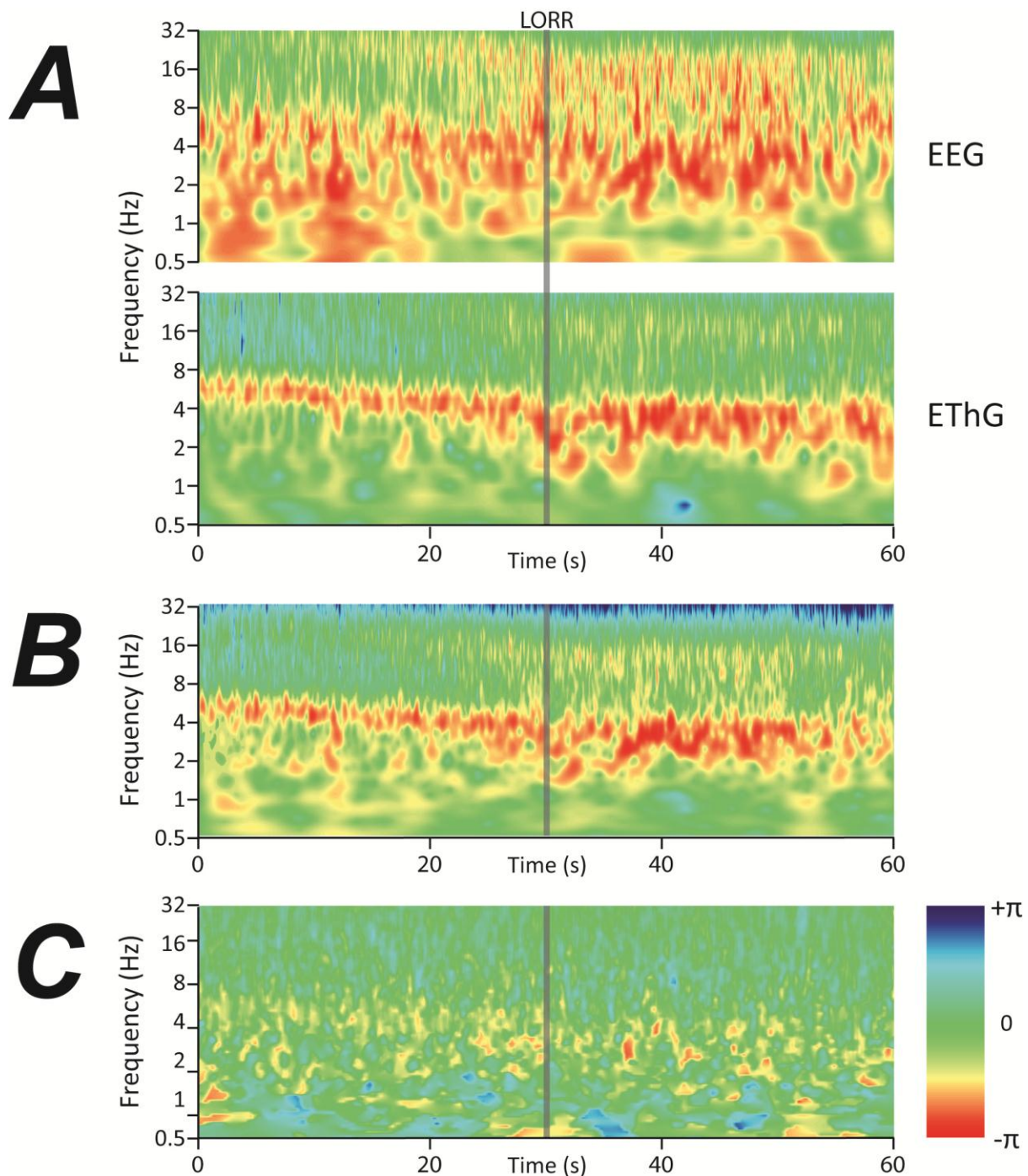
Figure 3.11 Loss of righting reflex induced by propofol is associated with a delta frequency transition in the thalamus.

A. Averaged morlet power spectra (n=4) for both EEG and EthG. In both cases, the waking theta rhythm frequency falls to become continuous with a delta oscillation. In the thalamus at LORR there is a switch in frequency which remains stable in the delta range after LORR. Note the increase of events in the spindle frequency range increasing to a maximum at LORR. LORR is marked by the grey line at 30s. **B.** Averaged cross wavelet transform for the same data as in A. Regions in which the EEG and thalamus share common high power follow the the pattern observed in the thalamus. **C.** Averaged phase coherence spectrum for the same data as in A. Before LORR the phase is −π/2, i.e.: the thalamus waveform is 90° in front of the cortex. cortex as indicated byt the yellow sections to the left of the spectrogram. After LORR there is a predominance of phase shift towards −π, i.e.: the thalamus and EEG are in antiphase where there is an increase in the red components on the right of the spectrogram.

3.4.3 Midazolam LORR

Midazolam LORR was performed as described in section 3.1.5. The mean dose required for LORR was 10.1 ± 1.4 mg/kg (n=3). Figure 3.12a shows the averaged Morlet power spectra for the EEG and EThG. The EEG shows the same pattern as previously. Interestingly, the EThG has little delta power prior to LORR unlike the EEG. A theta oscillation consistent with active wakefulness is present prior to LORR. There is some reduction in frequency, but not to the same extent as propofol. A frequency shift to delta does occur but not until 10-15s after LORR. There is also increase in covariant power at this point. Figure 3.12b shows the averaged cross wavelet transform. The highest common power is in the theta band prior to LORR, which does not alter at LORR. Note the coherence in the spindle band which occurs from 30s prior to LORR, in contrast to propofol and dexmedetomidine. Figure 3.12c shows the phase coherence spectrum of the EEG when compared to the EThG. There are no significant changes in phase correlation either side of LORR in either theta or delta bands.
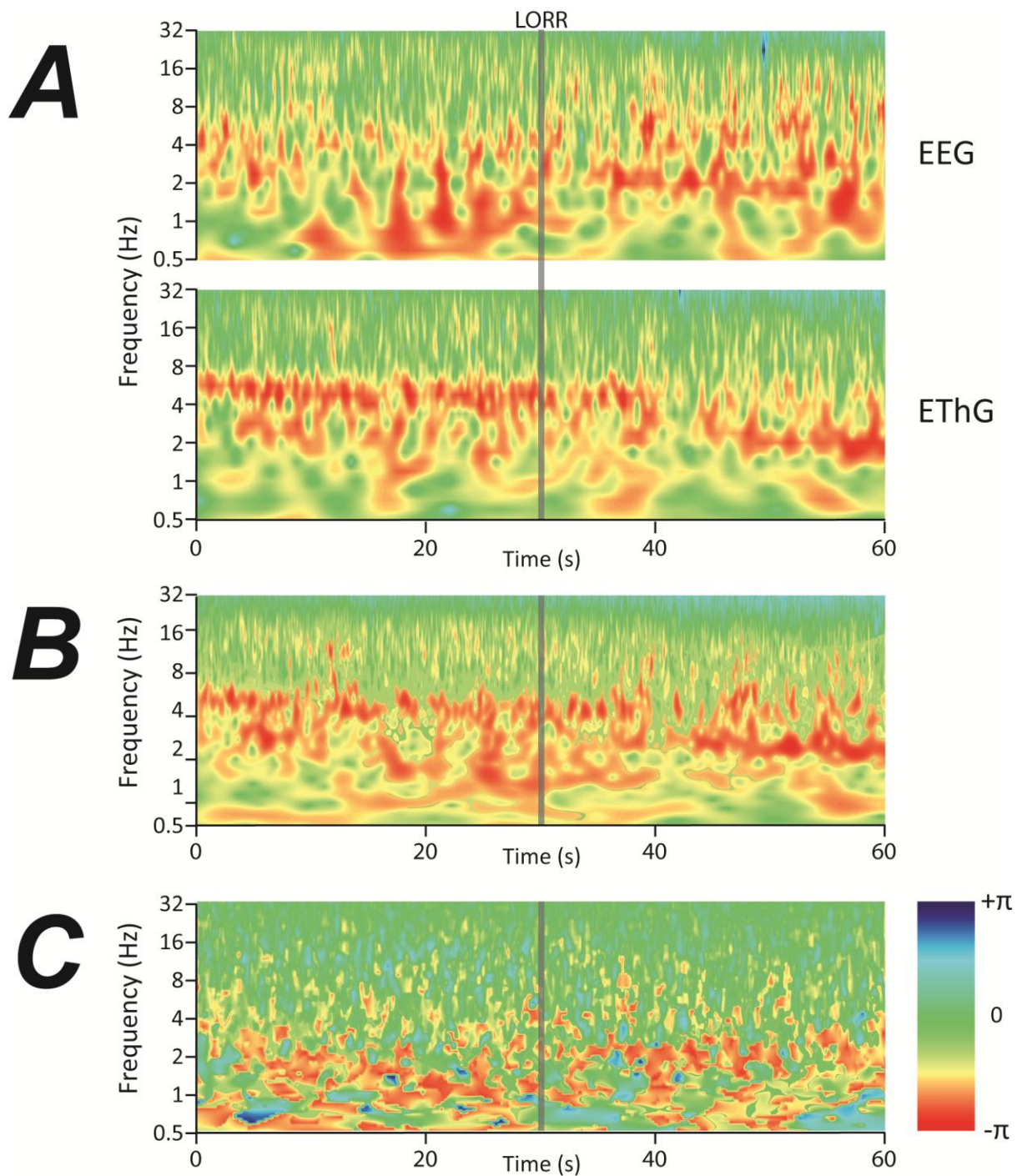
Figure 3.12 Midazolam LORR is not associated witha adelta frequency shift or phase change.
A. Averaged Morlet power spectra for EEG and EthG (n=3). In both cases, there is a delta oscillation before and after LORR. There is no change in frequency either side of LORR. The change in delta oscillation frequency occurs after LORR and is most prominent in the thalamus. LORR is marked by the grey line at 30s. **B.** Averaged cross wavelet transform for the above data. There is a high degree of correlation acorss the delta range both before and after LORR. **C.** Averaged phase coherence spectrum for the same data. For the areas of delta either side of LORR where there is high power coherence the phase is $-\pi/2$ across the entire time span.

3.4.4 Electrode placement verification

Following the end of experimental recordings, brains were fixed by transcardial perfusion with formalin and sliced in 100μm sections to verify the electrode placement. Figure 3.13 shows the placement of the electrode tips based on these slices. Electrodes aimed at the CMT (n=3) were successfully placed. Electrodes aimed at the GMv (n=3) were not successful. One had the tip in the optic tract and the other two were in the lateral geniculate nucleus of the thalamus. No differences between the recordings were observed on this basis.
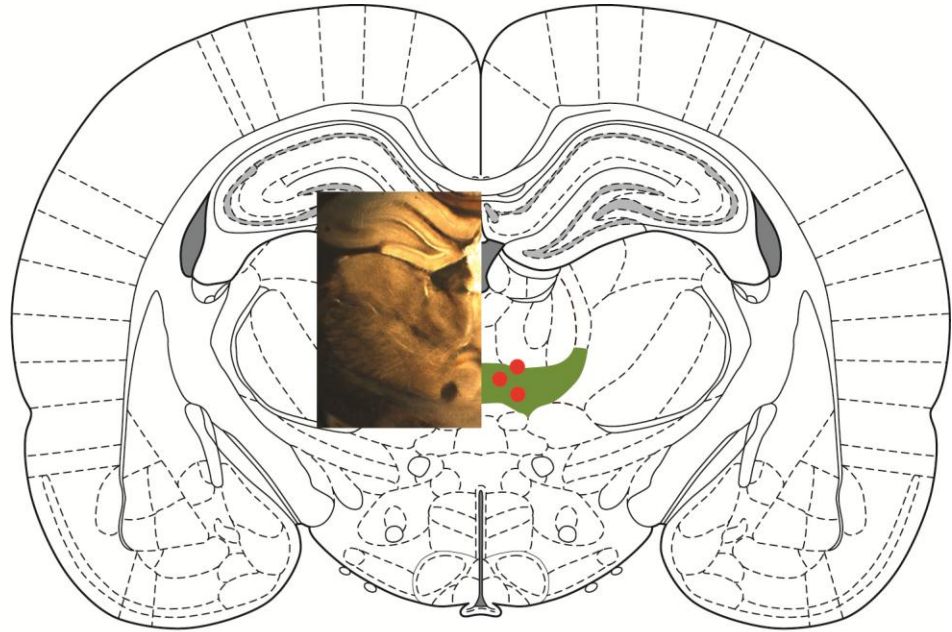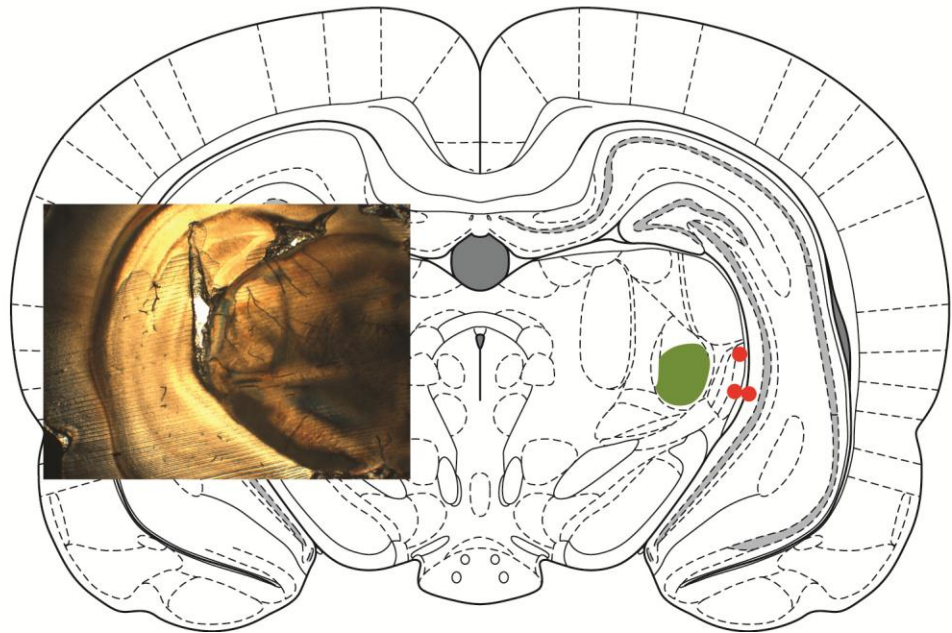
Figure 3.13 Histological verification of electrode placement for EthG.
A. Coronal section of the brain 3.2mm posterior to bregma with imbeded micrograph if histological sample. The central medial thalamus is highlighted in green. The location of the tips of the electrodes from three seperate animals indicated by red markers. **B**. Coronal section of the brain 4.9mm posterior to bregma with imbeded micrograph of histological sample. The ventral portion of the medial geniculate nucleus is highlighted in green. The location of the tips of the three elctrodes from three seperate animals indicated by red markers. Schematic diagrams in A and B reproduced and modified from Paxinos and Watson (2002).

3.5 Correlations of anaesthesia and sleep

Previous observations of sleep and anaesthesia in steady states have shown a high degree of similarity (Franks, 2008). However the results in this chapter suggest that transitions from wake into NREM and anaesthesia are fundamentally different. Sleep appears to onset with a rapid theta to delta switch, whereas anaesthesia with propofol and dexmedetomidine involves a switch within the delta frequency.

Recent clinical studies have shown that patients heavily sedated with dexmedetomidine to give brief responses to auditory stimuli (i.e. remained conscious) had the same EEG characteristics as stage II sleep (i.e. unconscious) (Mason *et al.*, 2009).

To investigate this phenomenon further, the EEG recordings of dexmedetomidine LORR and NREM sleep were investigated. The hypothesis being that following the start of dexmedetomidine infusion but prior to LORR, a theta to delta switch may be present in a similar fashion to that seen at the onset of NREM according to the algorithm used. Similarly, periods of established NREM were analysed for changes in delta frequency as seen at dexmedetomidine LORR.

3.5.1   Delta oscillations in stage I sleep are comparable to dexmedetomidine sedation

Results shown previously (sections 3.1.3 and 3.3.1) show that delta is established in the EEG at least 30s prior to LORR induced by dexmedetomidine. However, the conscious EEG is predominantly a theta rhythm of 7Hz. Figure 3.14b shows the averaged Morlet power spectrum of 6 EEG recordings prior to dexmedetomidine LORR. The data were aligned in the time domain for a transition from theta to delta. The theta rhythm is the same as during active wakefulness without drug delivery, being interspersed with paroxysms of delta. The mean frequency of theta prior to NREM (6.4 ± 0.7Hz, n=8) was not significantly different from the theta produced during dexmedetomidine infusion prior to delta (6.9 ± 0.8Hz, n=6) (p>0.1, Student's t-test). As with transitions from wake to NREM (Figure 3.8b) there is a rapid theta to delta switch. The delta frequency at the start of NREM (3.2 ± 1.1Hz, n=8) was not significantly different from the delta produced during dexmedetomidine sedation (3.7 ± 0.7Hz, n=6) (p>0.1, Student's t-test). In contrast to NREM there are few events in the spindle frequency range following the switch to delta. Figure 3.14a shows a typical waveform during a transition from theta to delta for dexmedetomidine sedation. Note that in contrast to the example waveform of NREM in figure 3.6a there are no spindles present.

3.5.2 Delta switches during NREM

Given the similarity in the theta to delta switch for the onset for NREM and dexmedetomidine sedation, periods of NREM were compared to EEG transitions for dexmedetomidine LORR. Figure 3.14c show the averaged Morlet power spectrum for 6 NREM recordings with delta frequency switches. The data was calibrated in the time domain for the frequency switches. A delta frequency switch does occur, although the frequency of the spindles remains unaltered. The delta frequency immediately prior to dexmedetomidine LORR (3.1 ± 0.7Hz, n=7) was significantly less than the delta in NREM (4.2 ± 0.5Hz, n=6) (p<0.01, Student's t-test). The delta frequency immediately after dexmedetomidine (1.9 ± 0.4Hz, n=7) LORR was significantly less than for NREM following the delta frequency shift (2.6 ± 0.5Hz, n=6) (p< 0.05, Student's t-test).
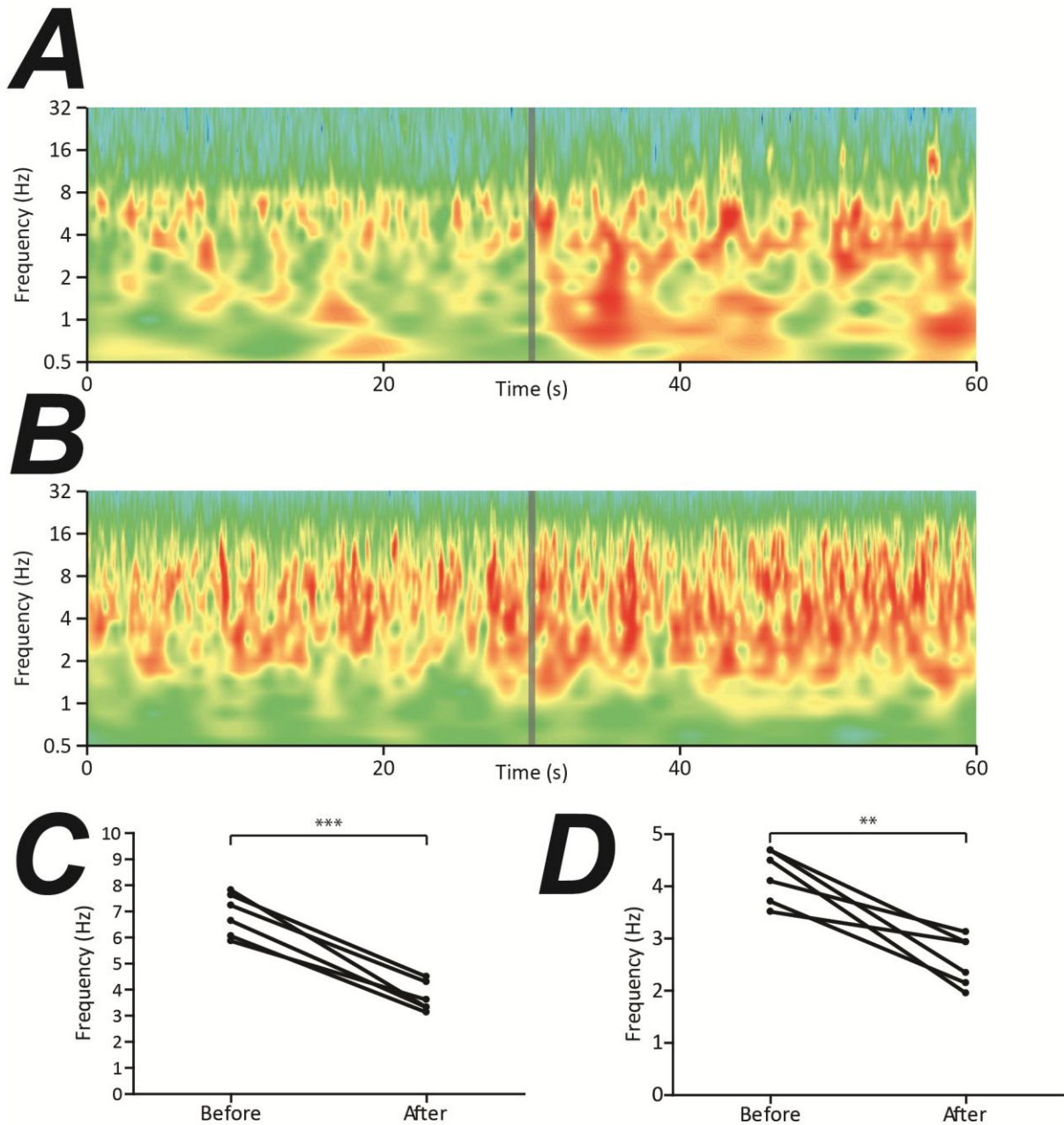
Figure 3.14 Correlations of dexmedetomidine sedation and NREM sleep.
Data showing the theta-to-delta switch in dexmedetomidine sedation and the delta-to delta switch in NREM. It is hypothesised that dexmedetomidine LORR is electrophysiologically analogous to deepening NREM, whereas the Wake-to-NREM transition is analogous to the start of dexmedetomidine sedation. **A.** Averaged Morlet power spectrum of theta to delta transitions during dexmedetomidine sedation (n=6). The transition is instantaneous as with the wake to NREM transition. Note the lack of events in the spindle frequency range. **B.** Averaged Morlet power spectrum for delta frequency switches during NREM sleep. There is an instantaneous reduction in delta frequency but no change in the frequency in spindles. **C.** Peak frequencies before and after theta-delta switches in dexmedetomidine sedation. There is a significant change in frequency (6.9 ± 0.8Hz to 3.7 ± 0.7 Hz, p<0.001 T-test, n=6). **D.** Peak frequencies before and after delta switches in NREM sleep. There is a significant decrease in frequency (4.2 ± 0.5Hz to 2.6 ± 0.5Hz, p<0.001 T-test, n=6).

4 Anaesthetic observations from depth recordings

4.1 Recording of LFP from deep brain structures

Following the observations of thalamic activity during LORR, localised components of the thalamocortical system were investigated to see how electrical activity in these regions corresponded to each other during natural sleep and anaesthetic induced LORR. Electrical activity in the form of local field potentials (LFP) may be recorded from electrodes placed in the brain tissue. This gives a localised electrical activity from a couple of hundred cells in the local vicinity of the electrode, rather than the globalised activity of the extra-dural EEG. Localised recording falls into two broad categories, unipolar and bipolar.

4.1.1 Unipolar Recording

Unipolar recording is most commonly employed due to the simplicity of the electrode configuration required. Moreover when specifically investigating sleep and anaesthesia with reference to the slow oscillation, bipolar recording may abolish the K-complex from the EEG since it occurs simultaneously over the cortex and will be subtracted from the waveform (Amzica *et al.*, 2002). Recent rodent *in vivo* models of sleep and anaesthesia using unipolar recording have indicated that changes in brain electrical activity occur instantaneously over large areas (Gervasoni *et al.*, 2004; Hwang *et al.*, 2010).

 In order to investigate the suitability of unipolar recording from multiple brain nuclei, a rat was implanted with single electrodes in the central medial nucleus of the thalamus and the primary auditory cortex as well as EEG skull electrodes. The ground was a skull screw over the vomer bone of the nose. Recording electrical activity in a tether-free configuration requires ground to be on the animal, the vomer was chosen as it is not directly over the brain and should have minimal neurogenic electrical activity.

 Figure 4.1a shows the EEG (a) and LFP from the primary auditory cortex (A1) (b) and the CMT (c) during active wakefulness. Note that the overlay of the three traces (d) shows a high degree of similarity in both waveform amplitude and frequency. Figure 4.1b shows the corresponding Morlet power spectra for these three recordings and confirms that the frequency and power structure of the three waveforms is nearly identical over very short time periods. Note the slightly fragmented theta rhythm with paroxysms of delta in each power spectrum, consistent with the earlier findings of the EEG during active wakefulness. Figure 4.1c shows the cross wavelet transform of A1 and the CMT. There is a high degree of correlation between the two signals over all the frequencies revealed from the Morlet power spectrum across the entire recording length. Figure 4.1d shows the phase

coherence spectrum of A1 and the CMT showing the waveforms are in phase over all frequencies for the length of the recording period.
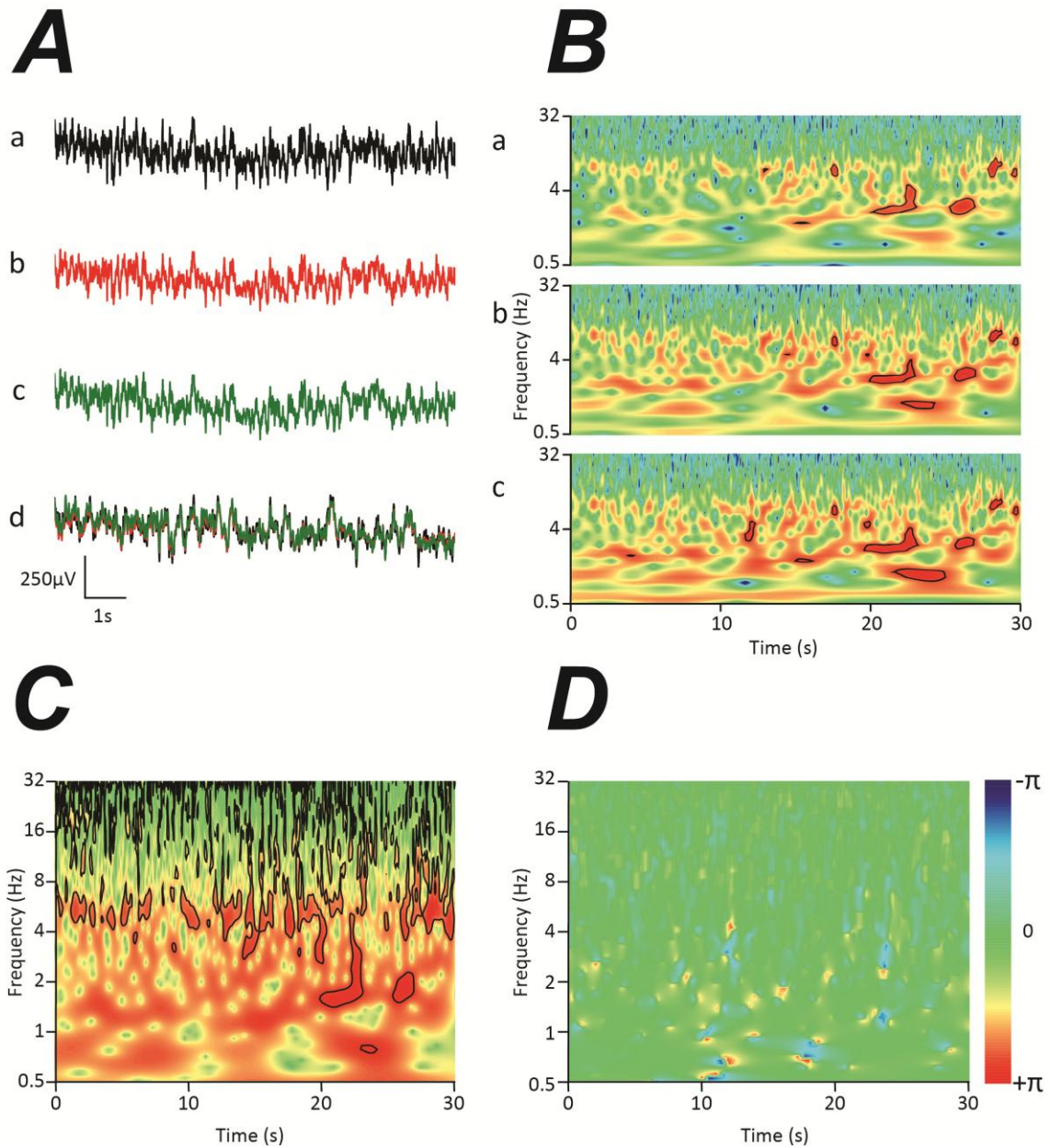
Figure 4.1 Unipolar recording from multiple brain regions with a common reference.
A. Waveforms of the EEG (a), A1 (b) and CMT (b) recorded simultaneously in an actively conscious rat. Note the high degree of similarity in the signal appearance exemplified when the waveforms are overlaid (d). **B.** Morlet wavelet power spectra of EEG (a), A1 (b) and CMT (c) showing a high degree of similarity in the fine structure of the waveforms over time. Note that all three signals show a robust theta (5-12Hz) rhythm consistent with an active behaviour in the rat. **C.** Cross wavelet power spectrum of the EEG and CMT including 95% confidence levels showing a high degree of coherence in power over a wide frequency range in both signals. **D.** Phase coherence spectrum of the EEG and CMT showing no phase deviation over time or frequency between the two signals, the signals are in phase, i.e. the phase difference is 0.

To investigate the cause of the dominating frequency observed in the three channels, one animal chronically instrumented with screw electrodes over the vomer, parietal cortex and a depth electrode in the barrel cortex was anaesthetised with 2% isoflurane and mounted in a stereotaxic frame. Unipolar recordings were made with respect to true ground, which was the inside of a Faraday cage. Figure 4.2a shows the potentials recorded from each electrode. The amplitude of the signal from the cortical screw was greatest, however the signal from the vomer electrode was of smaller but comparable amplitude. The signal from the depth electrode in the barrel cortex was of greatly reduced amplitude. Figure 4.2b shows the FFT power spectra for typical 60s recordings from each electrode. The peak frequency at 3Hz is the same from each electrode, however the power is significantly different being twice as much from over the parietal cortex compared to the vomer. The power in the vomer electrode is 10 times greater than in the barrel cortex. This suggests that potentials recorded at depth from single electrodes with respect to a ground on the vomer will be dominated by electrical activity at the vomer. Note that the relative frequency components of the vomer and parietal cortex are the same.
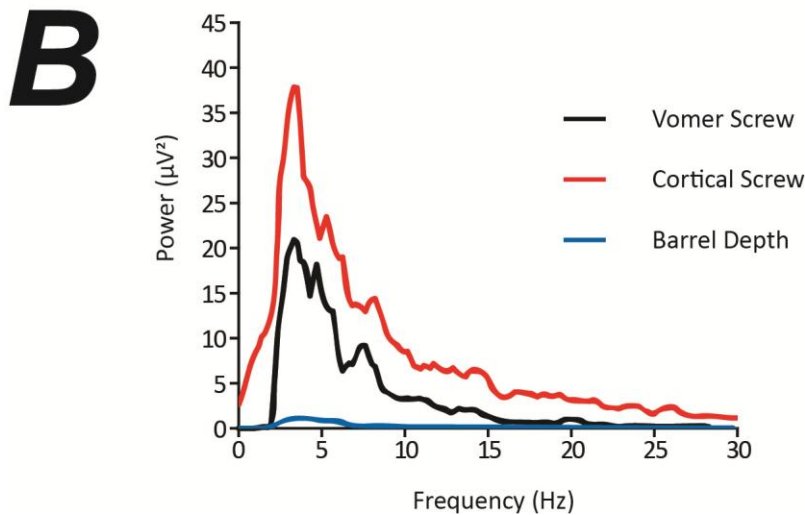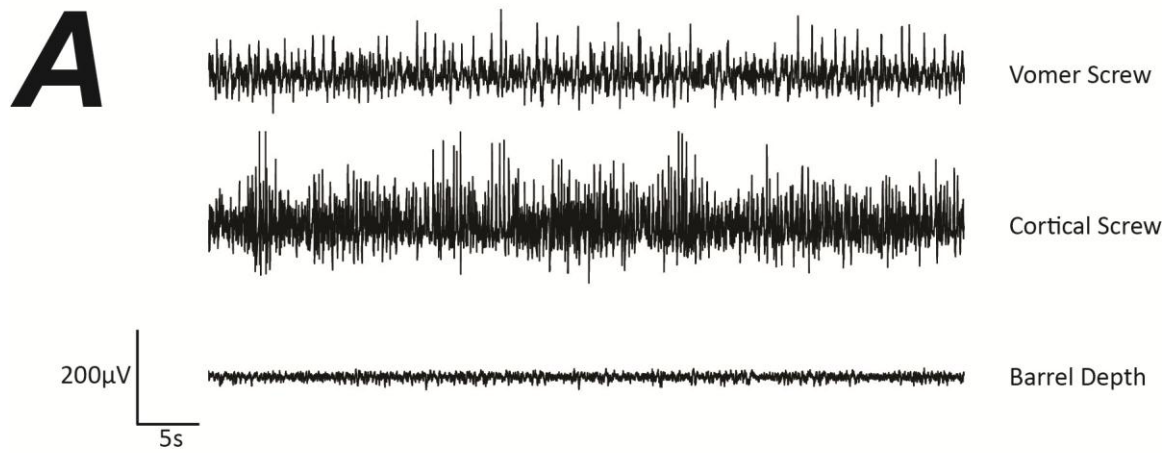
Figure 4.2 Electrical activity at the nasal vomer is sufficient to dominate a depth electrode recording.
 A. Simultaneous unipolar recordings from the nasal vomer, extra-dural parietal cortex and barrel cortex (depth recording). The extra-dural recording from over the cortex has the largest amplitude, although the signal from the vomer is of comparable size. By contrast, the signal recorded at depth from the barrel cortex has a very small amplitude. **B.** FFT power spectra for the waveforms shown above. The frequency components from the vomer and extra dural cortical recording are the same, with reduced power in vomer, showing the vomer as a poor choice for placement of a reference electrode.

4.1.2 Bipolar Recording

The principle problem with employing unipolar recording in an un-tethered setup is that each waveform appeared to have components of the reference waveform structure from what was fundamentally an EEG signal. This flaw in methodology has previously been acknowledged (Vyssotski *et al.*, 2006) and must result from a dominant frequency being present in the reference electrode that masks smaller amplitude signals in the recording electrodes. In order to remove this contamination and maintain a differential recording, the reference needs to be close to the site of recording, but far enough away to give an adequate signal. In a differential recording, this would result in equal components of the electrical activity from ground being present in both the recording and reference electrode and subtracted from the final signal. To this end a localised bipolar recording was employed. Figure 4.3a shows a schematic of the bipolar recording electrode. The electrodes consist of parallel insulated electrodes with exposed tip profiles that give a tip impedance of 1MΩ at 1kHz. The tip separation is 125μm. Figure 4.3b shows a typical acute recording from the CMT of a rat under 2% steady state isoflurane anaesthesia. The signal-to-noise ratio of the waveform was judged to be acceptable as the waveform was not digitized and no mechanical artefacts were present. The Morlet power spectrum shows that the principle oscillation within the waveform is a low frequency delta of 1-2Hz. Figure 4.3c shows a coronal schematic of the rat brain 3.2mm posterior to bregma. The CMT is highlighted in red. Figure 4.3d shows typical bipolar recordings from the cingulate cortex and CMT in a chronically instrumented animal during active wakefulness. Unlike the unipolar recordings in figure 4.1a, the waveforms from these bipolar recordings differ in frequency and amplitude suggesting that recordings are specific to their location, without influence from distal sites.
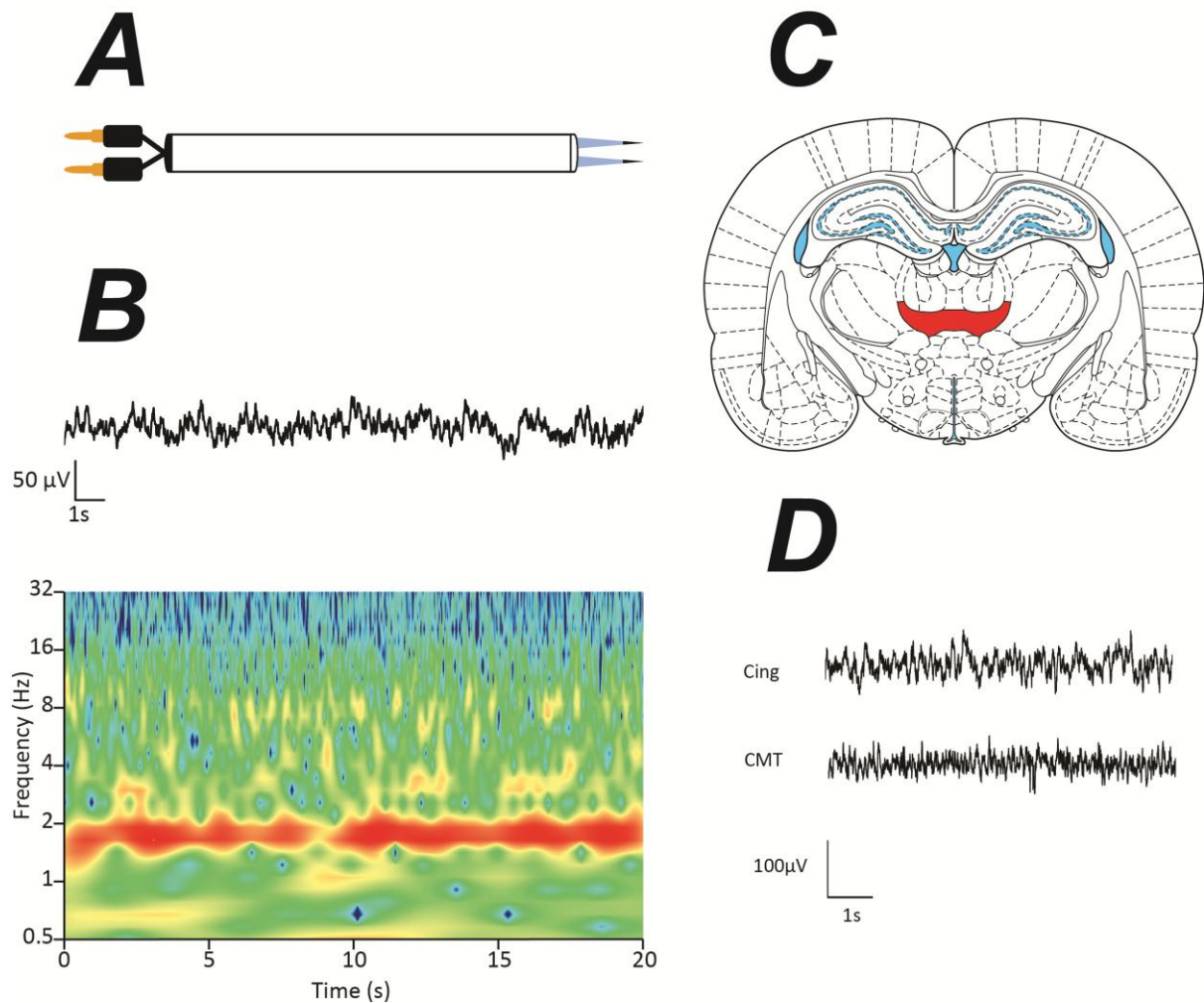
Figure 4.3 Bipolar electrode recording from deep brain structures.
A. Schematic of the bipolar electrodes used for chronic implantation and recording in rats. The electrodes consist of two parylene insulated tungsten wires with exposed tips. Electrode tip separation is 125μm and the tip impedance is 1MΩ. **B.** Data from an acute recording of the central medial thalamus of a rat under isoflurane anaesthesia. The waveform amplitude is 50μV compared to 5μV recorded by concentric bipolar electrodes at the same site (data not shown). The Morlet power spectrum shows strong delta power at 1-2Hz and a theta rhythm of 8Hz with lower power. **C.** Schematic of a coronal section of the rat brain 3.2mm anterior to bregma showing the segment of the central medial thalamus (highlighted in red) used for acute and chronic recordings. **D.** Simultaneous bipolar recordings from the cingulate and CMT showing waveforms differing in appearance, in comparison to unipolar recordings.

4.2 Determining suitable recording sites

The corticothalamic system is often simplified as a continuous loop between the thalamus and cortex, however the anatomy is more complex (see figure 1.1). Somatosensory input from the brainstem is transmitted to first order areas of the thalamus such as the ventrobasal nucleus (vibrissae) or the medial geniculate nucleus (auditory). The ascending projections of these nuclei are exclusive to corresponding areas of the parietal cortex involved in primary sensory processing such as the barrel cortex (vibrissae) and primary auditory cortex. The corticofugal projections are sent to higher order nuclei of the thalamus such as the visual pulvinar which project to numerous cortical regions concerned with primary sensory processing and associational cortical area involved in cross modality processing. A third group of thalamic nuclei, the midline and intralaminar nuclei possess properties of both first and higher order nuclei, receiving both primary sensory input and cortical excitation. These nuclei also project to the striatum and other areas of the brain.

The central medial thalamus has recently received attention for its role in arousal from anaesthesia and has been proposed as a consciousness switch (Alkire *et al.*, 2009; Alkire *et al.*, 2007). The ventrobasal nucleus (VB) and the corresponding barrel cortex were chosen as being representative of the first order thalamic and cortical regions of the thalamocortical system. The cingulate cortex was chosen due to its location in the frontal cortex and inputs from the midline and intralaminar thalamus (Van der Werf *et al.*, 2002).

4.3 Active consciousness

The electrical activity of the four thalamocortical regions was first determined during active consciousness in the rotating cylinder prior to drug infusion for LORR experiments. The cylinder was rotating at 5rpm, the same speed as during LORR experiments. The normal EEG recorded from extra-dural screw studs was shown in 3.1.2 to be a type I theta rhythm of 7Hz consistent with previous findings. The thalamocortical system is synonymous with delta oscillations and therefore determining whether a theta oscillation occurred in any parts of the thalamocortical system during active wakefulness was investigated.

4.3.1 Corticothalamic relationship

The relationship between the thalamus and cortex was considered in terms of its connectivity. The relationship of VB and the barrel cortex was investigated as an example of a first order thalamocortical relay and the cingulate and CMT were investigated together as an example of the thalamocortical system with higher order properties.

Figure 4.4a shows typical waveforms recorded from the cingulate and CMT. The CMT has a low amplitude fast frequency rhythm as would be expected during wakefulness and is consistent with the EEG findings in figure 3.2a. Whilst the cingulate also has a fast component similar to the CMT, it is clear that the waveform is predominantly a slower frequency, not in keeping with previous EEG findings. Figure 4.4b show the averaged Morlet power spectra of 60s recordings from both the cingulate and CMT (n=10 each) during active wakefulness. The cingulate exhibits a high power delta frequency over a large range of frequencies from 1-5Hz. There is a low power theta present at 6-7Hz unlike the skull EEG experiments presented previously. By contrast, the CMT demonstrates a continuous theta rhythm around 8Hz with bursts of delta and is comparable to the skull EEG data shown in figure 3.2c. Figure 4.4c shows the cross wavelet transform of the same data. The correlation in high power is predominantly within the delta band and is over the whole of the frequency range, consistent with the delta of the cingulate and the delta bursts seen within the CMT. There is a low power correlation in the theta range of 6-7Hz, below the peak theta of 8Hz observed in the CMT. Figure 4.4d shows the averaged phase coherence spectrum for the same data and is calculated as the CMT with reference to the cingulate. Only phase data above 95% significance as determined by the Monte Carlo calculation was included in the averaging. There is little phase coherence above 95% significance less than 2Hz. The average phase of in the delta range (1-5Hz) is -0.008 ± 0.015 radians (n=10) and -0.013 ± 0.13 radians for theta (5-8Hz), i.e. the cingulate and CMT are in phase for both the delta and theta ranges.
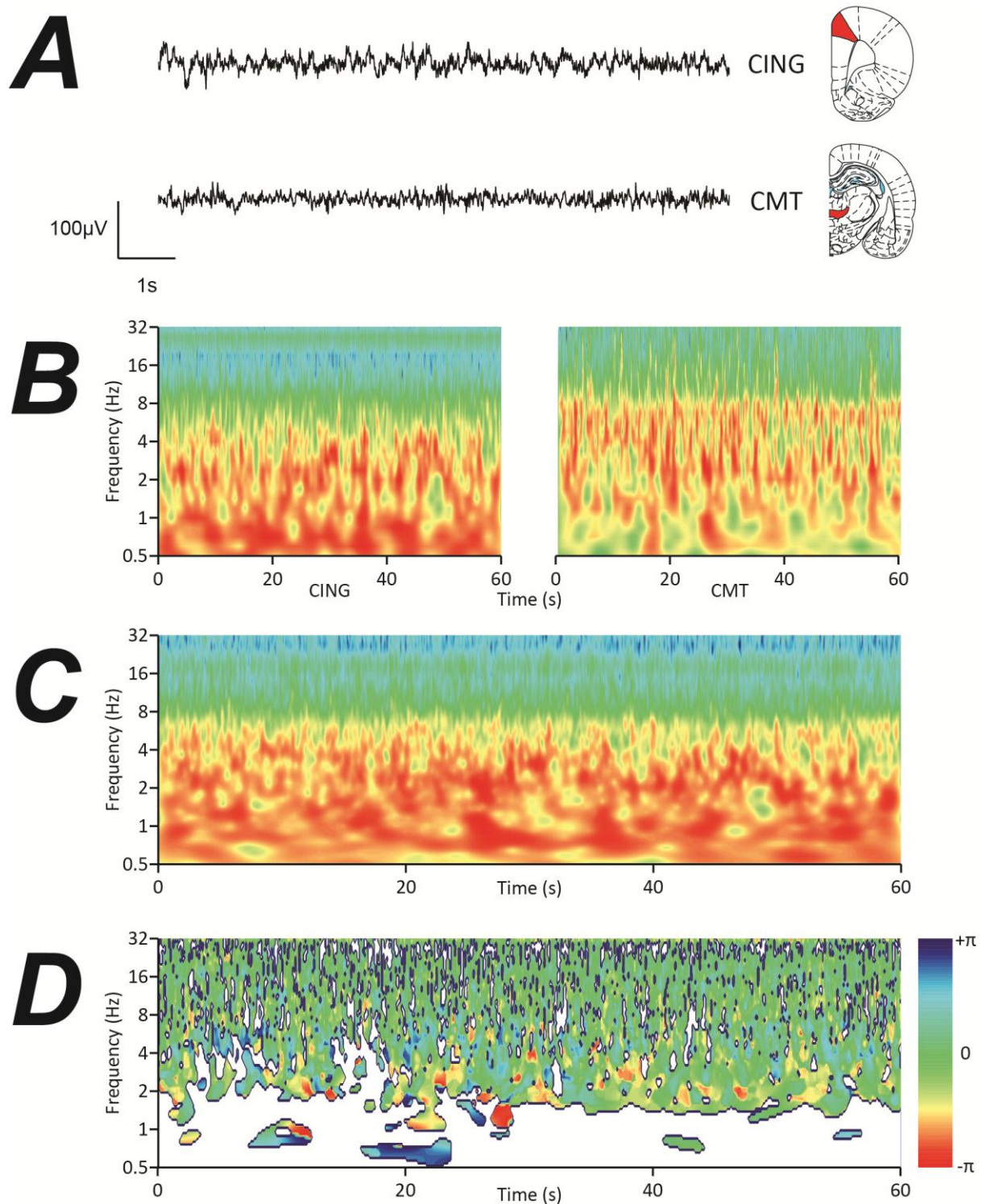
Figure 4.4 Activity of cingulate and CMT during active wakefulness.
A. Typical waveforms for the cingulate and CMT during active wakefulness. The CMT has a small frequency fast waveform, whereas the cingulate has a higher amplitude slow component as well as fast components. **B.** Averaged Morlet power spectra of cingulate and CMT. The cingulate has a predominantly delta oscillations and theta is absent, whereas the CMT has a theta oscillation with bursts of delta. **C.** Cross wavelet transform of the cingulate and CMT. The highest power covariance is in delta with no covariant power in the theta range. **D.** Average phase correlation of the cingulate and CMT. There is no overall phase difference during consciousness for any frequency over the spectrogram.

Figure 4.5a shows typical waveforms recorded from the barrel cortex and VB. Both waveforms are low voltage and fast frequency. Figure 4.5b shows the averaged Morlet power spectra of 60s recordings from both the barrel and VB (n=10 each). The barrel cortex like the cingulate is dominated by power in the delta frequency range, although unlike the cingulate has a prominent theta oscillation also at 7-8Hz. VB has a more consistent and dominant theta oscillation, similar to the CMT and has bursts of delta. Figure 4.5d shows the averaged cross wavelet transform of the same data. The correlation is highest in power for the burst of delta, however unlike the cross correlation of the cingulate and CMT, there is a greater power in the theta range which is continuous. Figure 4.5d shows the averaged phase coherence spectrum for all of the phases calculated above 95% significance. The phase relationship of the barrel to VB in the delta range is -0.001 ± 0.02 radians and 0.007 ± 0.013 radians for theta, i.e. the barrel cortex and VB are in phase during consciousness.
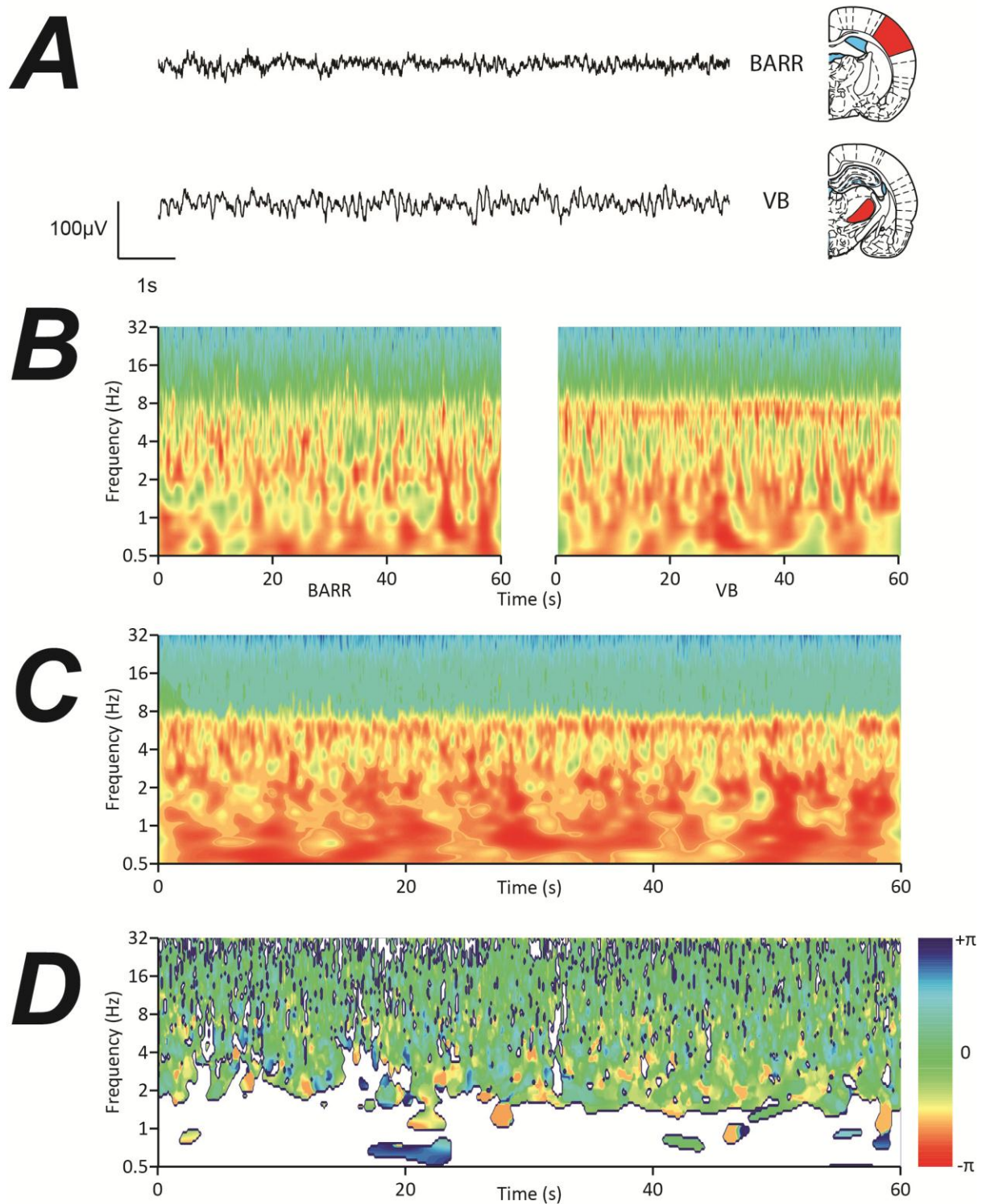
Figure 4.5 Activity of barrel and VB during active wakefulness.
A. Typical waveforms of the barrel and VB. VB has a low amplitude fast frequency waveform. The barrel also has a fast frequency component, but contains a slow frequency component of greater amplitude. **B.** Averaged Morlet power spectra for barrel and VB. VB activity is predominantly theta with some bursts of delta. The barrel has a much lower powered theta compared to delta. **C.** Averaged cross wavelet transform of barrel and VB. There is high covariant power in theta and for the delta bursts. **D.** Averaged phase correlation for barrel and VB. The signals are in phase across all frequencies during active wakefulness.

4.3.2 Corticocortical relationship

In addition to receiving projections from VB the barrel cortex also has significant inputs from multiple cortical regions. Since there was no significant phase difference between the cortex and thalamus during active consciousness, the corticocortical relationship was investigated. Figure 4.6a shows the averaged cross wavelet transform and averaged phase coherence spectrum for the cingulate and barrel cortices (n=10 each). The highest power coherence within the cortex is within the delta range. There is coherence within the theta range, although it is of much lower power. The theta coherence does not appear to be continuous as with the relationship of barrel to VB, but instead is of short bursts. Note in the phase coherence spectrum that there is a reduced amount of data above 95% significance compared to the corticothalamic phases shown previously. Despite the high power coherence in the delta region, there is much less of this above 95% significance compared to the theta range. The average phase relationship -0.006 ± 0.04 radians for delta and 0.005 ± 0.008 radians for theta, i.e. the cortex is in phase for both delta and theta during consciousness.

4.3.3 Thalamothalamic relationship

Given the anatomical connectivity described in section 4.2 and the corticothalamic and corticocortical phase relationships described above, it follows that the phase within different areas of the thalamus should also be synchronous during active consciousness, regardless of whether they are functionally connected.

Figure 4.6b shows the averaged cross wavelet transform and averaged phase coherence spectrum for the CMT and VB. Note how the power coherence is much greater in the theta range compared with the corticothalamic and corticocortical analysis. The theta coherence is continuous over time and there are bursts of power coherence in the delta range. The phase coherence spectrum shows that unlike the corticothalamic and corticocortical phase relationships, only frequencies in the theta and gamma ranges are above 95% significance. The phase of the CMT in relation to VB is -0.04 ± 0.03 radians, i.e. the CMT and VB are also in phase during active wakefulness.
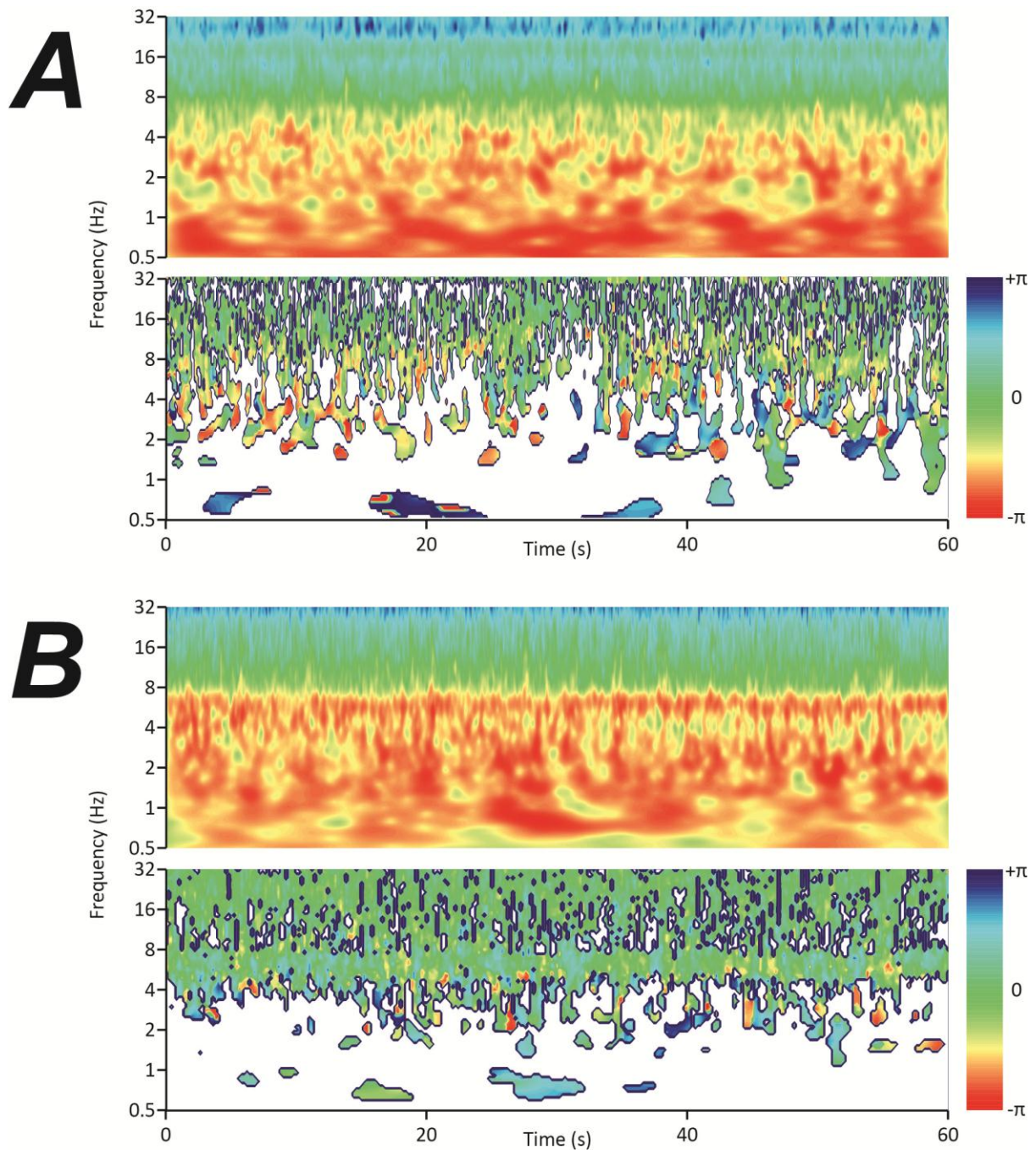
Figure 4.6 Corticocortical and Thalamothalamic coherence during active consciousness.
A. Averaged cross wavelet transform and phase correlation for cingulate and barrel. Covariant power is in the delta range, there is no covariant power in theta. There is little significant covariant power within the cortex during wakefulness. The cingulate and barrel are in phase throughout active wakefulness. **B.** Averaged cross wavelet transform and phase correlation for CMT and VB. The highest covariant power is within theta, and the signals are in phase throughout consciousness.

89

4.4 Dexmedetomidine

Dexmedetomidine was investigated in more detail using localised thalamocortical recordings because of the downwards shift in delta frequency seen at LORR from scalp EEG recordings shown previously. The LORR experiments were conducted in the same manner as previously described.

4.4.1 Corticothalamic relationship

The predominant oscillation in the scalp EEG recordings was delta, which occurred both prior to and after LORR, with different frequency peaks. Since delta is generated by the thalamocortical loop, closer investigation of the synchrony between the thalamus and cortex might reveal the cause of the downward shift in the delta oscillation at LORR.

Figure 4.7a shows typical waveforms from the cingulate and CMT around LORR. Notice that the amplitude of the waveforms is similar before and after LORR, in contrast to the increase in amplitude following LORR in the scalp EEG (figure 3.3a). Figure 4.7b shows the averaged Morlet power spectra for the cingulate and CMT during dexmedetomidine LORR (n=10 each). The cingulate cortex has a low powered delta rhythm of approximately 3 Hz prior to LORR which switches in frequency to 2Hz following LORR and increases in power. This is consistent with the EEG findings previously in figure 3.3b. By contrast the CMT exhibits both tuned delta and theta prior to LORR. In this average the two oscillations are seen to be continuous throughout the time domain. However in individual recordings, the waveform switches between delta and theta oscillations, every 1-2 seconds, coinciding with the frequency at which the animal corrects its stance in the rotating tube. At LORR, the oscillation becomes a higher powered delta oscillation at a lower frequency than the delta prior to LORR and the same frequency as for the cingulate. Note that in the cingulate there is no evidence of spindle activity. In the CMT, there are minimal events within the spindle range and fewer than evident in the scalp EEG recordings shown in figure 3.3b. Figure 4.7c shows the cross wavelet transform for the cingulate and CMT for the same data as in 4.7b. The coherence in power is in the delta frequency range. Prior to LORR it is at a higher frequency of 3 Hz and drops to 2Hz following LORR and also increases in power, and mirrors the cingulate power spectrum. Note that there is no coherence in the theta range prior to LORR, despite there being theta power in the CMT power spectrum. Figure 4.7d shows the phase coherence spectrum for all data above 95% significance for the same recordings. There is little significant data below 2Hz. In the delta frequency band, the areas of significance follow the high power areas in the cross wavelet transform. The phase relationship in the delta prior to LORR is 0.03 ± 0.09 radians and changes to -2.4 ± 0.05 radians after LORR (p<0.0001, t-test).
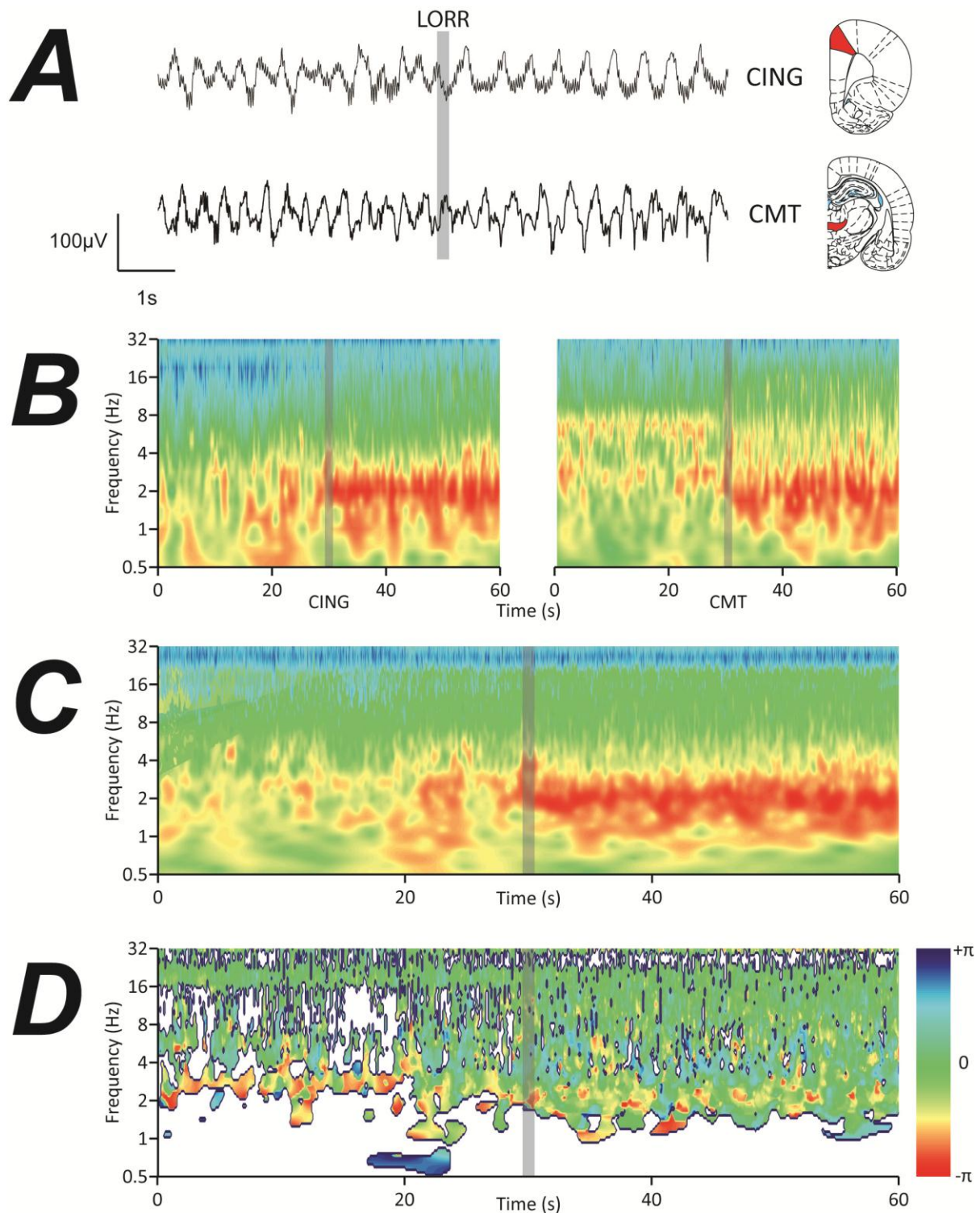
Figure 4.7 Simultaneous frequency changes occur in cingulate and CMT at dexmedetomidine LORR.
A. Typical waveforms for cingulate and CMT at dexmedetomidine LORR. There is little change in amplitude for either signal immediately around LORR. **B.** Averaged Morlet power spectra of the cingulate and CMT. The cingulate has a predominantly delta prior to LORR. At LORR the frequency shifts downwards to 2Hz. The CMT has a mixture of theta and delta power prior to LORR. At LORR theta is abolished and the delta frequency shifts downwards to 2Hz and spindles occur. The l increase in power occurs several seconds after LORR. **C.** Averaged cross wavelet transform of cingulate and CMT. The coherence prior to LORR in delta at 3Hz, this coherent power decreases in frequency at LORR to 2Hz. **D.** Phase difference correlation of cingulate and CMT from all significant power in the XWT. There is little significant power coherence below delta. In the delta range the phase prior to LORR is 0.03 ± 0.09 radians and -2.4 ± 0.05 afterwards.

Figure 4.8a shows typical waveforms from the barrel cortex and VB during LORR. Note in the barrel cortex that there is an obvious reduction in the frequency after LORR. The barrel also has fewer frequency components in the waveform structure than VB, which is more complex. VB becomes a reduced frequency following LORR. Figure 4.8b shows the averaged Morlet power spectra of the barrel cortex and VB for dexmedetomidine LORR. The barrel cortex has a delta frequency prior to LORR of 3Hz. Following LORR this delta frequency drops in frequency to 2Hz. Whilst this delta frequency shift mirrors the cingulate cortex, note the abundance of spindles that are not found in the cingulate. VB predominantly has a theta oscillation prior to LORR with some bursts of delta, and resembles the finding of the drug free conscious recordings in figure 4.5b. At LORR there is a frequency reduction to a 2Hz delta, as in the barrel cortex, CMT and cingulate. Note that VB also has an abundance of spindles at the same frequency range as in the barrel cortex. Figure 4.5c shows the averaged cross wavelet transform for the same data as in figure 4.5b. Prior to LORR there is power coherence in both the delta and theta ranges, as seen in the cingulate and CMT correlation. Following LORR the greatest correlation is in the delta frequency range that is lower in frequency than prior to LORR, consistent with the frequency reduction in the cingulate and CMT correlation. Note that there is also good power correlation in the spindle frequency range. Figure 4.8d shows the phase coherence spectrum for data above 95% significant in the cross wavelet transform. There is little significant data below 2Hz. The phase prior to LORR is 0.06 ± 0.06 radians and changes to -0.2 ± 0.006 radians after LORR (P<0.0001, t-test).
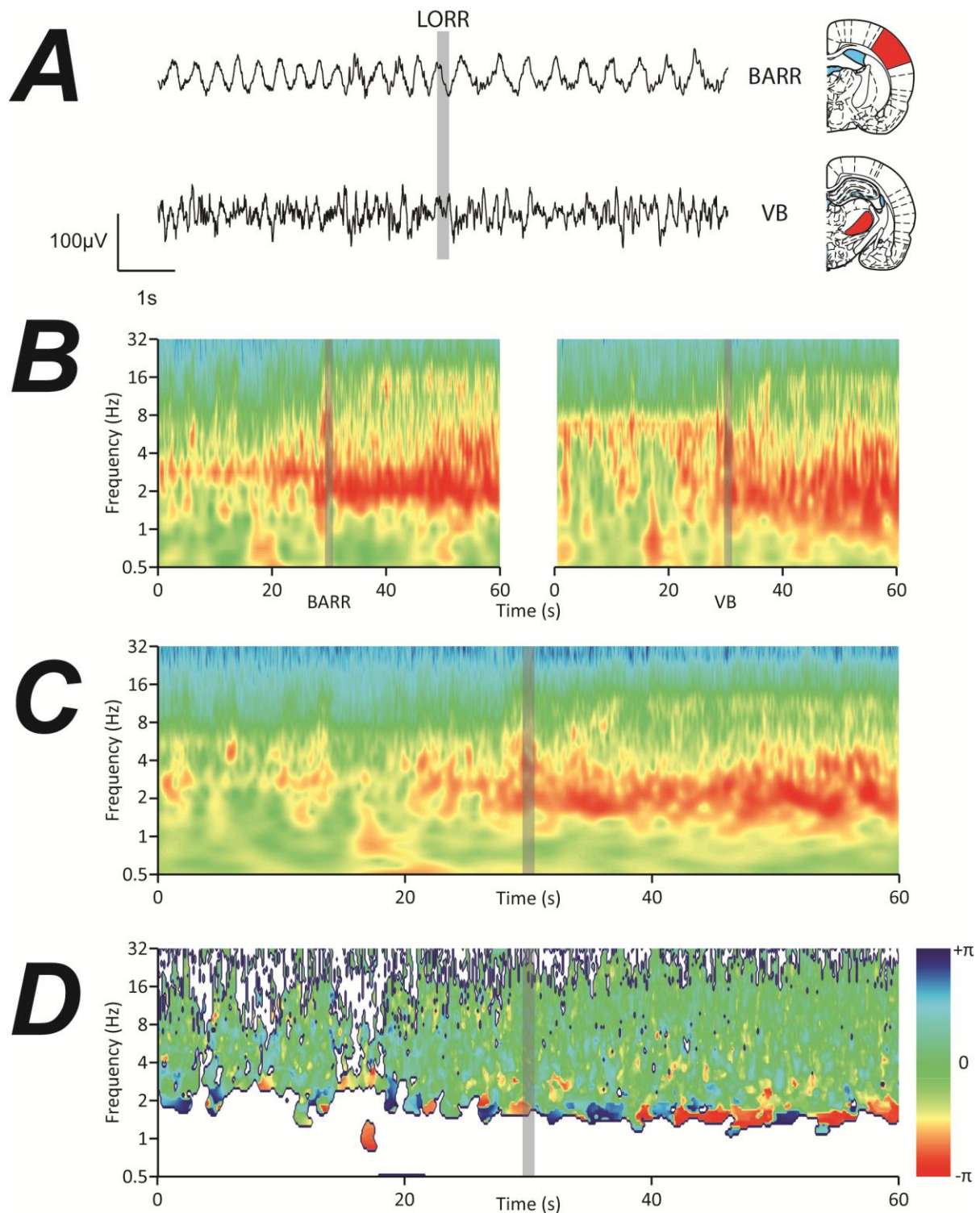
Figure 4.8 Simultaneous frequency changes occur in barrel and VB at dexmedetomidine LORR.
A. Typical waveforms for barrel and VB at dexmedetomidine LORR. There is little change in amplitude for either signal immediately around LORR. Note the disappearance of faster frequencies in the VB signal at LORR. **B.** Averaged Morlet power spectra of barrel and VB. The barrel has a predominantly delta at 3Hz prior to LORR. At LORR the frequency shifts downwards to 2Hz. VB has a theta oscillation prior to LORR. At LORR theta is replaced by a delta frequency of 2Hz. Spindles occur in both signals. **C.** Averaged cross wavelet transform of barrel and VB. The coherence prior to LORR in sparse, but becomes more coherent at LORR with a 2Hz delta. **D.** Phase difference correlation of barrel and VB from all significant power in the XWT. There is little significant power coherence below delta. In the delta range the phase after LORR is -0.2 ± 0.006.

93

4.4.2 Corticocortical relationship

Having established that the corticothalamic coherence is conserved in independent sites of the thalamocortical system, the correlation of different parts of the cortex was investigated. Figure 4.9a shows the averaged cross correlation transform and phase coherence spectra for the cingulate and barrel cortex during dexmedetomidine LORR. Prior to LORR, the power coherence is a 3Hz oscillation. At LORR a reduction in the frequency of peak correlation occurs to 2Hz which is also greater in power. Note that there is some correlation in the spindle frequency, although the event frequency is much less than seen in the barrel and VB. The phase correlation of delta within the cortex prior to LORR is 0.22 ± 0.02 radians prior to 0.54 ± 0.09 radians after LORR (p>0.05, t-test) i.e. the cingulate was in front of the barrel cortex throughout the recording.

4.4.3 Thalamothalamic relationship

Figure 4.9b shows the averaged cross wavelet transform and phase coherence spectrum of the CMT and VB during dexmedetomidine LORR. Prior to LORR, the predominant power coherence is in the theta range with bursts of delta, as seen in the drug-free conscious recordings. At LORR this power coherence shifts to a lower frequency of 2Hz. Note that in the 3-4s prior to LORR, there is a linear reduction in the frequency of power correlation, followed by the downward shift. Note that there is little coherence in the spindle frequency range. The phase relationship for delta is 0.03 ± 0.06 radians prior to LORR and -0.46 ± 0.09 radians afterwards (p<0.01, t-test).
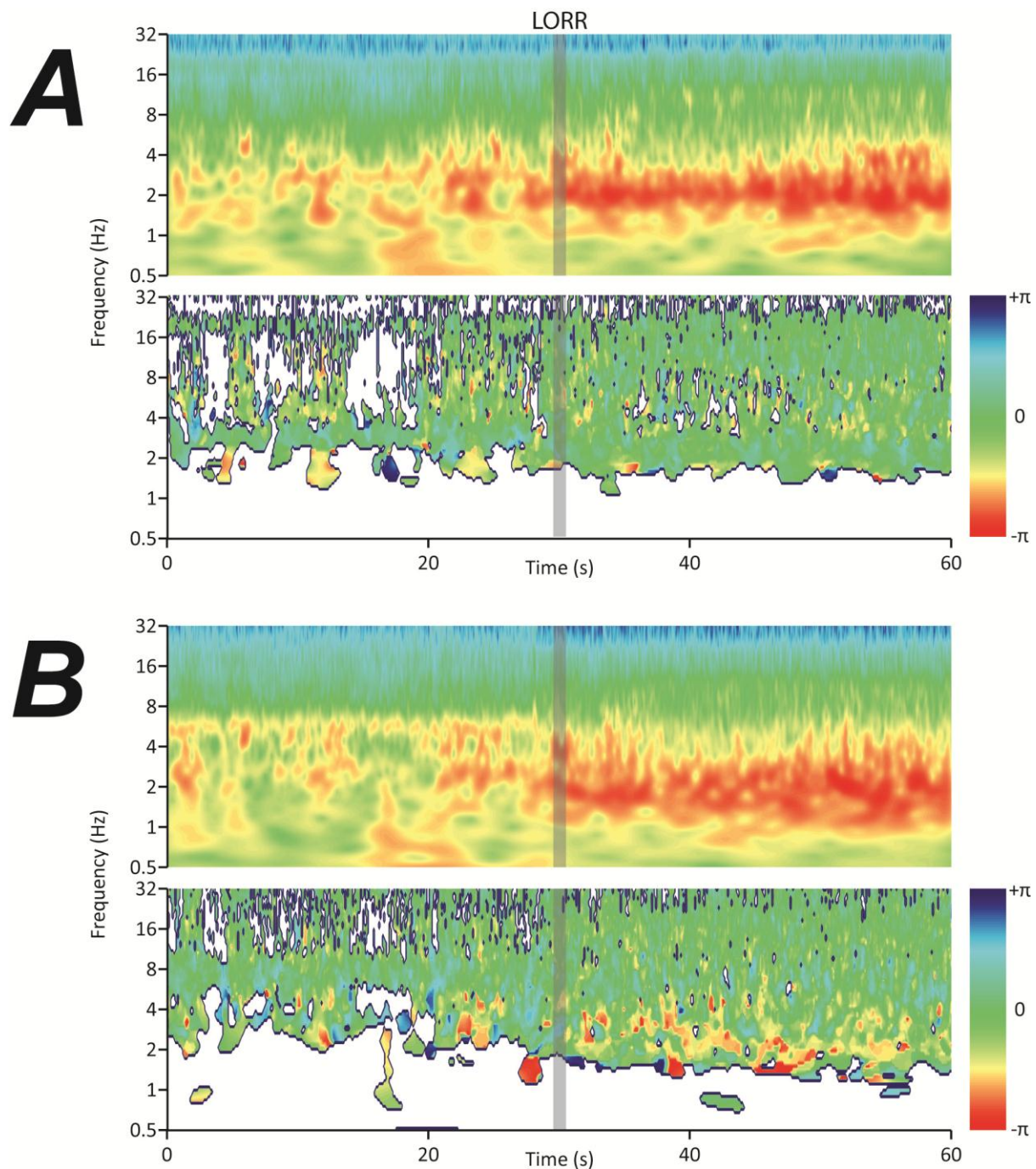
Figure 4.9 Corticocortical and thalamothalamic coherence in dexmedetomidine LORR.
A. Averaged cross wavelet transform and phase correlation spectra for cingulate and barrel. The cingulate and barrel have covariant power at 3Hz prior to LORR and 2Hz after LORR. The change of frequency occurs at LORR. The phase average phase difference is 0.22 ± 0.02 radians prior to 0.54 ± 0.09 radians after LORR, the cingulate leading the barrel throughout the recording. **B.** Averaged cross wavelet transform and phase correlation spectra for CMT and VB. The CMT and VB have covariant power in theta prior to LORR, switching to delta at 2Hz at LORR. The signals are in phase during conscious theta. The phase in delta after LORR is -0.46 ± 0.09 radians, the CMT leading VB.

4.5 Propofol

Given that the delta frequency shift seen in the EEG with dexmedetomidine was conserved in the cortex and CMT, but not VB, the activity in these areas was investigated for propofol. The LORR experiments were performed as previously described in section 3.1.4.

4.5.1 Corticothalamic relationship

Experimental data shown in figure 3.11 suggests that the thalamus closely follows the frequency changes of the EEG through propofol LORR. In order to determine the relevance of comparing the EEG and EThG to the thalamocortical system, the corticothalamic relationship was investigated using localised recording.

Figure 4.10a shows the typical waveforms of the cingulate and CMT during propofol LORR. There is little change in the waveform amplitude of the cingulate following LORR. By contrast, the CMT amplitude starts to increase in amplitude around 3s prior to LORR to reach maximum amplitude at LORR. Note following LORR there is an obvious change in the waveform frequency. Figure 4.10b shows the averaged Morlet power spectra for the cingulate and CMT during propofol LORR (n=6 each). The cingulate does not have high power in the theta frequency range, as previously shown in 4.4b. Instead, there is a delta oscillation of 2-4Hz. At LORR the 2-4Hz oscillation persists but there is an increase in the theta frequency power. By contrast the CMT has an 8Hz theta frequency prior to LORR with bursts of theta, as seen during active wakefulness. Five seconds prior to LORR there is a marked increase in theta and delta power and the theta frequency declines until LORR occurs. The frequency after LORR is dominated by delta, but also has power in the theta range. Figure 4.10c shows the cross wavelet transform of the same data. Prior to LORR there is little power correlation between the cingulate and CMT apart from some of the delta bursts. Following LORR, the greatest correlation is in delta at 3Hz, but there is correlation across the delta range and also in theta up to 7Hz. Figure 4.10d shows the phase coherence spectrum for all data above 95% significance for propofol LORR. The phase relationship is -0.55 ± 0.28 radians in the delta band after LORR.
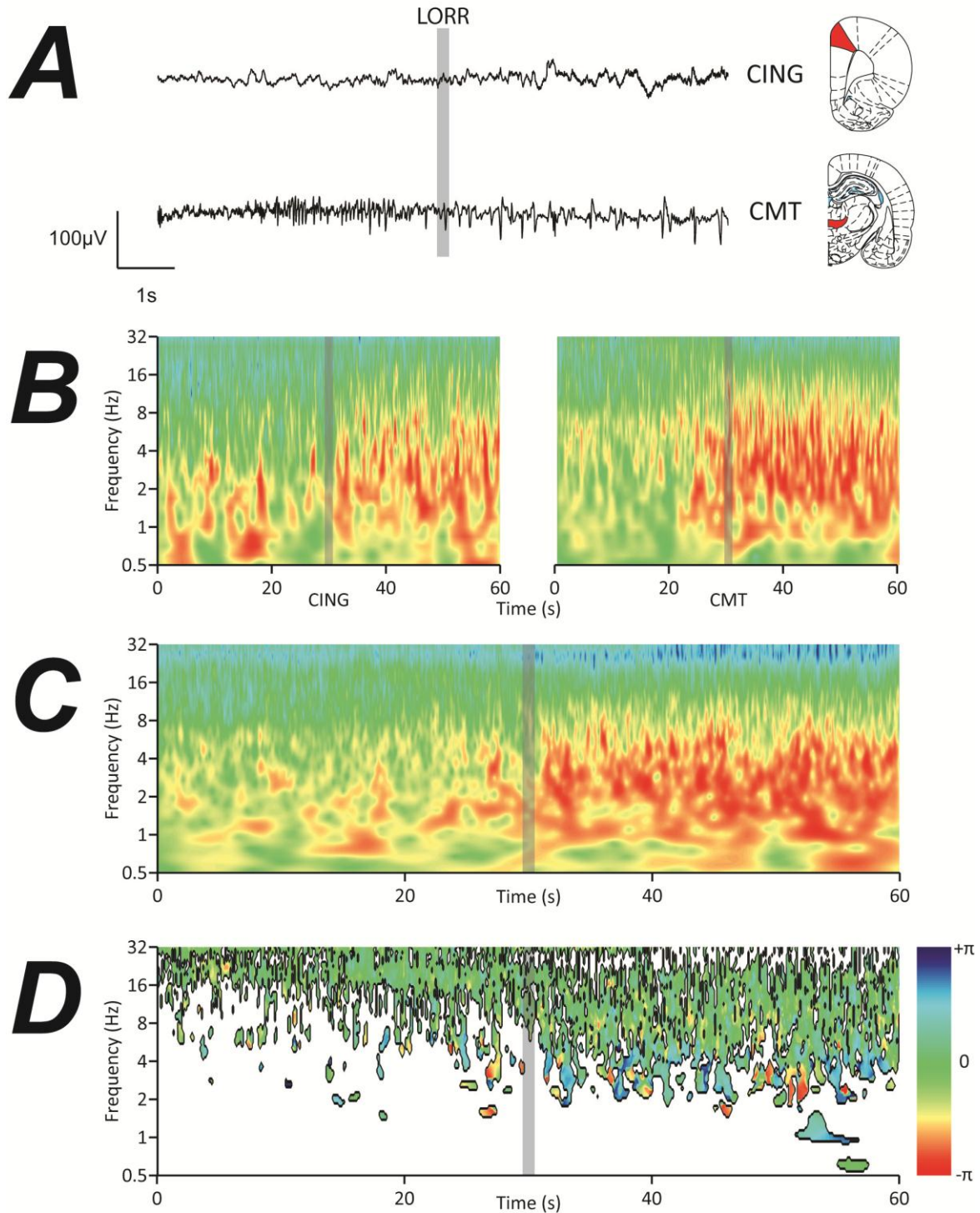
Figure 4.10 Frequency change in cingulate and CMT at propofol LORR.
A. Typical waveforms for the cingulate and CMT during propofol LORR. The waveform of the cingulate changes little around LORR. There is a small increase in amplitude afterwards. Five seconds before LORR, where there is an increase of amplitude and faster components in the waveform. Slow components become more prominent at LORR. **B.** Averaged Morlet power spectra for cingulate and CMT. The frequency of delta does not change during transitions in the cingulate. Spindles appear at LORR in the cingulate. The CMT has an increase in power 5s prior to LORR and a progressive decrease in frequency to result in delta and spindles at LORR. **C.** Averaged cross wavelet transform of cingulate and CMT. There is little covariant power before LORR. At LORR there is large covariant power in delta and spindles. **D.** Phase correlation of cingulate and CMT. There is little significant covariant power prior to LORR. After LORR the phase average phase difference is -0.55 ± 0.28 radians, the CMT leading the cingulate.

Figure 4.11a shows typical waveforms from the barrel cortex and VB for propofol LORR. The barrel cortex has a low amplitude fast frequency waveform. Following LORR there is a sudden increase in waveform amplitude and decrease in the frequency. VB also has a small amplitude fast frequency waveform 10s before LORR. A change in frequency and amplitude starts 4s before LORR. At LORR there is a further increase in waveform amplitude and decrease in frequency. Figure 4.11b shows the averaged Morlet power spectra for the barrel cortex and VB. Both barrel cortex and VB have low powered theta prior to LORR with bursts of delta. 3-4s prior to LORR there is a decrease in the theta frequency in both barrel cortex and VB. At LORR there is a large increase in both delta and theta power. There are few distinguishable events in the spindle range compared to recordings with dexmedetomidine (figure 4.8b). Figure 4.11c shows the averaged cross wavelet transform for the barrel cortex and VB. Prior to LORR there is correlation in theta and also some delta bursts as seen during active wakefulness (figure 4.4c). 3-4s prior to LORR, there is correlation in power for the decrease in theta frequency. Following LORR, there is correlation in delta and theta. Figure 4.11d shoes the phase coherence spectrum for the barrel cortex and VB. The phase relationship prior to LORR is -0.02 ± 0.01 radians and -0.11 ± 0.06 radians afterwards (p<0.05, t-test).
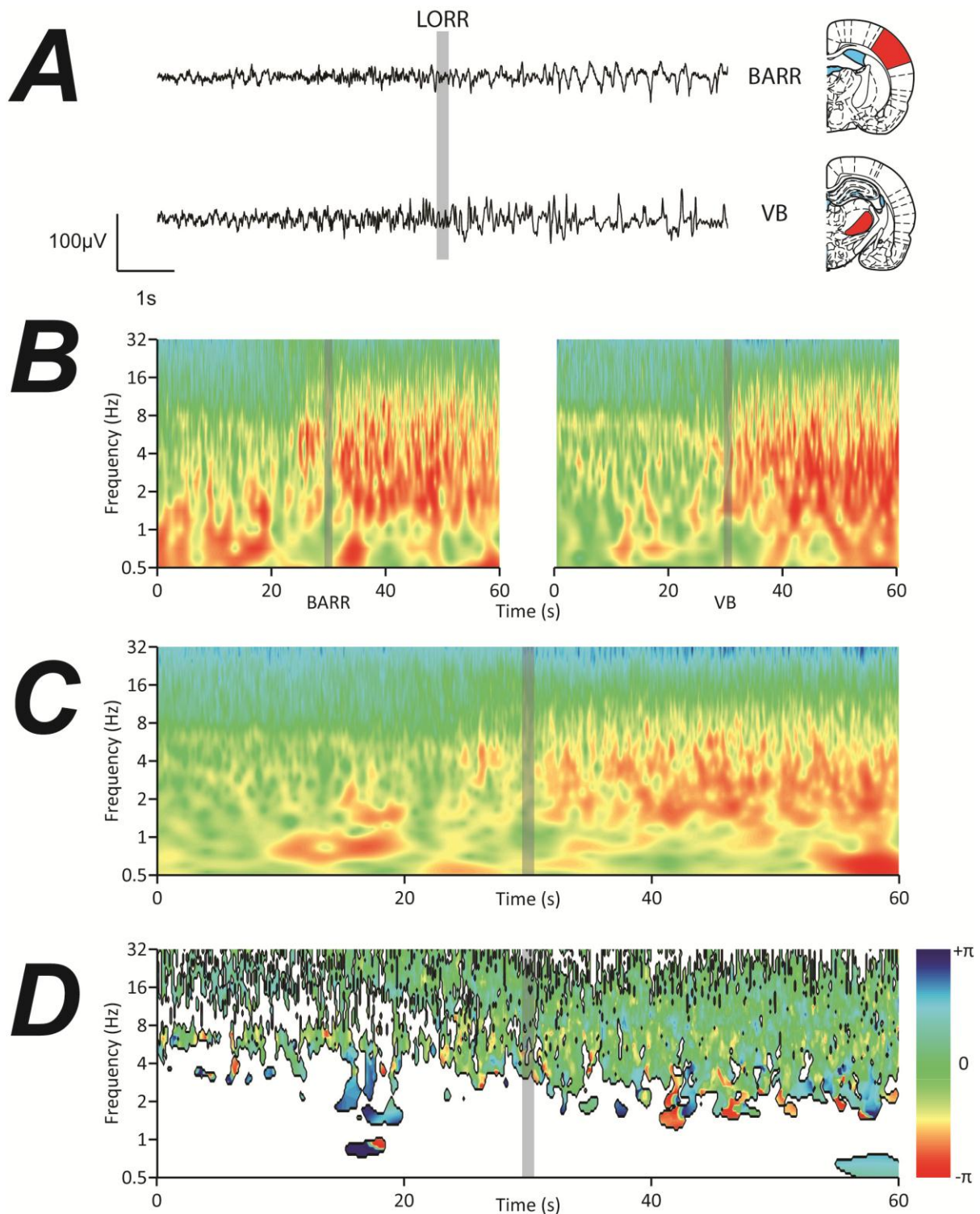
Figure 4.11 Simultaneous frequency changes in barrel and VB at propofol LORR.
A. Typical waveforms from barrel and VB. Increase in amplitude start 5s before LORR. There is an obvious change to a slower waveform at LORR for both signals. **B.** Averaged Morlet power spectra for barrel and VB. For both areas, the signal starts as a theta. As propofol infusion progresses, the theta frequency reduces and becomes delta and spindles at LORR. **C.** Averaged cross wavelet power spectrum. Bicovariant power is in theta prior to LORR and delta and spindles after LORR. **D.** Phase correlation spectrum for barrel and VB. Most significant covariant power was in theta prior to LORR and delta afterwards. Signals were in phase before LORR with a phase difference of -0.11 ± 0.06 radians in delta after LORR.

4.5.2 Corticocortical relationship

For dexmedetomidine LORR the cingulate and barrel cortex correlated in power in the delta frequency range both before and after LORR. Figure 4.12a shows the averaged cross wavelet transform and the phase coherence spectrum for the cingulate and barrel cortex. Unlike dexmedetomidine, there is only sporadic correlation between the cingulate and barrel cortex within the delta range prior to propofol LORR. No correlation in theta is seen. Following LORR, much more correlation is evident in delta and theta. The phase prior to LORR is 0.24 ± 0.12 radians and 0.17 ± 0.09 radians afterwards ($p > 0.05$, t-test), the cingulate leading the barrel throughout.

4.5.3 Thalamothalamic relationship

The CMT and VB had correlation in theta frequencies prior to dexmedetomidine LORR but not delta. Figure 4.12b shows the averaged cross wavelet transform and the phase coherence spectrum for the CMT and VB for propofol LORR. As with dexmedetomidine, the CMT and VB have a correlation in theta prior to LORR. Several seconds prior to LORR this coherence increases and the frequency of theta decreases. Note how at the same time there is an increase in the coherence in delta which continues after LORR. The coherence after LORR is in both delta and theta, as seen in the corticothalamic relationship for propofol. The phase prior to LORR is 0.73 ± 0.43 radians and -0.43 ± 0.13 afterwards ($p < 0.001$, t-test).
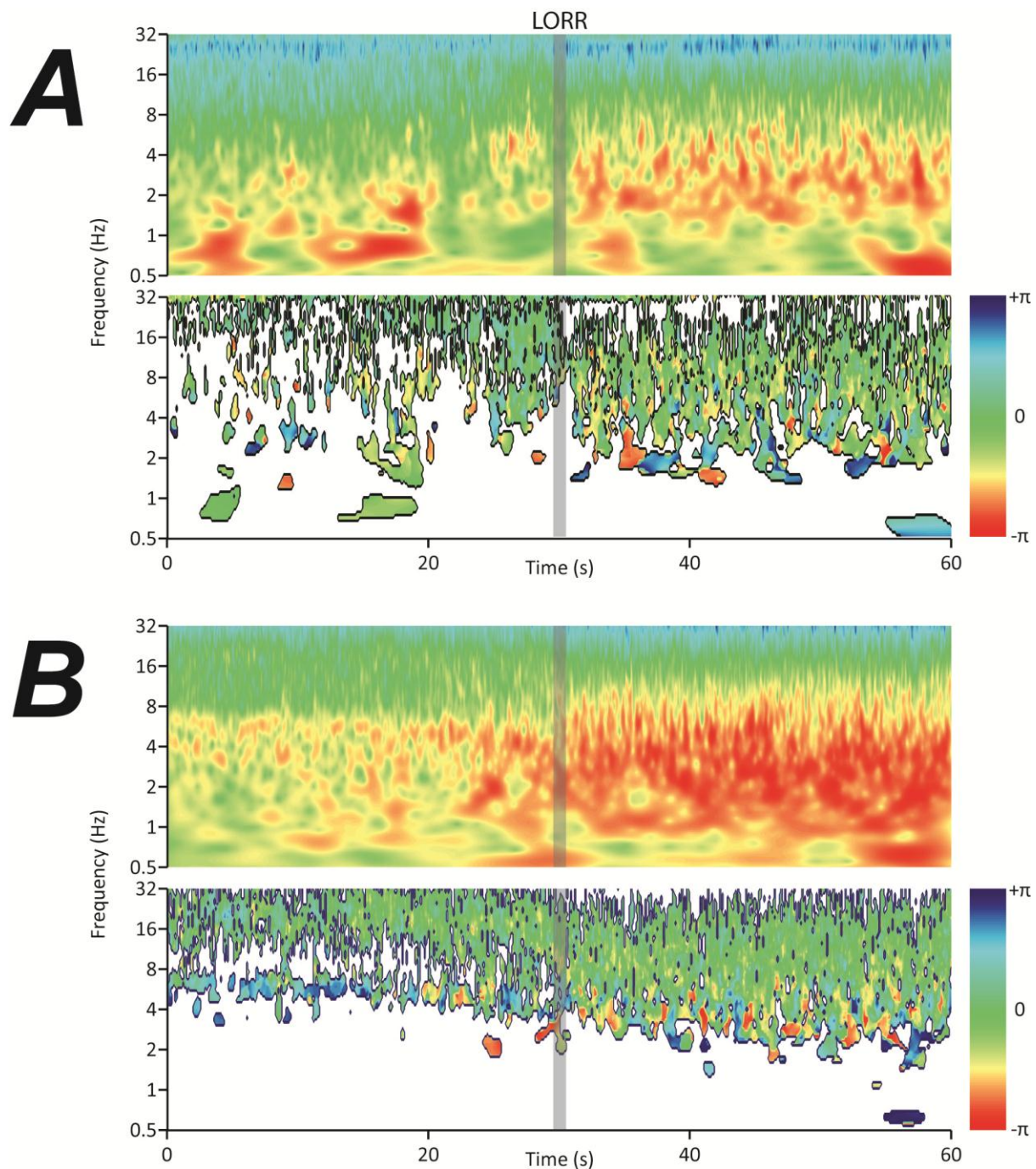
Figure 4.12 Corticocortical and Thalamothalamic coherence in propofol LORR.
A. Averaged cross wavelet transform and phase correlation spectrum for cingulate and barrel. There is little significant covariant power prior to LORR within the cortex, but most is within delta. There is a greater covariant power after LORR and this is within delta and spindle ranges. The phase difference after LORR is 0.17 ± 0.09 radians afterwards, the cingulate leading the barrel. **B.** Averaged cross wavelet transform and phase difference spectra in CMT and VB. Covariant power within the thalamus is found within theta prior to LORR with an average phase difference of 0.73 ± 0.43 radians, VB leading the CMT. This covariant power reduces in frequency 5s before LORR and reaches a steady delta frequency at LORR with a phase difference of -0.43 ± 0.13 radians, the CMT leading VB.

4.6 Effect of sensory input on delta frequency

In order to prevent mechanical noise artefacts around the point of LORR, it was necessary to stop rotation of the cylinder immediately as LORR occurred. To determine whether the reduction in delta frequency seen at LORR with dexmedetomidine was due to a reduction in sensory input, one rat was anaesthetized with intravenous dexmedetomidine at 20µg/kg. Soon after LORR was achieved, the rat was placed in the rotating cylinder and LFP was simultaneously recorded from the barrel cortex. The cylinder alternated between 0 and 3.5rpm every 100s. Figure 4.13s show the Morlet power spectrum for this recording. There is a delta frequency shown throughout the recording. There is no difference in delta frequency or fine structure of the power spectrum regardless of whether the cylinder was rotating or stationary. Figure 4.13b shows the FFT power spectrum of the average of all waveforms during both 0 and 3.5rpm rotation of the cylinder (n=3 each). There is no difference in peak delta frequency or power for each condition.
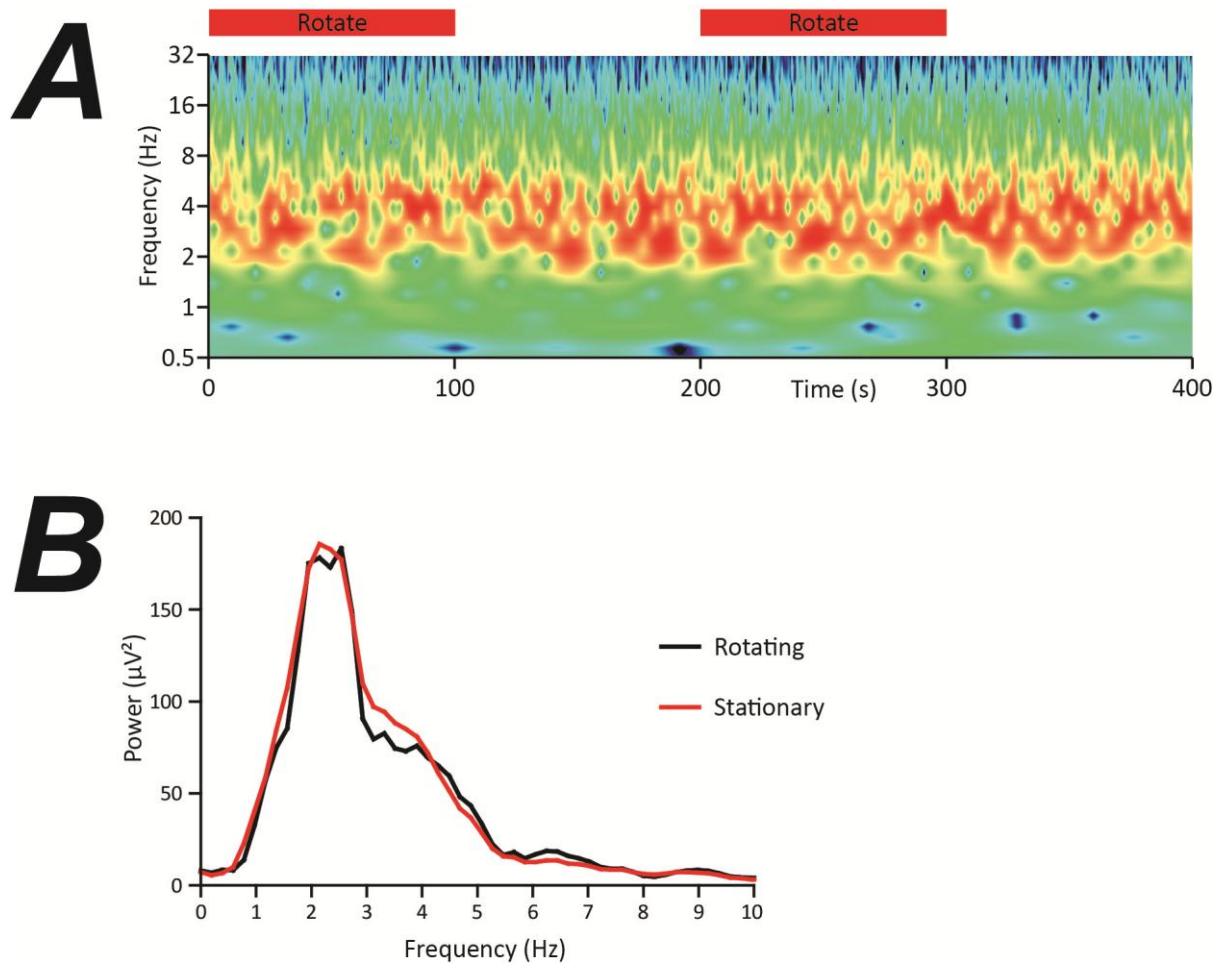
Figure 4.13 The delta frequency shift of dexmedetomidine LORR is not due to a change in external stimulatory input.

A. Morlet power spectrum of a recording from the barrel cortex under dexmedetomidine anaesthesia. The red bars above the spectrum indicate whether the cylinder was rotating or stationary. There is no difference in the fine structure or peak power frequency for a rotating or stationary cylinder. **B.** Averaged FFT power spectra from 60s recordings during cylinder rotation and a stationary cylinder (n=3 each). There is no difference in power or peak frequency.

5 Sleep observations from depth recordings

5.1 Establishing Wake-to-NREM transitions from EEG

Given that the cingulate cortex has a predominantly delta oscillation during wakefulness (Figure 4.4b) and that Wake-to-NREM transitions in the EEG were characterised by a theta to delta switch (Figure 3.8b), it is unlikely that transitions could be identified using the sleep scoring algorithm on cingulate recordings. Previous studies have suggested that theta does not have a high power in the cortex during wakefulness, but does in the thalamus (Gervasoni *et al.*, 2004). One rat was implanted with EEG skull electrodes as well as depth electrodes and natural sleep was recorded during the light period. The EEG data was scored using the algorithm previously described and data from the cingulate, barrel cortex, CMT and VB analysed by Morlet wavelet analysis, to determine which data nucleus would give the best approximation of the EEG data for sleep scoring.

Figure 5.1 shows a typical example of a Wake to NREM transition from the EEG, CMT, and cingulate from this animal. Figure 5.1a shows the waveforms of wake to NREM transitions and 5.1b shows the Morlet power spectra of the same data. The Morlet power spectrum for the EEG is consistent with the averaged data shown from other animals in figure 3.8b. During wakefulness, there is a theta rhythm of 7Hz interspersed with bursts of delta. As the animal transits into NREM the power in the recording changes from predominantly theta to delta. As with previous findings there is power across the delta, theta and spindle ranges. The Morlet power spectrum of the CMT mirrors the pattern shown in the EEG. By contrast, the Morlet power spectrum of the cingulate cortex shows predominantly delta during wakefulness, with some low power in the theta range.

The CMT and cingulate were both scored for wake and NREM using the previously described algorithm (Costa-Miserachs *et al.*, 2003) for three periods scored as Wake-to-NREM using EEG data. The CMT recordings scored the same as the EEG for Wake-to-NREM whereas the cingulate scored as doubts. The CMT was therefore chosen to score sleep in all other animals. Not all animals were implanted with EEG electrodes as well as depth electrodes for sleep recording, as this would require the use of an extra neurologger and increase the technical complexity of the recordings.
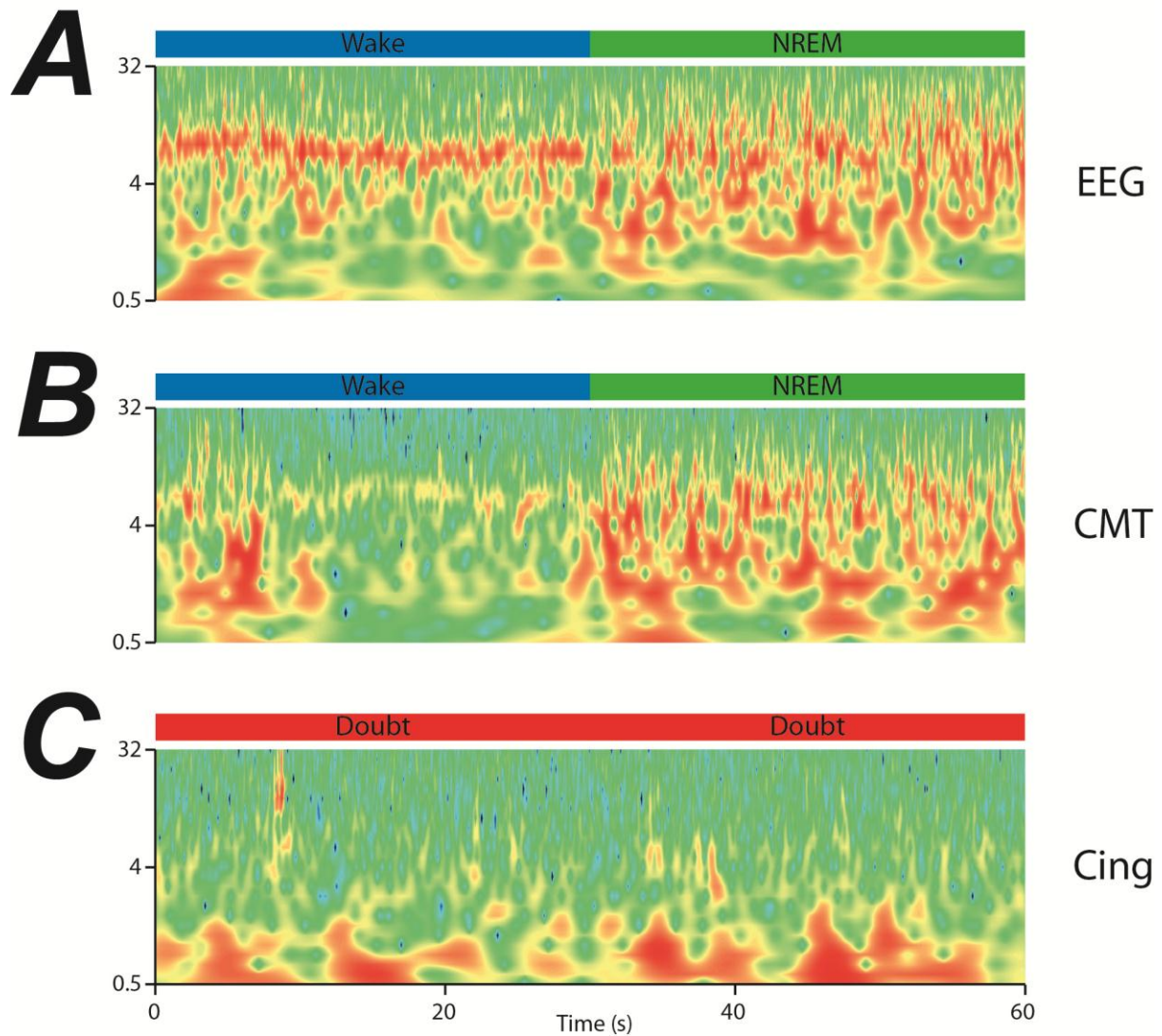
Figure 5.1 The CMT can be used to score Wake-to-NREM transitions in place of the EEG.
Morlet power spectra for EEG (**A**) CMT (**B**) and cingulate (**C**) recorded simultaneously. Data scored for Wake-to-NREM transitions using a previously established algorithm (Costa-Miserachs *et al.*, 2003) in 4s epochs. The EEG signal (**A**) showed a theta-to-delta switch as shown in chapter 3. The CMT signal (**B**) mirrored this transition and scored the same in 5s epochs. By contrast, the cingulate (**C**) which had mostly low frequency delta even during wake produced a large amount of doubt scores, due to delta and a high amplitude EMG (not shown).

5.2 Wake to NREM transitions

Previous findings in rats (Gervasoni *et al.*, 2004) have demonstrated that at the onset of sleep there are global forebrain transitions. However this study recorded from first order thalamus and primary sensory cortex. To investigate whether transitions occur simultaneously in intralaminar and first order thalamus, LFPs from animals instrumented for LORR experiments were recorded during the light phase (19:30-7:30) and Wake-to-NREM transitions investigated. Having characterised NREM from depth recordings, wake to NREM transitions were characterised based on sleep scoring of the CMT waveform. On average, each animal had 8 periods of consolidated sleep. Transitions from wakefulness into these prolonged periods were analysed. A total of 15 transitions were analysed from 5 animals.

5.2.1   Corticothalamic relationship

Figure 5.2a shows typical waveforms for the cingulate and CMT for Wake-to-NREM transitions. At The transition from wakefulness to NREM, there is little change in the cingulate amplitude. By contrast the CMT waveform shows a fast frequency low amplitude waveform approaching the transition, this then switches to a greater amplitude with slower components within the waveform. Figure 5.2b shows the averaged Morlet power spectra for all cingulate and CMT Wake-to-NREM transitions. Consistent with the active wake recordings in section 4.3, the cingulate exhibits no theta power prior to NREM, but instead a low frequency delta oscillation. At the transition, there is little change in the frequency or power components, although a delta of 3Hz is seen 10s after the transition and spindles 5s after that. By contrast the CMT has a low power theta during wakefulness, and switches to delta and spindles at the transition. Interestingly, there is a change in delta frequency 15s after the transition, from 3Hz to 2Hz, analogous to the delta frequency shift at LORR. This delta frequency switch does not appear to be replicated in the cingulate. Figure 5.2c shows the averaged cross wavelet transform of the cingulate and CMT for all Wake-to-NREM transitions. Covariant power before Wake-to-NREM transition is in delta below 2Hz. At the transition the covariant power switches to delta with a peak at 3Hz with spindles. The power covariance increase 15s after transition, which corresponds to the delta frequency shift in the CMT. Figure 5.2d shows the averaged phase correlation for significant covariant power between the cingulate and CMT for all Wake-to-NREM transitions. There is little significant covariant power before the onset of NREM. The cingulate and CMT are in phase for delta during NREM.
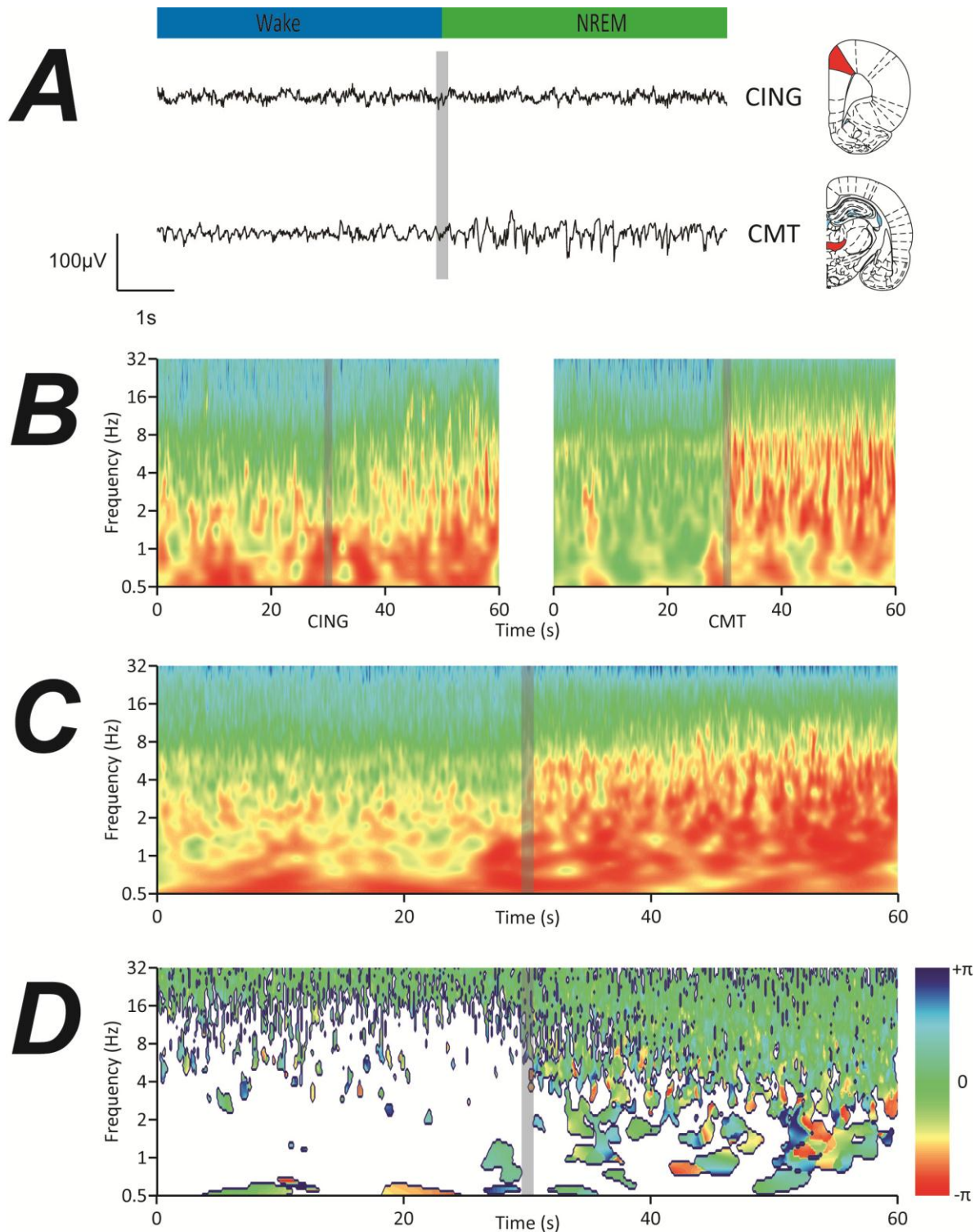
Figure 5.2 Abrupt changes in the CMT prior to cingulate at NREM onset.
A. Typical waveforms for cingulate and CMT at onset of NREM. Little change in amplitude or frequency occurs in the cingulate at the onset of NREM. The CMT has a sudden increase in waveform amplitude and concurrent slower component in the waveform. **B.** Averaged Morlet power spectra for cingulate and CMT. Before NREM, the cingulate has low delta power. Sleep spindles and increases in higher frequency delta power do not occur until 10s after NREM has started. The CMT shows theta as with active wakefulness and switches to delta and spindles at NREM. **C.** Averaged cross wavelet transform for cingulate and CMT. Covariant power is low prior to NREM. At NREM delta covariant power increases. Covariant power does not occur within spindles until 10-15s after NREM onset **D.** Averages phase correlation for cingulate and CMT. There is little significant covariance prior to NREM the phase difference after NREM is -0.022 ± 0.029 radians.

Figure 5.3a shows typical waveforms for barrel and VB during Wake-to-NREM transitions. Both waveforms consist of low amplitude fast frequency oscillations during this period. Figure 5.3b show averaged Morlet power spectra for barrel and VB. The barrel has low power in theta prior to the transition. VB also has theta during the conscious phase. This continues after the transition and becomes delta and spindles 15s after the Wake-to-NREM transition. This timing corresponds with the switch in CMT frequency from 3-2Hz. The delta in VB is 2Hz. Figure 5.3c shows the averaged cross wavelet transform for all Wake-to-NREM transitions for barrel and VB. Covariant power in theta is present during waking and continues through the transition to change to delta and spindles 10-15s after the transition. Figure 5.3d shows the averaged phase correlation between barrel and VB. The signals are in phase for theta and for delta.
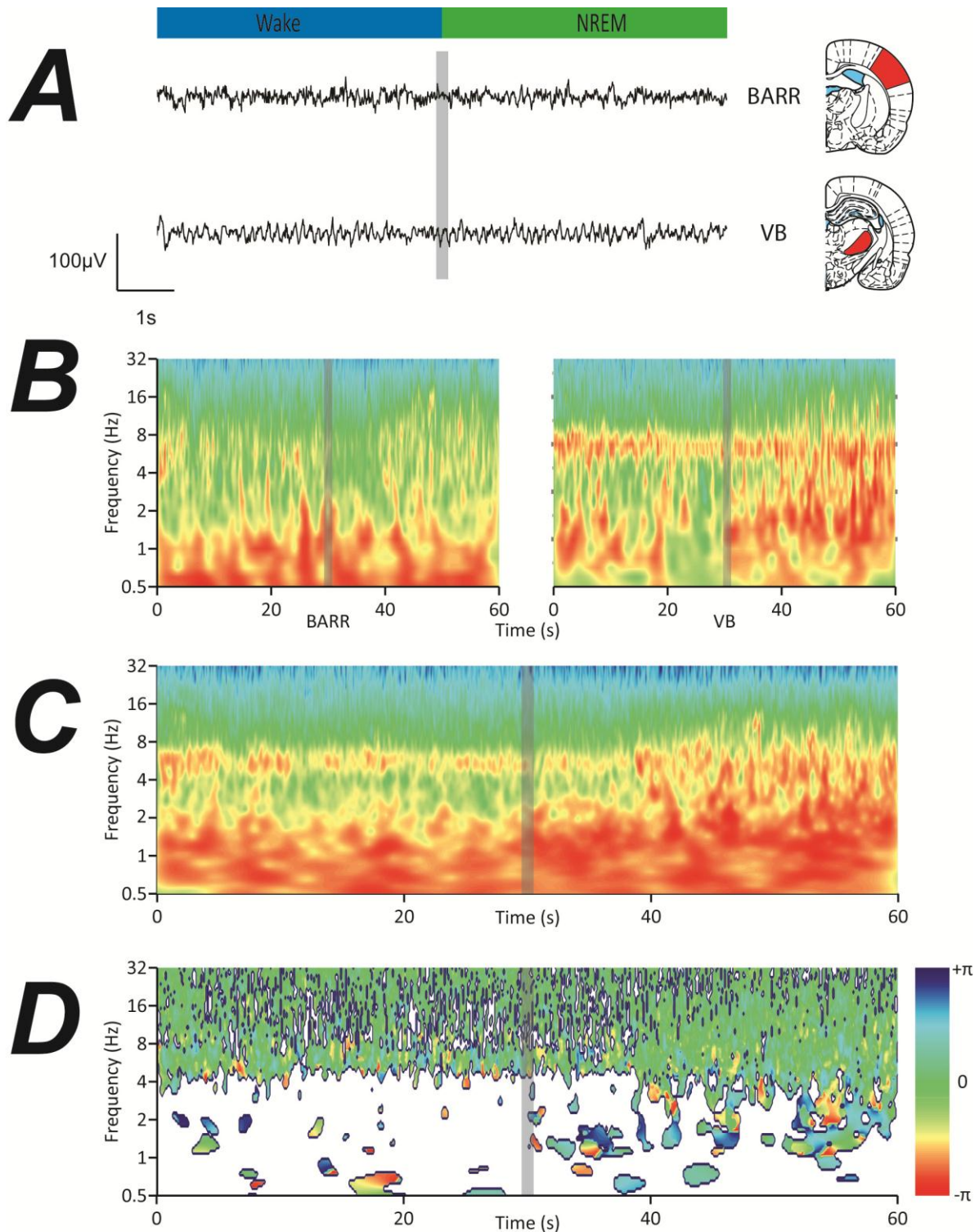
Figure 5.3 Concurrent changes in barrel and VB occur after CMT in NREM. A.
Typical waveforms for the barrel and VB during Wake-to-NREM transitions as scored by CMT. There is no change in appearance of the waveform either side of he scored transition. **B.** Averaged Morlet analysis for transitions. Both barrel and VB have low powered theta and transition to delta occurs 15s after the Wake-to-NREM transition scored by the CMT. The barrel has low delta frequency high power. **C.** Averaged cross wavelet transform for barrel and VB. Covariant power in theta continues to 15s after the Wake-to-NREM transition point. Covariant power in delta and spindles occurs 15s after NREM starts. **D.** Averaged phase correlation of barrel and VB. On average the signals are in phase for both theta and delta.

5.2.2 Corticocortical relationship

For Wake-to-NREM transitions, the barrel and cingulate did not have covariant power in delta at 2-4Hz until 10s after the scored transitions into NREM. Figure 5.4a shows the averaged cross wavelet transform and the phase correlation spectrum for the cingulate and barrel cortex. No covariant power is evident within theta. The signals were on average in phase for this delta.

5.2.3 Thalamothalamic relationship

The CMT and VB had a small correlation in theta prior to NREM. Figure 4.12b shows the averaged cross wavelet transform and the phase coherence spectrum for the CMT and VB for propofol LORR. At the onset of NREM, covariant power in delta increases. Maximal covariant power in delta and the start of covariant power in the spindle range occurs 10-15s after the scored transition into NREM.
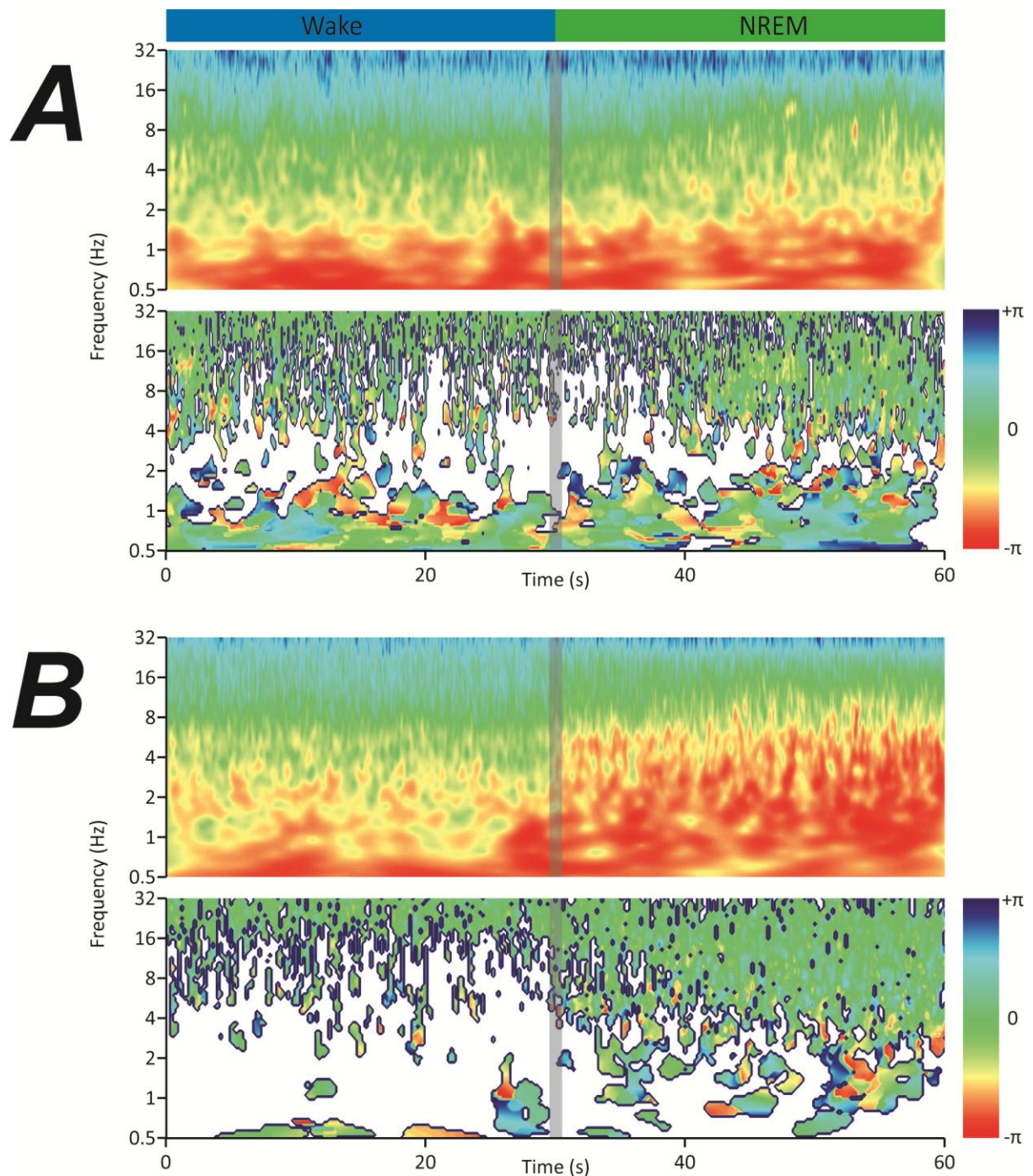
Figure 5.4 Corticocortical and Thalamothalamic coherence in Wake-to-NREM transitions
A. Averaged cross wavelet transform and phase correlation spectra for cingulate and barrel. Covariant power in delta of 3-4Hz does not occur until 10s after transitions. Covariant power less than 2Hz occurs throughout transition. The cingulate and barrel are in phase for the 3-4Hz delta. **B.** Averaged cross wavelet transform and phase correlation spectra for CMT and VB. Covariant power is present in theta before transition. After transitions covariant power is in delta and spindle ranges.

5.3 Electrode Placement

Following completion of all LORR and sleep experiments, animals were deeply anaesthetised and brains fixed by transcardial perfusion of ice cold PBS followed by 4% formalin. Brains were removed, post-fixed, sliced and stained with Cresyl violet to confirm the location of the electrode tips by their tracts. All electrodes included in the analysis were correctly positioned as shown below.
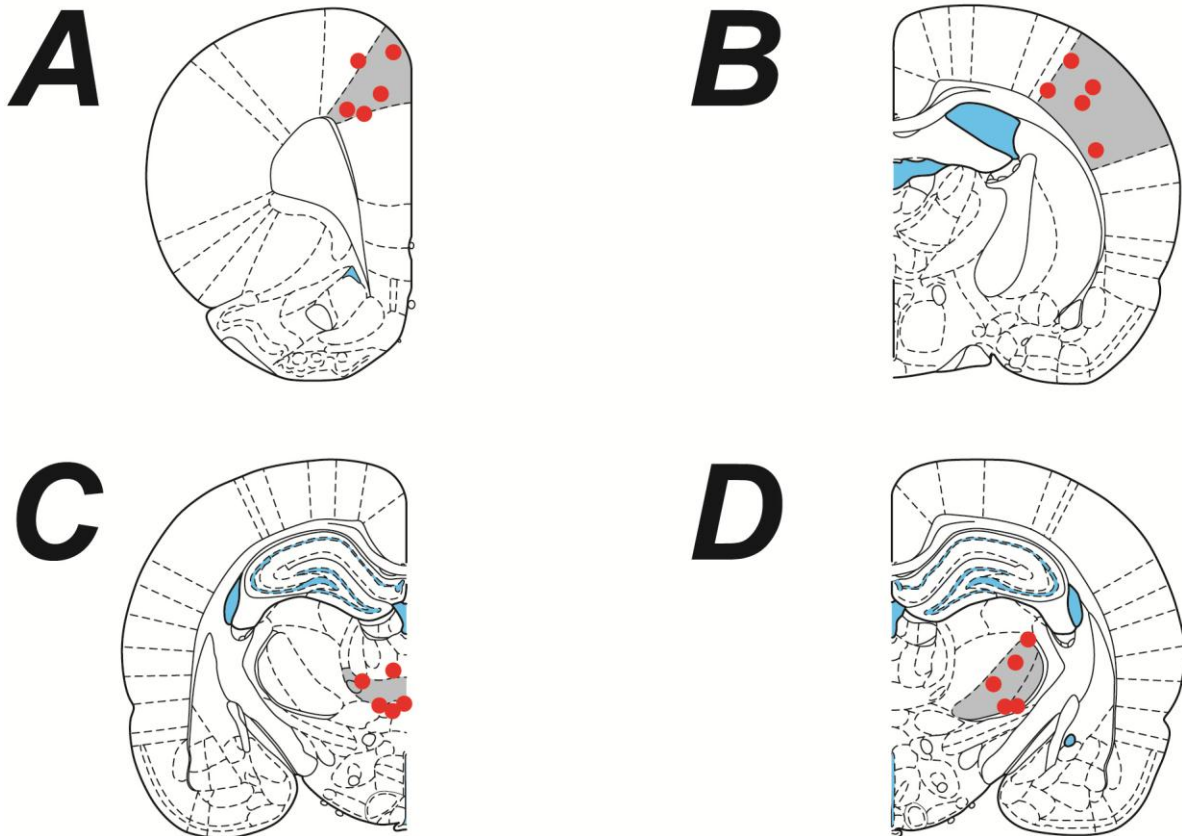
Figure 5.5 Electrode tip placement determined by tracts in histological slices.
Only animals with correct electrode placement were used for data analysis. Schematics shown for cingulate (**A**), barrel (**B**), CMT (**C**), and VB (**D**).

6   Discussion

6.1 Rationale for Study

There have been many previous studies looking at various electrophysiological aspects of sleep and anaesthesia. However the majority of these studies have investigated sleep and anaesthesia during steady state conditions (Crunelli *et al.*, 2010; Dossi *et al.*, 1992; Steriade *et al.*, 1993b). Pharmacological (Alkire *et al.*, 2009; Alkire *et al.*, 2007) and brain imaging (Kinomura *et al.*, 1996) studies have implicated the role of the thalamus in regulating wakefulness, as have studies in human patients with brain injury (Schiff, 2008). However, more recent brain lesion studies have questioned the importance of the thalamus in this regulatory role (Constantinople *et al.*, 2011; Fuller *et al.*, 2011).

Recently there have been several studies that have investigated electrophysiological changes during transitions from wakefulness in to sleep or anaesthesia (Gervasoni *et al.*, 2004; Hwang *et al.*, 2010; Magnin *et al.*, 2010; Velly *et al.*, 2007). They come to differing conclusions on the dynamics of the thalamocortical system for the onset of sleep and anaesthesia.

Velly et al. (2007) recorded local field potentials from the cortex and subthalamic nucleus in patients with advanced Parkinson Disease during induction of anaesthesia with propofol. They concluded that cortical parameters of SEF_{90}, MPF and Da reduced in the cortex prior to the subthalamic nucleus by approximately 10 minutes. These parameters did not reduce to comparable levels in the subthalamic nucleus until after the patients were deemed to have become unconscious. SEF_{90} (Spectral edge frequency) is defined as the frequency below which 90% of the total power of a given signal is found. MPF (median power frequency) is defined as the frequency below which 50% of the power is found. Both are often used as a correlate of depth of sleep and anaesthesia (Drummond *et al.*, 1991). Dimensional activation (Da) is a measure of the consistency between points found within a signal and is therefore determines a degree of entropy. A high Da score indicates more variability within a signal and is correlated with wakeful EEG, whereas a low Da score indicates a less chaotic signal, likely to be produced by a more synchronised network as occurs during sleep. By contrast, Magnin et al. (2010), recording from patients with refractory epilepsy, demonstrated that at the onset of natural sleep, the same parameters reduced in the thalamus on between 30s and nearly 5 minutes before the cortex in nearly all patients. Both of these studies are compromised by recording from physiologically abnormal brains in patients that were also taking medication.

There are two notable investigations into the role of the thalamus in unconsciousness in animals. Hwang et al. (2010) used the forced walking test in mice and recorded from primary sensory and motor cortices and ventrolateral thalamus during propofol and ketamine/xylazine loss of motion (LOM). The waveforms in the study suggest that changes in both the thalamus and cortex occur simultaneously around LOM and that the reduction in SEF did not occur until several seconds after LOM. This may indicated that LOM is not a suitable surrogate for loss of consciousness for some forms of anaesthesia. Gervasoni (2004) investigated sleep in rats, also recording from the primary sensory cortex and ventral posterior thalamus. This study showed a high degree of synchrony across the forebrain during different behavioural states.

None of these studies have attempted to dissect the importance of differing parts of the thalamus with regards to loss of consciousness. Furthermore conflicting opinion remains as to the importance of the thalamus for LOC. The object of this study was to determine how the thalamus and cortex interact during transitions into unconsciousness of both natural sleep and anaesthesia, using EEG and depth recordings from chronically implanted rats.

6.2 Characterising EEG Signatures for Sleep and Anaesthesia

Rats chronically implanted with skull screw electrodes were used to characterise transitions from wakefulness to unconsciousness for both natural sleep and for anaesthesia. Sleep recordings were conducted in the home cage during the light period, 7:30pm – 7:30am. Anaesthetic LORR recordings were conducted in a continuously rotating chamber using a remotely operated intravenous infusion.

6.2.1 Anaesthetic Measurements

LORR was used as a measure of consciousness since data from humans suggests that LOC, defined as the failure to respond to a verbal command, occurs as similar blood drug concentrations as LORR in animals (Franks, 2006). Furthermore in this paradigm LORR indicates the failure to respond to an external stimulus. Numerous protocols exist for assessing LORR. Hwang et al. (2010) compared the latency to LORR with latency to LOM in the forced walking test. Whilst no difference was found with propofol, ketamine/xylazine resulted in a significant increase in time for LORR compared to LOM. Since the immobility of actions of α_2-agonists has been demonstrated to result in large part from actions on spinal motor neurones, this would account for the discrepancy seen in this study. To this end, LORR in a continuously rotating tube was deemed a better end point to investigate LOC in animals, particularly for agents such as dexmedetomidine.

The dynamic effects dexmedetomidine on EEG rhythms were investigated. Many previous experiments have shown dexmedetomidine to produce delta oscillations and spindles (Bol *et al.*, 1997; Huupponen *et al.*, 2008; Mason *et al.*, 2009) both cardinal signatures of the thalamocortical system (Steriade *et al.*, 1993c). Unlike many anaesthetics used to induce LOC, dexmedetomidine may be given as an intravenous bolus but does not produce LORR until sometime afterwards, in this case over one minute. At present there is not a mechanistic explanation for this, although this may represent a delay of in equilibrating the brain drug concentration with that of blood. However it may also indicate the time taken for run-down of the noradrenergic system and therefore have important implications in determining the mechanism for LOC. The intravenous dose of 20µg/kg has been used previously as a reliable dose for inducing LORR in rats (Zecharia *et al.*, 2009). Dexmedetomidine produced delta oscillations and spindles prior to LORR. The production of robust delta oscillations in the conscious rat by dexmedetomidine has previously been reported (Bol *et al.*, 1997). The finding of a switch in the delta oscillation at LORR is a novel finding. The peak power frequencies immediately prior to and after LORR in these experiments were significantly different. Since this shift occurred over a short time frame, it is unlikely to be due to a large change in brain drug concentration. Little is known about the mechanism determining the frequency of thalamocortical oscillations. NREM and differing anaesthetics appear to clamp the slow and delta oscillations at different frequencies

(Steriade *et al.*, 1993e). This frequency switch may represent a change in the thalamocortical network that induces LOC, although much more detailed experiments would be required to investigate this. Spindles in dexmedetomidine hypnosis have previously been reported in humans (Huupponen *et al.*, 2008; Mason *et al.*, 2009) and rats (Bol *et al.*, 1997; Huupponen *et al.*, 2008). Interestingly, the report in paediatric patients (Mason *et al.*, 2009) showed that dexmedetomidine could produce sleep spindles in patients that were heavily sedated but still deemed to be conscious and were comparable to stage II NREM. An in depth analysis of dexmedetomidine spindles revealed them to be similar in frequency but longer in duration than those in NREM, and also that the spindle event frequency of dexmedetomidine was greater than for NREM (Huupponen *et al.*, 2008), although this may be related to the depth of unconsciousness achieved by dexmedetomidine administration and the degree of inhibition of ascending arousal (Amzica *et al.*, 2002). Dexmedetomidine has been proposed to exert its effects by blocking the presynaptic α_{2a} receptors of the locus coeruleus (Correa-Sales *et al.*, 1992). The reticular thalamus, which is responsible for the initiation of spindles (Steriade *et al.*, 1987), receives many ascending excitatory inputs (Pare *et al.*, 1988). This may explain why blockade of noradrenergic transmission by dexmedetomidine produces spindles.

The dynamic effects of propofol on EEG rhythm were investigated. Previous studies have demonstrated that propofol produces delta oscillations in rats and man during heavy sedation and following LOC (Dutta *et al.*, 1997; Gugino *et al.*, 2001; Jugovac *et al.*, 2006). The mean dose of 11.1mg/kg initially appears higher than previous reports for LORR in rats (Zecharia *et al.*, 2009), however, it is important to consider that the total dose used in these experiments was given over more than 30s, rather than as a bolus. This was important to observe dynamic changes in the EEG rhythm rather than produce instantaneous LORR and associated EEG changes. Previous studies investigating the pharmacodynamic effects of propofol on rat EEG have looked at steady state plasma drug concentrations (Dutta *et al.*, 1997) rather than dynamic infusions as in this study. Nevertheless, there are noticeable similarities in the EEG changes, namely that as the dose of propofol infused increases, there is a reduction theta power and an increase in delta power. In the present study, this is demonstrated as a continuous change in frequency over time, suggesting that the EEG frequency may be set by propofol in a dose dependant manner. The observation of a switch in frequency at the point of LORR is novel. This is particularly interesting given that the increase in brain drug concentration over this short time period must presumably be small, and indeed, infusion was stopped at LORR. Furthermore a comparable frequency shift was also seen in dexmedetomidine LORR. The frequency in peak power was from the delta band both immediately prior to and after LORR. The peak power frequencies were different for propofol and dexmedetomidine; this may

indicate different neural mechanisms leading to LORR. Propofol was also shown to induce spindle oscillations prior to LORR and interestingly the frequency of the spindles decreased with an increase in propofol infusion. This frequency change stopped at LORR, although this is likely to be due to termination of the infusion. Sleep spindles have previously been reported in propofol anaesthesia (Bergamasco *et al.*, 2003; Ferenets *et al.*, 2006; Feshchenko *et al.*, 1997; Leslie *et al.*, 2009; Wolter *et al.*, 2006). However, most of these studies investigate spindles at deep anaesthesia and rather than transitions in to anaesthesia. One study (Ferenets *et al.*, 2006) compared spindles of NREM to spindles of propofol. Spindle events of the two classes were different in several ways. Whilst spindles in NREM have a classically described waxing and waning appearance (Bazhenov *et al.*, 2000; De Gennaro *et al.*, 2003), propofol spindles have an abrupt onset and taper off in amplitude. Furthermore, propofol spindles are of a higher frequency than during NREM, although the frequency of spindles in NREM does vary throughout NREM. This difference in spindle frequency between NREM and propofol anaesthesia was reproducible in this study. Mechanistic investigations into spindles have been conducted in NREM and barbiturate anaesthesia (Contreras *et al.*, 1996b; Fuentealba *et al.*, 2004b) however no such studies have been performed detailing propofol induced spindles, although given the intimacy of spindles with the slow oscillation (Amzica *et al.*, 2002), this difference in frequency may be of the same origin as the difference in frequency in the slow oscillation determined by various anaesthetics (Steriade *et al.*, 1993e). The slow oscillation frequency increases depth of sleep and anaesthesia increases (Amzica *et al.*, 2002) as the decrease in ascending arousal reduces the duration of the UP state and so hastening the oscillation. The reticular thalamus also receives ascending excitatory projections (Pare *et al.*, 1988) and may therefore also affect spindle frequency. This would suggest a hypothalamic target for propofol.

The dynamic effects of midazolam on the EEG were also investigated. Midazolam has been shown not to increase delta power in the rat EEG at LORR (Jugovac *et al.*, 2006) and modelling data suggests that it has a preferential effect on the cortex rather than thalamic relay neurones (Judge *et al.*, 2009). In the present study, experiments confirmed that whilst midazolam did produce a robust delta oscillation prior to LORR, there was no change in peak power frequency at LORR, confirming previous findings. Interestingly there is a notable change in delta frequency and power that occurred 10-15s after LORR. Whilst some spindle events were seen in the EEG following LORR, these were not comparable in number to dexmedetomidine or propofol. Midazolam has been shown to produce spindles (Feshchenko *et al.*, 1997), although clearly in the present study, does not do so prior to LORR unlike propofol and dexmedetomidine. It seems from these findings unlikely that midazolam is recruiting the thalamocortical system to cause LORR, indeed recent reports in humans suggest that

midazolam causes LORR by a direct action on the cortex disrupting long range synchrony (Ferrarelli *et al.*, 2010).

6.2.2   Sleep Measurements

A previously defined algorithm was used to score sleep recordings as Wake, NREM and REM (Costa-Miserachs *et al.*, 2003). This algorithm designates a score to an epoch of EEG data, dependant on the ratio of theta to delta and on EMG amplitude.

Conscious EEG activity was characterised by a theta frequency of 7Hz, there was no difference in frequency of theta recorded in the home cage compared to in the rotating cylinder. The theta recorded during REM was of a higher frequency of 8Hz. Both of these findings are consistent with the findings of Kramis et al. (1975) who first noted that there are two types of theta oscillation in the rat brain. Whilst pharmacology was not performed to characterise the theta rhythm fully, both frequencies are consistent with the type I or atropine resistant theta described in this investigation. Type II theta is by comparison rare in un-anaesthetised rats and is seen during alert immobility or prior to movement (Sainsbury *et al.*, 1987).

Wake-to-NREM transitions were characterised from skull recordings over the parietal cortex. Interestingly the transitions from theta to a predominantly delta rhythm of sleep appeared to occur instantaneously. The EMG amplitude however would move to baseline noise around 10s prior to this transition. Previous reports have suggested that inactive conscious rats have an EEG consisting of large irregular activity (LIA) (Vanderwolf, 1969) essentially large delta power, although this does not occur in these recordings. However the LIA phenomenon could well explain the delta bursts seen during both wakefulness in the home cage and prior to drug administration in the LORR experiments. The EEG of NREM was found to consist predominantly of delta oscillations; however the waveform also had significant power in the theta range as well as the spindle range. Interestingly, the slow (<1Hz) oscillation was not apparent during the early stages of NREM, however the 3dB point of the Neurologger for the high pass filter is at 0.4Hz (Robledo, unpublished findings). So it is unlikely that the slow oscillation of 0.2-0.3Hz (Steriade *et al.*, 1993e) of sleep would be readily identifiable in the current study. The peak power frequency of early NREM was found to be 3-4Hz delta.

Gervasoni et al. (2004) have investigated LFP changes in the thalamocortical system using wavelet analysis, however the time scale over which the data was plotted does not allow accurate interpretation of the transitions. In this study, the nature of the Wake-to-NREM transitions was found to be abrupt in the EEG. The EMG findings were generally not so abrupt, with the EMG

amplitude tapering to baseline several seconds prior to the onset of NREM. It is of course impossible to determine when exactly the rat becomes unconscious with NREM, particularly since dexmedetomidine produced delta prior to LORR. The Gervasoni et al. (2004) study used the polygraph and visual behavioural analysis to score sleep. However the EMG data from the current study suggest that visual behavioural analysis of sleep is likely to show the onset of NREM occurring before the dramatic theta-to-delta transitions of the EEG.

The use of Morlet wavelet analysis has enabled an accurate time dissection of brain state transitions. The Morlet analysis of the Wake-to-NREM transitions shows a clearly defined theta rhythm prior to NREM. However the spectrogram of NREM seems to show equal power across the delta, theta and spindle ranges, unlike the FFT power spectrum, which clearly shows a peak power in delta with power decreasing with increasing frequency in a near linear fashion. This discrepancy is due to scaling in the Morlet power spectrum. Frequency is represented on a harmonic scale, and so contours in the z-axis can be the same for large power over a small frequency range (e.g. 3-4Hz of delta) as low power over large frequency ranges (e.g. 5-12Hz theta). Therefore FFT power spectra, whilst lacking sensitivity in the time domain, remain a useful adjunct to Morlet analysis.

Wake to NREM transitions were shown in the current study to be represented in the EEG by abrupt theta to delta transitions. This is a novel but not necessarily unexpected finding. There has been a great deal of investigation into sleep mechanisms in recent years focusing on hypothalamic pathways (Saper *et al.*, 2010). In particular a theory of hypothalamic sleep switching has been championed by Saper (2001) and revolves around excitatory nuclei of the brainstem including the locus coeruleus (noradrenergic), tuberomammillary nucleus (histaminergic) and dorsal raphe (serotinergic) providing competitive feedback to the sleep active, GABAergic ventrolateral preoptic nucleus. These nuclei all provide ascending projections to the thalamocortical system and other higher brain areas, and may be responsible for the sudden transitions observed in the EEG.

The spindles seen in the EEG of NREM for this study are at the same frequency as those in dexmedetomidine LORR experiments but lower than those of propofol, agreeing with previous observations (Ferenets *et al.*, 2006; Huupponen *et al.*, 2008).

6.2.3   Correlations of Sleep and Anaesthesia

Previous investigations in human patients have shown marked similarities in the EEG of dexmedetomidine sedation and stage II sleep (Huupponen *et al.*, 2008; Mason *et al.*, 2009). Importantly in these studies subjects remained responsive to stimuli and were therefore conscious, a cardinal feature of dexmedetomidine sedation (Souter *et al.*, 2007; Venn *et al.*, 1999).

The current study showed Wake-to-NREM as being characterised by a theta-to-delta switch and dexmedetomidine LORR by delta-to-delta switch. To investigate whether dexmedetomidine sedation prior to LORR was similar to NREM, dexmedetomidine LORR recordings were analysed for theta-to-delta switches prior to LORR. The theta-to-delta switches in both the dexmedetomidine experiments and the Wake-to-NREM transitions had the same peak power frequencies for theta and delta. Whilst NREM consisted of high delta power, moderate theta power and spindles immediately after the switch, in dexmedetomidine, there were very few spindles. This may have been due to the animals receiving constant stimulation in terms of the rotating cylinder in contrast to animals in the sleep experiments that were in their home cage. Behavioural end points other than LORR were not recorded during LORR experiments; therefore the theta-to-delta switch of dexmedetomidine cannot be attributed to the start of sedation per se. Furthermore markers of sedation such as spontaneous activity and neck angle would be difficult to assess accurately in an animal that is constantly being stimulated to move. However given that dexmedetomidine has been demonstrated to recruit endogenous sleep pathways (Nelson *et al.*, 2003), the theta-to-delta switch in dexmedetomidine and NREM may indicate the same neuronal pathways being activated. Dexmedetomidine LORR was shown to be characterised by a delta frequency switch. Given that dexmedetomidine sedation appears to present early stage NREM (Huupponen *et al.*, 2008; Mason *et al.*, 2009) periods of NREM were investigated for similar switches in delta frequency. Whilst these switches were clearly visible in the EEG, they were of different frequency from those seen in dexmedetomidine LORR. Since no behavioural correlates were measured during sleep recordings, these frequency switches cannot be attributed to behavioural changes. Furthermore no change of EMG was seen to indicate that any postural changes would accompany the change in frequency. Given the manner in which dexmedetomidine LORR was measured, animals remained responsive to stimuli prior to LORR and this responsiveness halted at the point of LORR. Whilst greater stimuli or noxious stimuli may have the potential to cause arousal at this point, LORR certainly indicated a change in rousability. It is possible then that the delta frequency switch in NREM may represent a change in sleep stage to a deeper plane that requires a greater stimulus for arousal. Clearly further in depth behavioural investigation is required to investigate this.

6.3 Methodology for Depth Electrode Recording

Local field potentials have been recorded in brains using a variety of techniques and configurations. In the current investigation, the tether free set up required a ground electrode to be on the animal. For recording during active behaviour, positioning of the ground on an ear lobe or skin was unsuitable; furthermore screw electrodes positioned over the nasal vomer bone had sufficient electrical activity as to contaminate signals recorded from depth electrodes. This was demonstrated in a unipolar recording with respect to true ground. Since in a differential recording both the recording electrode and reference electrode both oscillate with respect to ground, important consideration needs to be given to placement of ground and reference electrodes. The issue of contamination of a depth recording from a cortical reference electrode has previously been considered by Vyssotski et al. (2006). This investigation coined the term "reference contamination" to describe electrical activity in a local field potential that was actually from a distal site. Furthermore they noted that the waveform was subject to a greater number of mechanical artefacts when the reference electrode was located on the skull in freely moving animals. The solution to this issue was to locate the reference electrode on the same depth electrode array as the LFP was recorded from. In practical terms, the same methodology was applied to the current study.

Bipolar recording in this fashion is rarely employed for LFP recordings, since many investigators utilise a tethered system for recording electrode activity, which allows for oscillation with respect to true ground. A tethered recording system would be severely limiting for LORR experiments in the rotating cylinder, although interestingly, the use of a lead line to infuse anaesthetic agents into a vascular access port on the back did not appear to hinder animal movements.

Whilst bipolar differential recording was suitable and necessary in this case, it is not without limitations. Bipolar recording necessitates that for a signal to be measured that is of significant amplitude above background noise there is an electrical potential between two localised points, in this case separated by 125µm. Certain oscillations such as the slow oscillation occur with such widespread synchrony that differential recording may cancel out the signal in the resulting waveform (Amzica *et al.*, 2002). This coupled with filtering characteristics of the Neurologger recording device may account for the failure to detect the slow oscillation in NREM in these experiments.

6.4 Coherence Analysis

The use of cross wavelet transform and phase difference analysis is relatively unused for neurophysiological data, although some recent investigations have employed it (Gervasoni *et al.*, 2004; Hu *et al.*, 2010; Li *et al.*, 2007).

Recording from different parts of the hippocampus Li et al. (2007) reported a change in power coherence and phase difference when changing from a pre-ictal to inter-ictal stages of a seizure. The cross wavelet transform is a measure of power bi-coherence for two signals (Grinsted *et al.*, 2004). Changes in power coherence are interpreted as an increase in synchronization in brain regions at a given frequency and time point. However high power coherence can be calculated is the power in one signal is very high, despite the power in the other signal being small (Gervasoni *et al.*, 2004; Grinsted *et al.*, 2004).

The phase difference of two signals has so far yet to be given a neurobiological mechanism. Physical explanations in terms of the waveform have been given (Li *et al.*, 2007) describing one waveform as "leading" the other. An interpretation of this may be that for a given oscillation frequency, if one neural population "leads" another, then it is likely that that neural population initiates the oscillation or is further upstream from the second population. The phase difference is therefore presumably the result of a delay in synaptic transmission from one population to the other. For example, given the accepted genesis of sleep spindles (De Gennaro *et al.*, 2003; Steriade *et al.*, 1987), one would expect that the phase difference in the 7-14Hz range between the reticular thalamus and the cortex would indicate the reticular thalamus "leading" the cortex. This causal relationship is however yet to be established.

Nonetheless, the use of power and phase coherence is becoming a useful tool to investigate neural networks and suggest models of causality in behavioural states (Gervasoni *et al.*, 2004).

6.5 Characterising Anaesthesia by Depth Electrode Recording

Recently investigators have started to examine short term changes in electrical brain activity during transitions from wakefulness to anaesthetic induced unconsciousness (Hwang *et al.*, 2010; Velly *et al.*, 2007). The conclusions drawn from each of these studies are contradictory. Velly et al. (2007) concluded that cortical deactivation occurred at LOC for propofol and sevoflurane anaesthesia in humans, whereas Hwang et al. (2010) demonstrated simultaneous changes in the thalamus and cortex for propofol and ketamine/xylazine LOM in mice. Both of these studies are subject to criticism in the methodology. Firstly The Velly study (2007) recorded from depth electrodes in Parkinson's patients. The location of the recording site could not be verified, furthermore the recording site was postulated to be the subthalamic nucleus, not actually a part of the thalamocortical system. Secondly, the analysis of dimensional activation assesses uniformity of an EEG signal (Rey *et al.*, 2007). Whilst this may be a measure of the chaos within a waveform, it does not describe the frequency changes occurring within the waveform as the brain transits into unconsciousness. Indeed a waveform that starts as a theta rhythm and changes to delta with sporadic spindles is likely to be more chaotic. The waveforms shown in the Hwang study (2010) seem to be very similar to each other suggesting an issue with an overriding oscillation common to all of the recording sites, as investigated in this study. Furthermore, Hwang et al. (2010) used to waveform data to illustrate the validity of a LOM test, rather than investigate changes in the brain per se.

Anaesthetic induced LORR was investigated for dynamic changes in LFP, power coherence and phase difference for propofol and dexmedetomidine. These drugs were chosen from the findings previously in this study for showing cardinal EEG signs of thalamocortical activity, namely delta and spindles, and changes in thalamocortical activity at LORR.

6.5.1   Active Wakefulness

The EEG previously shown in this study recorded from the occipito-parietal cortex demonstrated a high power theta oscillation with bursts of delta. Notably LFP recordings recorded from the barrel cortex did have a discernable theta rhythm, but with a much greater degree of delta. This is consistent with the findings of Gervasoni et al. (2004). Intracellular studies have shown difference in cortical oscillations dependant on active wakeful states, with quiet wakefulness resulting in low frequency activity (Petersen *et al.*, 2003). Interestingly, the cingulate cortex showed very little theta rhythm power and had a predominantly delta rhythm during consciousness, consistent with previous findings (Young *et al.*, 2009). Both the CMT and VB showed prominent theta oscillations, and appear similar to the EEG findings of active consciousness.

For all relationships analysed within the thalamocortical system, theta was in phase. Active theta is considered to be generated by the septo-hippocamal network (Buzsaki, 2002). Since the neocortex and thalamus both have extensive connectivity to the hippocampus, it is likely that the theta seen in this data is in phase, as both cortex and thalamus are being driven at theta by the hippocampus (Young *et al.*, 2009). Interestingly, there is little significant covariant power within the cortex during wakefulness. Recent findings have shown that the cortex has a long range zero lag synchrony at the theta frequency (Gollo *et al.*, 2011). This lack of significant coherence is presumably due to the large delta and small theta power in the cingulate.

6.5.2 Dexmedetomidine LORR

EEG findings earlier in this investigation showed that dexmedetomidine produced a robust delta prior to LORR and at LORR there was a delta frequency shift. This pattern was reproduced in the cortex and CMT, although not in VB. In VB there was a theta to delta switch at LORR. The CMT had a mixture of theta and delta prior to LORR. This is unlikely due to a differential sensitivity to dexmedetomidine within the thalamus, given the limited distribution of the adrenergic α_{2a} receptor (Nicholas *et al.*, 1993) and that the peak power frequency after LORR is the same in all 4 brain areas. VB receives numerous projections from the brainstem, the majority being from the trigeminal nucleus which carried sensory information from the vibrissae (Rhoades *et al.*, 1987) but none have been reported from the hypothalamus and pons where dexmedetomidine is thought to exert its effects (Correa-Sales *et al.*, 1992). By contrast, the midline and intralaminar nuclei receive significant ascending arousal from the hypothalamus, although the majority of this innervation is cholinergic (Jones *et al.*, 1985; Levey *et al.*, 1987). Further to this, given that the only ascending projections to the barrel cortex come from VB, it would be expected that the barrel cortex and VB would mirror each other in the frequency and time domain. However, the barrel cortex also receives a large number of connections from within the cortex (Lubke *et al.*, 2007) which is likely to account for the discrepancy during the sedated phase prior to LORR. Blockage of noradrenergic but not cholinergic drives can create a quiescent state within the cortex during wakefulness (Constantinople *et al.*, 2011) which would account for the synchronized delta oscillations during active wakefulness seen within these recordings. The reason for the importance of the noradrenergic drive over the cholinergic in this matter is unclear. The CMT receives direct projection from the LC (Krout *et al.*, 2002), providing an indirect action for dexmedetomidine on the CMT. The frequency shift at LORR results in all four nuclei having a delta oscillation at the same frequency, reflecting a wide ranging synchrony in the brain. The frequency transition occurs at the same time in both cortex and thalamus. The thalamic recordings in chapter 3 recorded from the CMT with respect to the lateral geniculate and the oscillation prior to LORR was of delta with a prominent theta, in contrast to the

bipolar recordings of the CMT in chapter 4. This is likely to be representative of concurrent activity from both a first order and intralaminar nucleus, and further highlights the requirement for a localised reference electrode in this setup.

 A change in the phase difference between thalamus and cortex was demonstrated at LORR. The waveform of the CMT lead the cingulate prior to LORR, there was a phase shift at LORR whereupon the CMT continued to lead the cingulate, but at a lower frequency. Cell firing in the thalamus has been shown to occur before the cortex in the slow oscillation despite the slow oscillation originating in the cortex (Contreras *et al.*, 1995) and dynamic changes in phase have been reported in the hippocampus during the onset of seizure activity (Li *et al.*, 2007). A small change was seen in between VB and the barrel cortex. There was a change in phase between the CMT and VB over LORR. Under ketamine/xylazine anaesthesia (Slezia *et al.*, 2011) using thalamic unit recording and cortical delta oscillations a differential phase relationship was found between first and higher order relay neurones (VB and Po respectively) and the cortical delta. Furthermore, the phase relationship was found to be frequency sensitive, with an increase in frequency resulting in phase advancement. In these dexmedetomidine experiments, frequency reduction was analysed and the converse phase relationship was seen. In contrast to the Slezia paper, there was no phase difference seen in the spindle frequency range in this study. This may have been due to animals being at a different depth of anaesthesia or may be an artefact of the analysis, the phases being washed out in the averaging, due to the transient nature of the oscillation.

The cause of phase advancement is currently poorly understood. Recent findings show that corticofugal excitatory input to relay cells can activate a T-type calcium channel current, responsible for depolarisation of relay cell, thus increasing the probability of cell firing (Bessaih *et al.*, 2008). Furthermore, corticothalamic feedback has been shown to be important for spatiotemporal synchrony of thalamocortical oscillations (Contreras *et al.*, 1996a). Phase change in cortical networks has been demonstrated by altering depolarising current injection, which did not alter the rate of firing (Tiesinga *et al.*, 2010), this may implicate an important change in thalamocortical projections and connectivity to the cortex. Therefore the hypothesis for the frequency and phase change shown here is that a reduced corticothalamic drive decreases the probability of thalamic relay cell firing and so decreases the delta frequency and hence causes the change in phase. Why this should occur with such a dramatic shift in frequency remains unclear although a useful insight may be gleaned from modelling data. Sheeba et al. (2008) modelled the thalamocortical system as simplistic coupled oscillators. Whilst this model does not take account of the intricacies of the intrathalamic and intracortical networks, it shows that changing the coupling parameters between the two oscillators

can result in a sudden shift in frequency between both the thalamus and cortex. The scope of this paper was towards arousal and increase in the coupling results in an increase in frequency, opposite to this investigation. The concept of a decrease in coupling between the cortex and thalamus suggested by this modelling would coincide with the hypothesis stated above. Interestingly, there was only a small phase change within the cortex, the cingulate being ahead of the barrel in phase. This is a predictable observation since the delta wave in the cortex has been demonstrated to travel from frontal to occipital (Ermentrout *et al.*, 2001; Massimini *et al.*, 2004). This synchrony appears to be preserved at LORR and suggests that long-range cortical networks are disrupted to cause LORR.

6.5.3   Propofol LORR

In contrast to dexmedetomidine, there was not a prolonged delta oscillation prior to LORR with propofol. This is most likely in large part due to the pharmacokinetic profile of propofol, which equilibrates into the brain very quickly since it is highly lipophilic. In retrospect, the propofol experiments may have gleaned more informative data by incrementally infusing steady state doses to closer mimic the slow equilibration of dexmedetomidine.

The LFPs of the barrel, CMT and VB demonstrated a continuous ramp from theta to delta, reaching a steady delta frequency at LORR. By contrast the cingulate had a predominantly delta oscillation prior to LORR and seemingly increased in frequency after LORR to the same delta frequency as the other nuclei. The stabilisation of the delta frequency at LORR is most likely due to cessation of the propofol infusion coupled with the rapid equilibration in the brain. Propofol modulates the $GABA_A$ receptor of which the β_3 subunit appears critical for causing LORR (Jurd *et al.*, 2003). The β_3 subunit is widely expressed throughout the cortex, thalamus and hypothalamus. There is evidence to show that the hypothalamic nuclei are sensitive to propofol which is dependent on the β_3 subunit (Zecharia *et al.*, 2009). Given the widespread distribution of this dependant receptor subunit, the possibility that propofol has a global effect on the brain to cause LORR remains a possibility.

The theta oscillation dominant in all but the cingulate prior to LORR had significant coherence in the first order thalamocortical relationship and the intrathalamic. Following LORR there was a greater degree of significant power coherence between the cingulate and the barrel and the cingulate and CMT. There was a small change in phase difference between the barrel cortex and VB through LORR, as seen in dexmedetomidine. The CMT lead the cingulate after LORR in delta for propofol, although the phase difference was much less than that in dexmedetomidine LORR. The biggest change in phase was between VB and CMT. This phase change was the same as for dexmedetomidine. The advancement of phase in thalamic relay neurones is thought to involve a prolonged hyperpolarisation of groups of neurones allowing the activation of the calcium dependant T-current

leading to a low threshold spike (Bessaih *et al.*, 2008). Bursting of the relay neuron rides on the back of this calcium transit (McCormick *et al.*, 1990). It is therefore possible that for both dexmedetomidine and propofol LORR, that the CMT reaches a comparable state of hyperpolarisation with comparison to VB allowing the phase difference demonstrated here. Moreover the midline and intralaminar nuclei have numerous projections to within the thalamus and other limbic areas, and might therefore be regulating the bursting and therefore the delta oscillation within VB. Further investigation would be required to confirm this.

6.6 Characterising Sleep by Depth Electrode Recording

Recent investigations into sleep (Magnin *et al.*, 2010) demonstrated that the dimensional activation (Da) of the thalamus deactivated significantly before that of the cortex in human natural sleep. This is in stark contrast to similar experiments in humans during induction of anaesthesia (Velly *et al.*, 2007). This would suggest that the mechanisms for the onset of sleep are radically different to that of anaesthesia, despite evidence to the contrary (Nelson *et al.*, 2002). Recent investigations in rats suggest that there are simultaneous global changes within the forebrain at the onset of sleep (Gervasoni *et al.*, 2004). The latter investigation presented data to suggest that local field potential changes could not be discriminated over a matter of minutes as with the Velly and Magnin studies however the changes in the thalamus and cortex were not analysed on shorter time scales, nor were the different parts of the thalamocortical system.

The sleep scoring system used for data collected by skull screw electrode (Costa-Miserachs *et al.*, 2003) proved not to be useful for scoring Wake and NREM for depth electrode recordings from the cortex. This was due to the large power of delta, seen even during wake. The algorithm relies on discriminating Wake from NREM by the ratio of delta power to theta power. Therefore filtering of the barrel or cingulate waveforms does not rectify the problem. From one animal that was implanted with skull and depth electrodes, the CMT was found to be a better correlate of the skull EEG for Wake-to-NREM than was the cingulate, because of the distinction of theta during wakefulness. The CMT was used to score Wake-to-NREM transitions for all other animals. The reason for the cingulate cortex producing slow delta oscillations during consciousness is unclear, particularly since the EEG rhythm of wakefulness was theta, with transient delta bursts. Previous investigations (Leung *et al.*, 1987) demonstrated different oscillations for the cingulate during different active states. Walking, rearing and head movements were associated with theta in the cingulate, whereas grooming and quiet wakefulness were associated with delta. Since the periods before the onset of NREM are most likely to be quiet given the low EMG amplitude demonstrated in Chapter 3, this low frequency activity is a predictable finding. Further investigation (Borst *et al.*, 1987) showed that the theta in the cingulate was dependant on cholinergic drive, likely from the basal forebrain. This may implicate a reduction in the basal forebrain drive to the cingulate as being a necessary condition for LOC.

The main finding of this investigation was that the LFP changes for Wake-to-NREM occurred in the CMT before the cingulate, barrel cortex and VB. Interestingly, the cingulate had LFP changes following a couple of seconds after the CMT, the barrel and VB changed in synchrony several seconds after that. Such differential changes in LFPs during transitions into unconsciousness have

been reported before in humans (Magnin *et al.*, 2010; Velly *et al.*, 2007), although the differences seen in these studies were in the range of minutes, not seconds. Electrophysiological Wake-to-NREM transitions are now recognised to take only a couple of seconds in rodents (Takahashi *et al.*, 2010), but 10s of seconds to minutes in humans (Wright *et al.*, 1995), although the reasons for this are unclear. The abruptness of the electrophysiological changes reported here would be consistent with the concept of the flip-flop switch (Saper *et al.*, 2010). This consists of several hypothalamic nuclei providing mutual inhibition, of which the GABAergic VLPO is deemed to be the most important for the onset of sleep (Lu *et al.*, 2000). Direct evidence of electrophysiological change within the thalamus occurring prior to the cortex in rodents is novel, however Takahashi et al. (Takahashi *et al.*, 2010) did note a time lag between the cessation of LC firing and the onset of basal forebrain firing at the onset of NREM in rats. Cell firing rates from the basal forebrain and hypothalamus show a switching behaviour occurring at the onset of NREM (Saper *et al.*, 2010). The projections of these hypothalamic nuclei are widespread and include the thalamus and the cortex. The correlation of this firing rate with thalamocortical LFPs is yet to be investigated, but is likely to be important for determining the importance of the thalamus in regulating arousal in the cortex.

A possible reason for the time discrepancy between VB and CMT showing sleep oscillations at the onset of NREM could be to do with this differing modulatory activity of first and higher order nuclei. For example, higher order nuclei have modulatory inputs from the GABAergic zona incerta (Bartho *et al.*, 2002) giving an indirect cortical modulation to the cortex not present in the first order nuclei. Furthermore ascending arousal to first order nuclei causes depolarisation in first order but hyperpolarization in higher order nuclei (Mooney *et al.*, 2004). This may also provide a mechanism for the different behaviours of VB and the CMT during dexmedetomidine sedation.

Findings in chapter 3 suggested that frequency shift within NREM were analogous to dexmedetomidine LORR. In the depth electrode studies frequency shifts in the CMT during NREM coincided with the theta-to-delta shift in VB, both of which occurred during dexmedetomidine LORR. However these results were not augmented by the same shifts in phase difference as the signals were in phase through the NREM recordings.

6.7 Conclusion

The CMT has been proposed as a consciousness switch (Alkire *et al.*, 2009; Alkire *et al.*, 2007; Miller *et al.*, 1990), however significant evidence to the contrary has recently been published (Constantinople *et al.*, 2011; Fuller *et al.*, 2011). The observation in this study that the CMT enters an electrophysiological sleep like state prior to the cortex adds weight to the argument that the midline nuclei may be important in cortical arousal and consciousness. Many electrophysiological studies on thalamic regulated cortical arousal (Constantinople *et al.*, 2011) focus on investigations on the primary thalamocortical loop such as VB and the barrel cortex. The data presented in this study question the validity of those experiments in the context of *in vivo* behaviour, given that the primary thalamocortical system enters an electrophysiological state of sleep after the higher order system. Furthermore VB seems to be unaffected by dexmedetomidine during sedation.

Whilst previous studies have suggested a similarity between dexmedetomidine hypnosis and natural sleep (Huupponen *et al.*, 2008; Mason *et al.*, 2009), this study presents novel data showing that the onset of early NREM is analogous to sedation with dexmedetomidine, whereas dexmedetomidine LORR is analogous to a change in sleep stage. Further investigation of this phenomenon is required to determine whether behavioural endpoints of arousal correlate to the electrophysiological transitions.

This study does not determine the either the cortex or thalamus as a putative anaesthetic target, but does shed light in the dynamic interaction that the two have in transitions into unconsciousness. The concept of phase difference and coherence has been employed infrequently for analysis of electrophysiological data (Li *et al.*, 2007). As such, the mechanisms for changes in phase between connected neural populations are not understood. Given the timing in the phase changes demonstrated in this study, it is likely that it represents a change in thalamocortical connectivity which may be crucial in understanding the regulation of consciousness. Two recent studies have thrown doubt over the role of the thalamus as a consciousness regulator in favour of it acting as a read-out of cortical activity (Constantinople *et al.*, 2011; Fuller *et al.*, 2011). These investigations gave evidence for the role of the basal forebrain in regulating consciousness, and future experiments must also focus on this area.

A1 Appendix: Inbred mouse strain differential sensitivity to dexmedetomidine LORR

The α_2 agonist dexmedetomidine has been suggested to exert its effects via presynaptic α_{2a} receptors in the locus coeruleus (LC) of the pons (Lakhlani *et al.*, 1997). Dexmedetomidine may be of particular interest to study as there is evidence that it recruits endogenous sleep pathways to induce its sedative effects (Nelson *et al.*, 2003). The LC is the principal CNS outflow of noradrenaline and its projections are found ubiquitously. Because of this complexity, a more detailed mechanism for dexmedetomidine LORR has yet to be put forward. Furthermore, racemic medetomidine still produces LORR in noradrenaline lacking dopamine beta-hydroxylase knockout mice (Gilsbach *et al.*, 2009).

There have been several studies in recent years documenting differing sensitivities to anaesthetics between various inbred mouse lines (Homanics *et al.*, 1999; Sato *et al.*, 2006; Sonner *et al.*, 2000), although none of these have documented α_2 agonist sedation or anaesthesia. A strain difference to dexmedetomidine LORR may prove to be a useful tool in elucidating the mechanism of anaesthetic LOC.

A1.1 129/SvJ mice are insensitive to dexmedetomidine LORR

Hybrids of C57/Bl6 and 129/SvEV mice are sensitive to medetomidine LORR (Gilsbach *et al.*, 2009) yet some studies report hybrids of the 129/SvJ may respond unreliably to attempts to perform LORR with dexmedetomidine (Ref). To test the relative sensitivity of C57/Bl6 and 129/SvJ mice for dexmedetomidine LORR, dose response curves were generated for both strain. Dexmedetomidine was delivered intraperitoneally and animals were placed in a cylinder continuously rotating at 3.5rpm. At the end of 15 minutes animals were scored as positive for LORR if they had been rolled onto their backs and made no purposeful attempt to right themselves.

The ED_{50} for C57/Bl6 was 124.7 ± 16.4µg/kg however 129/SvJ mice did not lose righting reflex at doses up to 2mg/kg (Figure A2.1a). Sequences of the α_{2a} receptor for both strains of mice were identical (Ref). To begin investigating whether this difference may be due to a single or multiple gene difference, an F1 hybrid of the two strains was bred and tested for dexmedetomidine sensitivity. The F1 showed the same sensitivity as the 129/SvJ parents (data not shown), suggesting the 129/SvJ were homozygous dominant negative. An F2 generation was bred since a single gene controlled phenotype would be unmasked in this generation, on the assumption that the grandparents were homozygous. All F2 animals were screened for LORR at 400µg/kg dexmedetomidine i/p, since this dose would guarantee LORR in C57/Bl6 mice. From 64 animals

screened, 46 were negative and 18 positive giving a ratio of 2.6:1. A classic Mendelian single gene model for LORR sensitivity would expect 3:1 ratio of negative:positive. The 2.6:1 ratio was not significantly different ($p > 0.99$, χ^2 test). All the animals that were negative in this screen were screened at 2mg/kg and all negative (data not shown). The sensitive F2 animals ($F2_s$) were back crossed with C57/Bl6 and the progeny (F2BC) screened for LORR at 400μg/kg, all of which were positive (Figure A2.1c) confirming the single gene model. Dose response curves were generated for $F2_s$ and F2BC animals and compared to C57/Bl6 (Figure A2.1d). The ED_{50} for $F2_s$ was approximately three times greater than for C57/Bl6 (330.7 ± 58.5μg/kg). Interestingly the ED_{50} of F2BC lay between C57/Bl6 and $F2_s$ (180.3 ± 31.8μg/kg) and all were significantly different, suggesting that whilst absolute sensitivity to dexmedetomidine LORR may be controlled by a single gene, there is a multi-gene background controlling relative sensitivity.
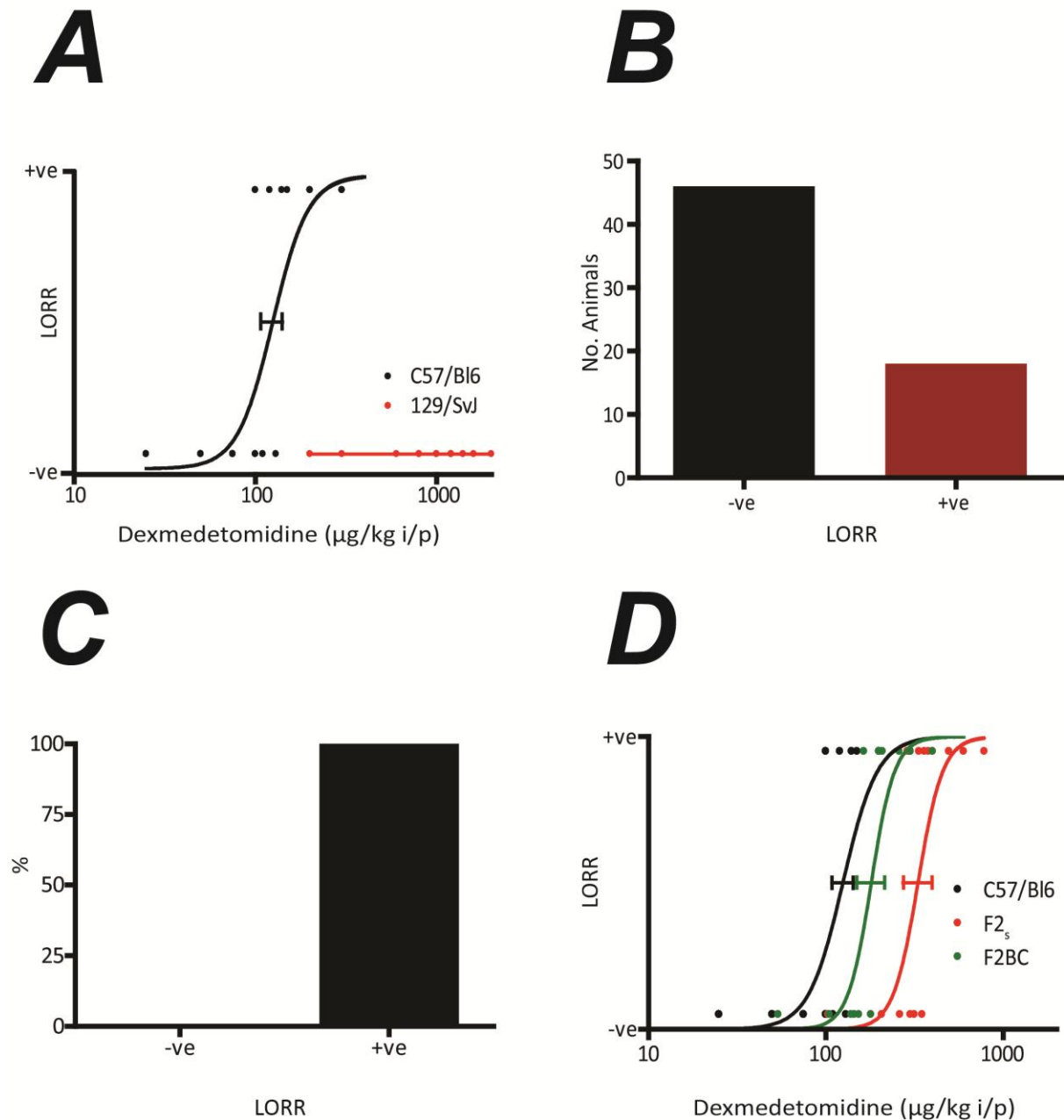
Figure A1.1 Sensitivity to dexmedetomidine follows as classical Mendelian regression.
A. Dose response curves with Waud analysis for C57/Bl6 and 129/SvJ mice for dexmedetomidine LORR. The ED_{50} for C57/Bl6 was 124.7 ± 16.4µg/kg. 129/SvJ did not lose righting reflex at doses up to 2mg/kg. F1 hybrids of both strains were also resistant at 2mg/kg (data not shown). **B.** F2 hybrids screened for LORR at 400µg/kg showed a ration of insensitive:sensitive ratio of 2.6:1, χ^2 test determined this was not significantly different from a 3:1 ratio expected with a single gene locus mechanism (p>0.99). **C.** Sensitive F2 animals ($F2_s$) were backcrossed with C57/Bl6 and the progeny (F2BC) screened for sensitivity to dexmedetomidine at 400µg/kg. All animals were sensitive. **D.** The three dexmedetomidine sensitive strains tested had different ED_{50} values for LORR. C57/Bl6 124.7 ± 16.4µg/kg, $F2_s$ 330.7 ± 58.5µg/kg and F2BC 180.3 ± 31.8µg/kg.

A1.2 C57/Bl6 and 129/SvJ are equally sensitive to dexmedetomidine sedation

Despite the resistance of 129/SvJ to dexmedetomidine LORR, they appeared to be heavily sedated at low doses by having reduced movement within the tube and low body and head posture. Dexmedetomidine is a potent muscle relaxant and may have caused postural changes due to effects on spinal motor neurones alone. To investigate whether this was a centrally mediated sedation, animals were chronically implanted with EEG electrodes and given dexmedetomidine 400µg/kg i/p. The conscious EEG was dominated by a theta rhythm of 7Hz for both C57/Bl6 (n=6) and 129/SvJ (n=4) animals (Figure A2.2a). Following administration of dexmedetomidine, C57/Bl6 animals lost righting reflex. Figure A2.2b shows the averaged Morlet power spectrum for these transitions. Prior to LORR there is a delta oscillation of 4-4.5Hz. At LORR this frequency shifts to 3.5Hz and the power increases. Figure A2.2c shows averaged Morlet power spectra for 129/SvJ animals at a comparable time period following i/p injection. There is a delta frequency of 4-4.5Hz the same as C57/Bl6, which does not make a frequency shift. 129/SvJ animals therefore have central effects of dexmedetomidine without losing righting reflex.
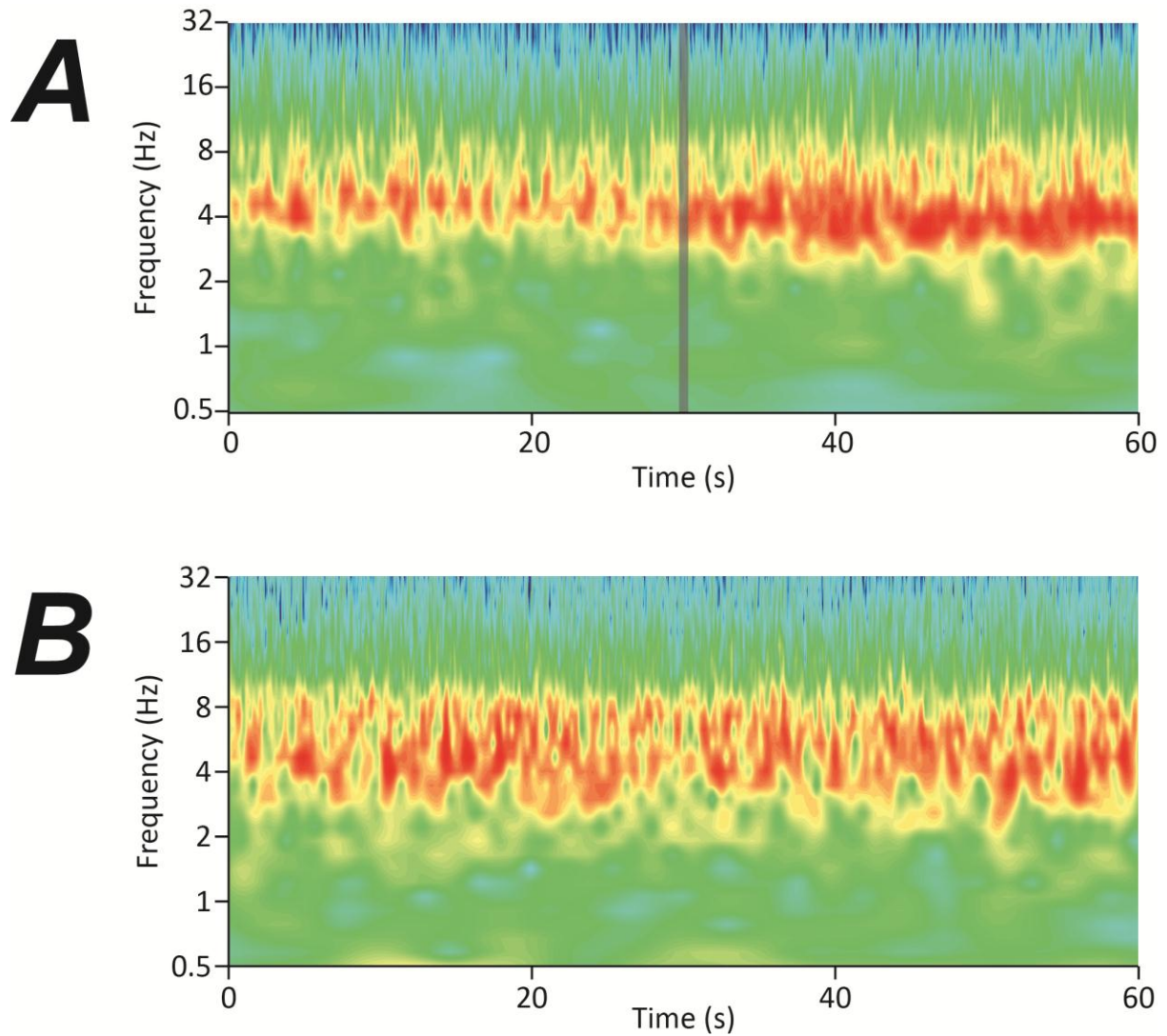
Figure A1.2 Dexmedetomidine produces delta oscillations in C57/Bl6 and 129/SvJ mice
A. Averaged morlet power spectrum of dexmedetomidine LORR EEG recordings in C57/Bl6 mice (n=6). Prior to LORR there is a a 4-4.5Hz delta oscillation in C57/Bl6 mice which shifts frequency to 3.5 Hz at the point of LORR. **B.** Averaged morlet power spectrum of dexmedetomidine EEG recordings in 129/SvJ mice (n=4). 129/SvJ are are not susceptible to LORR induced by dexmedetomidine. They still exhibit behavioural signs of sedation and also delta EEG oscillations similar to C57/Bl6 mice prior to LORR.

In order to compare the degree of sedation for each strain in a quantitative manner, animals were tested on a rotarod at sub anaesthetic doses of dexmedetomidine. Animals of both strains were trialled on the rotarod for innate performance with the rotarod accelerating at 0.5 revolutions min^{-2}. The speed at which they fell off or failed to keep up with the rotarod was recorded. C57/Bl6 fell off at 25.1 ± 2.3rpm whereas 129/SvJ fell off at a significantly slower speed 13.7 ± 4.2rpm ($p<0.01$ Student's T-test) (Figure A2.3a). Due to this disparity, populations of both strains were trained using the protocol in Figure A2.3b, consisting of 10 minute periods of constant speed every day increasing daily for 6 days. The performance evaluation was then repeated (Figure A2.3c). Following training, the C57/Bl6 animals did not improve in performance (25.2 ± 3.8rpm) and the 129/SvJ animals did improve to reach the same level of performance as C57/Bl6 (24.4 ± 3.1rpm) ($p>0.1$ Student's T-test) Figure (A2.3c). A dose response curve was then generated for each strain following i/p injection of dexmedetomidine on the rotarod at a constant speed of 15rpm (Figure A2.3d). ED_{50} values were comparable for both strains, 22.9 ±2.4µg/kg for C57/Bl6 and 19.7 ± 3.1µg/kg for 129/SvJ, therefore suggesting that the sedative component for dexmedetomidine in both C57/Bl6 and 129/SvJ is the same.
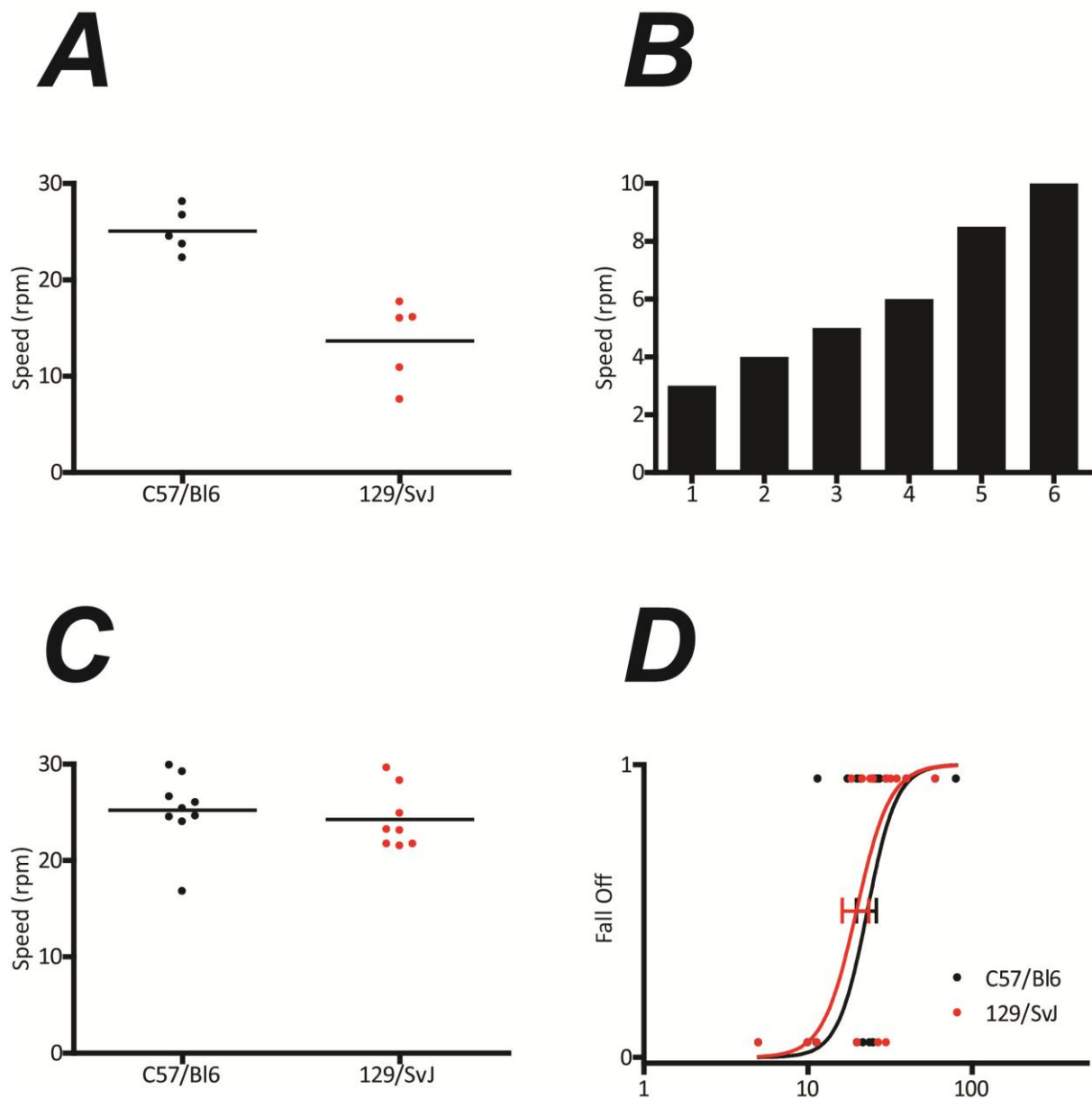
Figure A1.3 C57/Bl6 and 129/SvJ mice are both equally sensitive to dexmedetomidine in a rotarod assay.
A. Pre-training performance on the rotarod. Animals were placed on the rotarod at rest and accelerated at 0.5 revolutions min^{-2}. C57/Bl6 animals fell off at 25.1 ± 2.3 (s.e.m.) rpm whereas 129SvJ fell off at 13.7 ± 4.2 rpm (p<0.01 t-test). **B.** The rotarod training schedule consisted of daily 10 minute periods of constant speed. **C.** Post-training performance on the rotarod. C57/Bl6 fell off at 25.2 ± 3.8 rpm and 129/SvJ at 24.35 ± 3.1rpm (p>0.1). **D.** Dose response curve with Waud analysis for performance of the two strains after training at a constant speed of 15 rpm. Dexmedetomidine ED_{50} values were 22.9 ±2.4μg/kg for C57/Bl6 and 19.7 ± 3.1μg/kg for 129/SvJ (p>0.1).

A1.3 Dexmedetomidine LORR is stimulus sensitive

Previous studies have shown differences in strain sensitivity to various anaesthetics such as propofol, barbiturates and etomidate (Homanics *et al.*, 1999; Sato *et al.*, 2006; Sonner *et al.*, 2000). However these results differences have been small and no binary differences such as this have previously been reported for inbred mouse strains. One possible explanation for the binary difference in sensitivity to dexmedetomidine LORR but not sedation could be a fundamental difference in ascending arousal pathways. Studies in humans have shown that dexmedetomidine can produce a sedated but rousable state if sufficient environmental stimulus is given (Ref). To investigate this in mice, LORR experiments were conducted in C57/Bl6 mice in a cylinder rotating at three different speeds. For each speed, a dose response curve for LORR was generated (Figure A2.4). For dexmedetomidine, increasing the rotational speed from 3.5 to 5.0rpm increased the ED_{50} from $124 \pm 16.4\mu g/kg$ to $801.1 \pm 114.2\mu g/kg$ (Figure A2.4a). Increasing the speed further to 12 rpm abolished LORR up to doses of 2mg/kg, the dose that 129/SvJ animals failed to respond to at 3.5rpm and were determined LORR insensitive. For propofol however, rotational speeds of 3.5, 5.0 and 12rpm did not alter doses required to achieve LORR. A possible reason for this is that unlike most anaesthetics dexmedetomidine in rats has been shown not to diminish somatosensory evoked potentials (Li *et al.*, 2003), therefore whilst overall arousal may be reduced sensory information is still capable of reaching the cortex.

Dexmedetomidine has been postulated to cause unconsciousness by blocking ascending noradrenergic arousal (Correa-Sales *et al.*, 1992). These LORR results suggest that given sufficient stimulatory input, ascending arousal may override a dexmedetomidine blockade. It is possible that 129/SvJ mice lack such a pathway and have an alternative compensating pathway which is not dexmedetomidine sensitive. Further work to characterise differences in α_{2a} protein expression between these strains is required to investigate this theory.
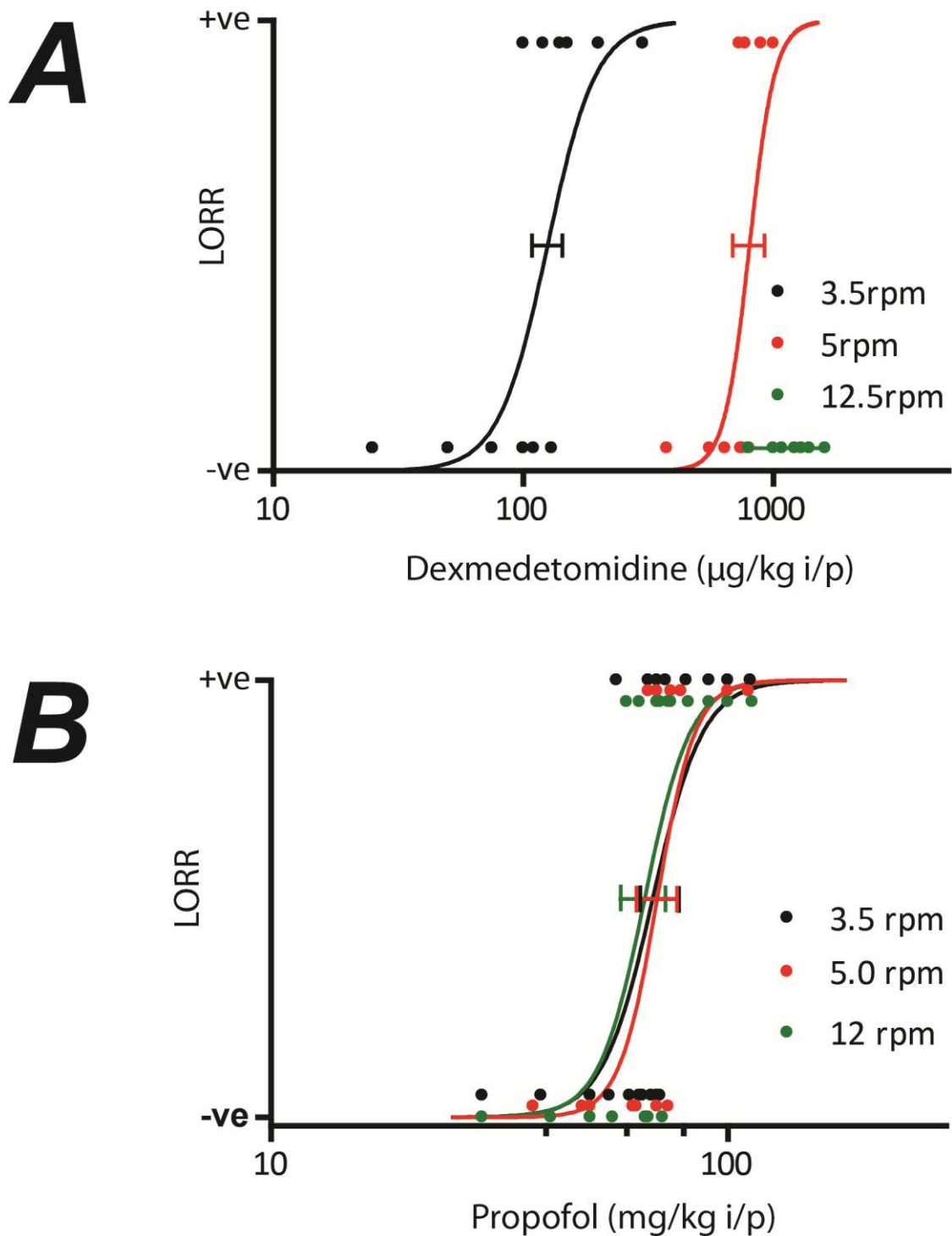
Figure A1.4 LORR by dexmedetomidine but not propofol is influenced by external stimulus.
A. Dose response curves with Waud analysis for dexmedetomidine LORR in C57/Bl6 mice under differing stimulus conditions. LORR was performed in a continuously rotating cylinder at varying speeds. ED_{50} values for 3.5 and 5.0 rpm were 124.7 ± 16.4µg/kg and 801.1 ± 114.2µg/kg respectively (p<0.01 t-test). Rotation at 12rpm effectively abolished LORR up to 1.6mg/kg. **B.** Dose response curves with Waud analysis for propofol LORR in C57/Bl6 mice under differing conditions. In the same conditions as A, LORR sensitivity to propofol was not affected by the rotational speed of the cylinder.

References

Achermann, P, Borbely, AA (1997) Low-frequency (< 1 Hz) oscillations in the human sleep electroencephalogram. *Neuroscience* **81**(1)**:** 213-222.

Adamantidis, AR, Zhang, F, Aravanis, AM, Deisseroth, K, de Lecea, L (2007) Neural substrates of awakening probed with optogenetic control of hypocretin neurons. *Nature* **450**(7168)**:** 420-424.

Adrian, ED, Matthews, BH (1934) The interpretation of potential waves in the cortex. *J Physiol* **81**(4)**:** 440-471.

Alkire, MT, Asher, CD, Franciscus, AM, Hahn, EL (2009) Thalamic microinfusion of antibody to a voltage-gated potassium channel restores consciousness during anesthesia. *Anesthesiology* **110**(4)**:** 766-773.

Alkire, MT, McReynolds, JR, Hahn, EL, Trivedi, AN (2007) Thalamic microinjection of nicotine reverses sevoflurane-induced loss of righting reflex in the rat. *Anesthesiology* **107**(2)**:** 264-272.

Amzica, F, Steriade, M (2002) The functional significance of K-complexes. *Sleep Med Rev* **6**(2)**:** 139-149.

Amzica, F, Steriade, M (1997) The K-complex: its slow (<1-Hz) rhythmicity and relation to delta waves. *Neurology* **49**(4)**:** 952-959.

Andersen, P, Andersson, SA, Lomo, T (1967) Nature of thalamo-cortical relations during spontaneous barbiturate spindle activity. *J Physiol* **192**(2)**:** 283-307.

Andrews, PR, Mark, LC (1982) Structural specificity of barbiturates and related drugs. *Anesthesiology* **57**(4)**:** 314-320.

Aston-Jones, G, Bloom, FE (1981) Activity of norepinephrine-containing locus coeruleus neurons in behaving rats anticipates fluctuations in the sleep-waking cycle. *J Neurosci* **1**(8)**:** 876-886.

Bal, T, McCormick, DA (1996) What stops synchronized thalamocortical oscillations? *Neuron* **17**(2)**:** 297-308.

Bal, T, von Krosigk, M, McCormick, DA (1995a) Role of the ferret perigeniculate nucleus in the generation of synchronized oscillations in vitro. *J Physiol* **483 (Pt 3):** 665-685.

Bal, T, von Krosigk, M, McCormick, DA (1995b) Synaptic and membrane mechanisms underlying synchronized oscillations in the ferret lateral geniculate nucleus in vitro. *J Physiol* **483 (Pt 3):** 641-663.

Bartho, P, Freund, TF, Acsady, L (2002) Selective GABAergic innervation of thalamic nuclei from zona incerta. *Eur J Neurosci* **16**(6)**:** 999-1014.

Bazhenov, M, Timofeev, I, Steriade, M, Sejnowski, T (2000) Spiking-bursting activity in the thalamic reticular nucleus initiates sequences of spindle oscillations in thalamic networks. *J Neurophysiol* **84**(2)**:** 1076-1087.

Bazhenov, M, Timofeev, I, Steriade, M, Sejnowski, TJ (1999) Self-sustained rhythmic activity in the thalamic reticular nucleus mediated by depolarizing GABAA receptor potentials. *Nat Neurosci* **2**(2)**:** 168-174.

Belelli, D, Peden, DR, Rosahl, TW, Wafford, KA, Lambert, JJ (2005) Extrasynaptic GABAA receptors of thalamocortical neurons: a molecular target for hypnotics. *J Neurosci* **25**(50)**:** 11513-11520.

Bergamasco, L, Accatino, A, Priano, L, Neiger-Aeschbacher, G, Cizinauskas, S, Jaggy, A (2003) Quantitative electroencephalographic findings in beagles anaesthetized with propofol. *Vet J* **166**(1)**:** 58-66.

Berger, H (1929) Über das Elektroenkephalogramm des Menschen. *Arch Psychiat Nervenkr* **99**(6)**:** 555-574.

Bessaih, T, Leresche, N, Lambert, RC (2008) T current potentiation increases the occurrence and temporal fidelity of synaptically evoked burst firing in sensory thalamic neurons. *Proc Natl Acad Sci U S A* **105**(32)**:** 11376-11381.

Bishop, G (1936) The interpretation of cortical potentials. *Cold Spring Harbor Symp Quant Biol* **4:** 305-319.

Blethyn, KL, Hughes, SW, Toth, TI, Cope, DW, Crunelli, V (2006) Neuronal basis of the slow (<1 Hz) oscillation in neurons of the nucleus reticularis thalami in vitro. *J Neurosci* **26**(9)**:** 2474-2486.

Bol, C, Danhof, M, Stanski, DR, Mandema, JW (1997) Pharmacokinetic-pharmacodynamic characterization of the cardiovascular, hypnotic, EEG and ventilatory responses to dexmedetomidine in the rat. *J Pharmacol Exp Ther* **283**(3)**:** 1051-1058.

Borst, JG, Leung, LW, MacFabe, DF (1987) Electrical activity of the cingulate cortex. II. Cholinergic modulation. *Brain Res* **407**(1)**:** 81-93.

Boucetta, S, Jones, BE (2009) Activity profiles of cholinergic and intermingled GABAergic and putative glutamatergic neurons in the pontomesencephalic tegmentum of urethane-anesthetized rats. *J Neurosci* **29**(14)**:** 4664-4674.

Bremer, F (1958) Cerebral and cerebellar potentials. *Physiol Rev* **38**(3)**:** 357-388.

Brown, EN, Lydic, R, Schiff, ND (2010) General anesthesia, sleep, and coma. *N Engl J Med* **363**(27)**:** 2638-2650.

Buzsaki, G (2002) Theta oscillations in the hippocampus. *Neuron* **33**(3)**:** 325-340.

Carter, AJ (1995) Antagonists of the NMDA receptor-channel complex and motor coordination. *Life Sci* **57**(10)**:** 917-929.

Cash, SS, Halgren, E, Dehghani, N, Rossetti, AO, Thesen, T, Wang, C, Devinsky, O, Kuzniecky, R, Doyle, W, Madsen, JR, Bromfield, E, Eross, L, Halasz, P, Karmos, G, Csercsa, R, Wittner, L, Ulbert, I (2009) The human K-complex represents an isolated cortical down-state. *Science* **324**(5930)**:** 1084-1087.

Caton, R (1875) The Electrical Currents of the Brain. *Br Med J* **2**(765)**:** 278.

Chiu, TH, Chen, MJ, Yang, YR, Yang, JJ, Tang, FI (1995) Action of dexmedetomidine on rat locus coeruleus neurones: intracellular recording in vitro. *Eur J Pharmacol* **285**(3)**:** 261-268.

Constantinople, CM, Bruno, RM (2011) Effects and mechanisms of wakefulness on local cortical networks. *Neuron* **69**(6)**:** 1061-1068.

Contreras, D, Destexhe, A, Sejnowski, TJ, Steriade, M (1996a) Control of spatiotemporal coherence of a thalamic oscillation by corticothalamic feedback. *Science* **274**(5288)**:** 771-774.

Contreras, D, Steriade, M (1995) Cellular basis of EEG slow rhythms: a study of dynamic corticothalamic relationships. *J Neurosci* **15**(1 Pt 2)**:** 604-622.

Contreras, D, Steriade, M (1996b) Spindle oscillation in cats: the role of corticothalamic feedback in a thalamically generated rhythm. *J Physiol* **490 (Pt 1):** 159-179.

Contreras, D, Steriade, M (1997) Synchronization of low-frequency rhythms in corticothalamic networks. *Neuroscience* **76**(1)**:** 11-24.

Correa-Sales, C, Rabin, BC, Maze, M (1992) A hypnotic response to dexmedetomidine, an alpha 2 agonist, is mediated in the locus coeruleus in rats. *Anesthesiology* **76**(6)**:** 948-952.

Costa-Miserachs, D, Portell-Cortes, I, Torras-Garcia, M, Morgado-Bernal, I (2003) Automated sleep staging in rat with a standard spreadsheet. *J Neurosci Methods* **130**(1)**:** 93-101.

Creutzfeldt, OD, Watanabe, S, Lux, HD (1966a) Relations between EEG phenomena and potentials of single cortical cells. I. Evoked responses after thalamic and erpicortical stimulation. *Electroencephalogr Clin Neurophysiol* **20**(1)**:** 1-18.

Creutzfeldt, OD, Watanabe, S, Lux, HD (1966b) Relations between EEG phenomena and potentials of single cortical cells. II. Spontaneous and convulsoid activity. *Electroencephalogr Clin Neurophysiol* **20**(1)**:** 19-37.

Crunelli, V, Cope, DW, Hughes, SW (2006) Thalamic T-type Ca2+ channels and NREM sleep. *Cell Calcium* **40**(2)**:** 175-190.

Crunelli, V, Hughes, SW (2010) The slow (<1 Hz) rhythm of non-REM sleep: a dialogue between three cardinal oscillators. *Nat Neurosci* **13**(1)**:** 9-17.

Cull-Candy, S, Brickley, S, Farrant, M (2001) NMDA receptor subunits: diversity, development and disease. *Curr Opin Neurobiol* **11**(3)**:** 327-335.

Cunningham, MO, Pervouchine, DD, Racca, C, Kopell, NJ, Davies, CH, Jones, RS, Traub, RD, Whittington, MA (2006) Neuronal metabolism governs cortical network response state. *Proc Natl Acad Sci U S A* **103**(14)**:** 5597-5601.

De Gennaro, L, Ferrara, M (2003) Sleep spindles: an overview. *Sleep Med Rev* **7**(5)**:** 423-440.

de Sousa, SL, Dickinson, R, Lieb, WR, Franks, NP (2000) Contrasting synaptic actions of the inhalational general anesthetics isoflurane and xenon. *Anesthesiology* **92**(4)**:** 1055-1066.

Deschenes, M, Madariaga-Domich, A, Steriade, M (1985) Dendrodendritic synapses in the cat reticularis thalami nucleus: a structural basis for thalamic spindle synchronization. *Brain Res* **334**(1)**:** 165-168.

Destexhe, A, Contreras, D, Steriade, M (1999) Spatiotemporal analysis of local field potentials and unit discharges in cat cerebral cortex during natural wake and sleep states. *J Neurosci* **19**(11)**:** 4595-4608.

Destexhe, A, Hughes, SW, Rudolph, M, Crunelli, V (2007) Are corticothalamic 'up' states fragments of wakefulness? *Trends Neurosci* **30**(7)**:** 334-342.

Devor, M, Zalkind, V (2001) Reversible analgesia, atonia, and loss of consciousness on bilateral intracerebral microinjection of pentobarbital. *Pain* **94**(1)**:** 101-112.

Dickinson, R, Franks, NP, Lieb, WR (1994) Can the stereoselective effects of the anesthetic isoflurane be accounted for by lipid solubility? *Biophys J* **66**(6)**:** 2019-2023.

Dickinson, R, Peterson, BK, Banks, P, Simillis, C, Martin, JC, Valenzuela, CA, Maze, M, Franks, NP (2007) Competitive inhibition at the glycine site of the N-methyl-D-aspartate receptor by the anesthetics xenon and isoflurane: evidence from molecular modeling and electrophysiology. *Anesthesiology* **107**(5)**:** 756-767.

Doi, A, Mizuno, M, Katafuchi, T, Furue, H, Koga, K, Yoshimura, M (2007) Slow oscillation of membrane currents mediated by glutamatergic inputs of rat somatosensory cortical neurons: in vivo patch-clamp analysis. *Eur J Neurosci* **26**(9)**:** 2565-2575.

Dossi, RC, Nunez, A, Steriade, M (1992) Electrophysiology of a slow (0.5-4 Hz) intrinsic oscillation of cat thalamocortical neurones in vivo. *J Physiol* **447:** 215-234.

Drummond, JC, Brann, CA, Perkins, DE, Wolfe, DE (1991) A comparison of median frequency, spectral edge frequency, a frequency band power ratio, total power, and dominance shift in the determination of depth of anesthesia. *Acta Anaesthesiol Scand* **35**(8)**:** 693-699.

Dutta, S, Matsumoto, Y, Gothgen, NU, Ebling, WF (1997) Concentration-EEG effect relationship of propofol in rats. *J Pharm Sci* **86**(1)**:** 37-43.

Eccles, JC (1951) Interpretation of action potentials evoked in the cerebral cortex. *Electroencephalogr Clin Neurophysiol* **3**(4)**:** 449-464.

Erchova, IA, Lebedev, MA, Diamond, ME (2002) Somatosensory cortical neuronal population activity across states of anaesthesia. *Eur J Neurosci* **15**(4)**:** 744-752.

Ermentrout, GB, Kleinfeld, D (2001) Traveling electrical waves in cortex: insights from phase dynamics and speculation on a computational role. *Neuron* **29**(1)**:** 33-44.

Ferenets, R, Lipping, T, Suominen, P, Turunen, J, Puumala, P, Jantti, V, Himanen, SL, Huotari, AM (2006) Comparison of the properties of EEG spindles in sleep and propofol anesthesia. *Conf Proc IEEE Eng Med Biol Soc* **1:** 6356-6359.

Ferrarelli, F, Massimini, M, Sarasso, S, Casali, A, Riedner, BA, Angelini, G, Tononi, G, Pearce, RA (2010) Breakdown in cortical effective connectivity during midazolam-induced loss of consciousness. *Proc Natl Acad Sci U S A* **107**(6)**:** 2681-2686.

Feshchenko, VA, Veselis, RA, Reinsel, RA (1997) Comparison of the EEG effects of midazolam, thiopental, and propofol: the role of underlying oscillatory systems. *Neuropsychobiology* **35**(4)**:** 211-220.

Franks, NP (2008) General anaesthesia: from molecular targets to neuronal pathways of sleep and arousal. *Nat Rev Neurosci* **9**(5)**:** 370-386.

Franks, NP (2006) Molecular targets underlying general anaesthesia. *Br J Pharmacol* **147 Suppl 1:** S72-81.

Franks, NP, Lieb, WR (1984) Do general anaesthetics act by competitive binding to specific receptors? *Nature* **310**(5978)**:** 599-601.

Franks, NP, Lieb, WR (1988) Volatile general anaesthetics activate a novel neuronal K+ current. *Nature* **333**(6174)**:** 662-664.

Fuentealba, P, Crochet, S, Timofeev, I, Bazhenov, M, Sejnowski, TJ, Steriade, M (2004a) Experimental evidence and modeling studies support a synchronizing role for electrical coupling in the cat thalamic reticular neurons in vivo. *Eur J Neurosci* **20**(1)**:** 111-119.

Fuentealba, P, Timofeev, I, Steriade, M (2004b) Prolonged hyperpolarizing potentials precede spindle oscillations in the thalamic reticular nucleus. *Proc Natl Acad Sci U S A* **101**(26)**:** 9816-9821.

Fuller, P, Sherman, D, Pedersen, NP, Saper, CB, Lu, J (2011) Reassessment of the structural basis of the ascending arousal system. *J Comp Neurol* **519**(5)**:** 933-956.

Gervasoni, D, Lin, SC, Ribeiro, S, Soares, ES, Pantoja, J, Nicolelis, MA (2004) Global forebrain dynamics predict rat behavioral states and their transitions. *J Neurosci* **24**(49)**:** 11137-11147.

Gilsbach, R, Roser, C, Beetz, N, Brede, M, Hadamek, K, Haubold, M, Leemhuis, J, Philipp, M, Schneider, J, Urbanski, M, Szabo, B, Weinshenker, D, Hein, L (2009) Genetic dissection of alpha2-adrenoceptor functions in adrenergic versus nonadrenergic cells. *Mol Pharmacol* **75**(5)**:** 1160-1170.

Goldstein, SA, Bockenhauer, D, O'Kelly, I, Zilberberg, N (2001) Potassium leak channels and the KCNK family of two-P-domain subunits. *Nat Rev Neurosci* **2**(3)**:** 175-184.

Gollo, LL, Mirasso, CR, Atienza, M, Crespo-Garcia, M, Cantero, JL (2011) Theta band zero-lag long-range cortical synchronization via hippocampal dynamical relaying. *PLoS One* **6**(3)**:** e17756.

Grinsted, A, Moore, JC, Jevrajeva, S (2004) Application of the cross wavelet transform and wavelet coherence to geophysical time series. *Nonlinear Processes in Geophysics* **11:** 561-566.

Gugino, LD, Chabot, RJ, Prichep, LS, John, ER, Formanek, V, Aglio, LS (2001) Quantitative EEG changes associated with loss and return of consciousness in healthy adult volunteers anaesthetized with propofol or sevoflurane. *Br J Anaesth* **87**(3)**:** 421-428.

Guillery, RW, Sherman, SM (2002) Thalamic relay functions and their role in corticocortical communication: generalizations from the visual system. *Neuron* **33**(2)**:** 163-175.

Halasz, P (1998) Hierarchy of micro-arousals and the microstructure of sleep. *Neurophysiol Clin* **28**(6)**:** 461-475.

Hallanger, AE, Levey, AI, Lee, HJ, Rye, DB, Wainer, BH (1987) The origins of cholinergic and other subcortical afferents to the thalamus in the rat. *J Comp Neurol* **262**(1)**:** 105-124.

Hofle, N, Paus, T, Reutens, D, Fiset, P, Gotman, J, Evans, AC, Jones, BE (1997) Regional cerebral blood flow changes as a function of delta and spindle activity during slow wave sleep in humans. *J Neurosci* **17**(12)**:** 4800-4808.

Homanics, GE, Quinlan, JJ, Firestone, LL (1999) Pharmacologic and behavioral responses of inbred C57BL/6J and strain 129/SvJ mouse lines. *Pharmacol Biochem Behav* **63**(1)**:** 21-26.

Hu, X, Xu, X, Tian, X (2010) Phase Synchronization Analysis of Multi-channel Local Field Potentials Based on High-resolution Wavelet Transform. *2010 Sixth International Conference on Natural Computation*.

Hughes, SW, Cope, DW, Blethyn, KL, Crunelli, V (2002) Cellular mechanisms of the slow (<1 Hz) oscillation in thalamocortical neurons in vitro. *Neuron* **33**(6)**:** 947-958.

Hughes, SW, Cope, DW, Crunelli, V (1998) Dynamic clamp study of Ih modulation of burst firing and delta oscillations in thalamocortical neurons in vitro. *Neuroscience* **87**(3)**:** 541-550.

Huupponen, E, Maksimow, A, Lapinlampi, P, Sarkela, M, Saastamoinen, A, Snapir, A, Scheinin, H, Scheinin, M, Merilainen, P, Himanen, SL, Jaaskelainen, S (2008) Electroencephalogram spindle activity during dexmedetomidine sedation and physiological sleep. *Acta Anaesthesiol Scand* **52**(2)**:** 289-294.

Hwang, E, Kim, S, Shin, HS, Choi, JH (2010) The forced walking test: a novel test for pinpointing the anesthetic-induced transition in consciousness in mouse. *J Neurosci Methods* **188**(1)**:** 14-23.

Jacob, V, Le Cam, J, Ego-Stengel, V, Shulz, DE (2008) Emergent properties of tactile scenes selectively activate barrel cortex neurons. *Neuron* **60**(6)**:** 1112-1125.

Jones, BE (2004) Activity, modulation and role of basal forebrain cholinergic neurons innervating the cerebral cortex. *Prog Brain Res* **145:** 157-169.

Jones, BE (2005) From waking to sleeping: neuronal and chemical substrates. *Trends Pharmacol Sci* **26**(11)**:** 578-586.

Jones, BE, Yang, TZ (1985) The efferent projections from the reticular formation and the locus coeruleus studied by anterograde and retrograde axonal transport in the rat. *J Comp Neurol* **242**(1)**:** 56-92.

Jones, EG (2002) Thalamic circuitry and thalamocortical synchrony. *Philos Trans R Soc Lond B Biol Sci* **357**(1428)**:** 1659-1673.

Jones, EG, Leavitt, RY (1974) Retrograde axonal transport and the demonstration of non-specific projections to the cerebral cortex and striatum from thalamic intralaminar nuclei in the rat, cat and monkey. *J Comp Neurol* **154**(4)**:** 349-377.

Jorm, CM, Stamford, JA (1993) Actions of the hypnotic anaesthetic, dexmedetomidine, on noradrenaline release and cell firing in rat locus coeruleus slices. *Br J Anaesth* **71**(3)**:** 447-449.

Judge, O, Hill, S, Antognini, JF (2009) Modeling the effects of midazolam on cortical and thalamic neurons. *Neurosci Lett* **464**(2)**:** 135-139.

Jugovac, I, Imas, O, Hudetz, AG (2006) Supraspinal anesthesia: behavioral and electroencephalographic effects of intracerebroventricularly infused pentobarbital, propofol, fentanyl, and midazolam. *Anesthesiology* **105**(4)**:** 764-778.

Jurd, R, Arras, M, Lambert, S, Drexler, B, Siegwart, R, Crestani, F, Zaugg, M, Vogt, KE, Ledermann, B, Antkowiak, B, Rudolph, U (2003) General anesthetic actions in vivo strongly attenuated by a point mutation in the GABA(A) receptor beta3 subunit. *FASEB J* **17**(2)**:** 250-252.

Kaur, S, Junek, A, Black, MA, Semba, K (2008) Effects of ibotenate and 192IgG-saporin lesions of the nucleus basalis magnocellularis/substantia innominata on spontaneous sleep and wake states and on recovery sleep after sleep deprivation in rats. *J Neurosci* **28**(2)**:** 491-504.

Kim, U, Bal, T, McCormick, DA (1995) Spindle waves are propagating synchronized oscillations in the ferret LGNd in vitro. *J Neurophysiol* **74**(3)**:** 1301-1323.

Kinomura, S, Larsson, J, Gulyas, B, Roland, PE (1996) Activation by attention of the human reticular formation and thalamic intralaminar nuclei. *Science* **271**(5248)**:** 512-515.

Kolmac, C, Mitrofanis, J (1999) Organization of the basal forebrain projection to the thalamus in rats. *Neurosci Lett* **272**(3)**:** 151-154.

Kramis, R, Vanderwolf, CH, Bland, BH (1975) Two types of hippocampal rhythmical slow activity in both the rabbit and the rat: relations to behavior and effects of atropine, diethyl ether, urethane, and pentobarbital. *Exp Neurol* **49**(1 Pt 1)**:** 58-85.

Krout, KE, Belzer, RE, Loewy, AD (2002) Brainstem projections to midline and intralaminar thalamic nuclei of the rat. *J Comp Neurol* **448**(1)**:** 53-101.

Kuizenga, K, Wierda, JM, Kalkman, CJ (2001) Biphasic EEG changes in relation to loss of consciousness during induction with thiopental, propofol, etomidate, midazolam or sevoflurane. *Br J Anaesth* **86**(3)**:** 354-360.

Lakhlani, PP, MacMillan, LB, Guo, TZ, McCool, BA, Lovinger, DM, Maze, M, Limbird, LE (1997) Substitution of a mutant alpha2a-adrenergic receptor via "hit and run" gene targeting reveals the role of this subtype in sedative, analgesic, and anesthetic-sparing responses in vivo. *Proc Natl Acad Sci U S A* **94**(18)**:** 9950-9955.

Landisman, CE, Long, MA, Beierlein, M, Deans, MR, Paul, DL, Connors, BW (2002) Electrical synapses in the thalamic reticular nucleus. *J Neurosci* **22**(3)**:** 1002-1009.

Lee, MG, Hassani, OK, Jones, BE (2005) Discharge of identified orexin/hypocretin neurons across the sleep-waking cycle. *J Neurosci* **25**(28)**:** 6716-6720.

Leresche, N, Jassik-Gerschenfeld, D, Haby, M, Soltesz, I, Crunelli, V (1990) Pacemaker-like and other types of spontaneous membrane potential oscillations of thalamocortical cells. *Neurosci Lett* **113**(1)**:** 72-77.

Leresche, N, Lightowler, S, Soltesz, I, Jassik-Gerschenfeld, D, Crunelli, V (1991) Low-frequency oscillatory activities intrinsic to rat and cat thalamocortical cells. *J Physiol* **441:** 155-174.

Leslie, K, Sleigh, J, Paech, MJ, Voss, L, Lim, CW, Sleigh, C (2009) Dreaming and electroencephalographic changes during anesthesia maintained with propofol or desflurane. *Anesthesiology* **111**(3)**:** 547-555.

Leung, LW, Borst, JG (1987) Electrical activity of the cingulate cortex. I. Generating mechanisms and relations to behavior. *Brain Res* **407**(1)**:** 68-80.

Levey, AI, Hallanger, AE, Wainer, BH (1987) Choline acetyltransferase immunoreactivity in the rat thalamus. *J Comp Neurol* **257**(3)**:** 317-332.

Li, BH, Lohmann, JS, Schuler, HG, Cronin, AJ (2003) Preservation of the cortical somatosensory-evoked potential during dexmedetomidine infusion in rats. *Anesth Analg* **96**(4)**:** 1155-1160, table of contents.

Li, X, Yao, X, Fox, J, Jefferys, JG (2007) Interaction dynamics of neuronal oscillations analysed using wavelet transforms. *J Neurosci Methods* **160**(1)**:** 178-185.

Lin, L, Faraco, J, Li, R, Kadotani, H, Rogers, W, Lin, X, Qiu, X, de Jong, PJ, Nishino, S, Mignot, E (1999) The sleep disorder canine narcolepsy is caused by a mutation in the hypocretin (orexin) receptor 2 gene. *Cell* **98**(3)**:** 365-376.

Lingenhohl, K, Pozza, MF (1998) Reevaluation of ACEA 1021 as an antagonist at the strychnine-insensitive glycine site of the N-methyl-D-aspartate receptor. *Neuropharmacology* **37**(6)**:** 729-737.

Liu, C, Au, JD, Zou, HL, Cotten, JF, Yost, CS (2004) Potent activation of the human tandem pore domain K channel TRESK with clinical concentrations of volatile anesthetics. *Anesth Analg* **99**(6)**:** 1715-1722, table of contents.

Loomis, AL, Harvey, EN, Hobart, G (1938) Distribution of disturbance-patterns in the human electroenchphalogram, with special reference to sleep. *J Neurophysiol* **1:** 413-430.

Loomis, AL, Harvey, EN, Hobart, G (1935a) Further Observations on the Potential Rhythms of the Cerebral Cortex during Sleep. *Science* **82**(2122)**:** 198-200.

Loomis, AL, Harvey, EN, Hobart, G (1935b) Potential Rhythms of the Cerebral Cortex during Sleep. *Science* **81**(2111)**:** 597-598.

Lu, J, Greco, MA, Shiromani, P, Saper, CB (2000) Effect of lesions of the ventrolateral preoptic nucleus on NREM and REM sleep. *J Neurosci* **20**(10)**:** 3830-3842.

Lubke, J, Feldmeyer, D (2007) Excitatory signal flow and connectivity in a cortical column: focus on barrel cortex. *Brain Struct Funct* **212**(1)**:** 3-17.

Luczak, A, Bartho, P, Marguet, SL, Buzsaki, G, Harris, KD (2007) Sequential structure of neocortical spontaneous activity in vivo. *Proc Natl Acad Sci U S A* **104**(1)**:** 347-352.

Macdonald, RL, Barker, JL (1978) Different actions of anticonvulsant and anesthetic barbiturates revealed by use of cultured mammalian neurons. *Science* **200**(4343)**:** 775-777.

Magnin, M, Rey, M, Bastuji, H, Guillemant, P, Mauguiere, F, Garcia-Larrea, L (2010) Thalamic deactivation at sleep onset precedes that of the cerebral cortex in humans. *Proc Natl Acad Sci U S A* **107**(8)**:** 3829-3833.

Manns, ID, Mainville, L, Jones, BE (2001) Evidence for glutamate, in addition to acetylcholine and GABA, neurotransmitter synthesis in basal forebrain neurons projecting to the entorhinal cortex. *Neuroscience* **107**(2)**:** 249-263.

Mason, KP, O'Mahony, E, Zurakowski, D, Libenson, MH (2009) Effects of dexmedetomidine sedation on the EEG in children. *Paediatr Anaesth* **19**(12)**:** 1175-1183.

Massimini, M, Huber, R, Ferrarelli, F, Hill, S, Tononi, G (2004) The sleep slow oscillation as a traveling wave. *J Neurosci* **24**(31)**:** 6862-6870.

McCormick, DA, Pape, HC (1990) Properties of a hyperpolarization-activated cation current and its role in rhythmic oscillation in thalamic relay neurones. *J Physiol* **431:** 291-318.

McKernan, RM, Whiting, PJ (1996) Which GABAA-receptor subtypes really occur in the brain? *Trends Neurosci* **19**(4)**:** 139-143.

Meuth, SG, Budde, T, Kanyshkova, T, Broicher, T, Munsch, T, Pape, HC (2003) Contribution of TWIK-related acid-sensitive K+ channel 1 (TASK1) and TASK3 channels to the control of activity modes in thalamocortical neurons. *J Neurosci* **23**(16)**:** 6460-6469.

Meyer, H (1899) Welche eigenschaft der anastheitca bedingt ihre narkotische wirkung? *Arch. Exp. Pathol. Pharmakol.* **42:** 109-118.

Miller, JW, Ferrendelli, JA (1990) Characterization of GABAergic seizure regulation in the midline thalamus. *Neuropharmacology* **29**(7)**:** 649-655.

Molle, M, Marshall, L, Gais, S, Born, J (2002) Grouping of spindle activity during slow oscillations in human non-rapid eye movement sleep. *J Neurosci* **22**(24)**:** 10941-10947.

Mooney, DM, Zhang, L, Basile, C, Senatorov, VV, Ngsee, J, Omar, A, Hu, B (2004) Distinct forms of cholinergic modulation in parallel thalamic sensory pathways. *Proc Natl Acad Sci U S A* **101**(1)**:** 320-324.

Morison, RS, Bassett, DL (1945) Electrical activity of the thalams and basal ganglia in decorticate cats. *J Neurophysiol* **8:** 309-314.

Moruzzi, G, Magoun, HW (1949) Brain stem reticular formation and activation of the EEG. *Electroencephalogr Clin Neurophysiol* **1**(4)**:** 455-473.

Mulle, C, Steriade, M, Deschenes, M (1985) Absence of spindle oscillations in the cat anterior thalamic nuclei. *Brain Res* **334**(1)**:** 169-171.

Nelson, LE, Guo, TZ, Lu, J, Saper, CB, Franks, NP, Maze, M (2002) The sedative component of anesthesia is mediated by GABA(A) receptors in an endogenous sleep pathway. *Nat Neurosci* **5**(10)**:** 979-984.

Nelson, LE, Lu, J, Guo, T, Saper, CB, Franks, NP, Maze, M (2003) The alpha2-adrenoceptor agonist dexmedetomidine converges on an endogenous sleep-promoting pathway to exert its sedative effects. *Anesthesiology* **98**(2)**:** 428-436.

Nicholas, AP, Pieribone, V, Hokfelt, T (1993) Distributions of mRNAs for alpha-2 adrenergic receptor subtypes in rat brain: an in situ hybridization study. *J Comp Neurol* **328**(4)**:** 575-594.

Niiyama, Y, Satoh, N, Kutsuzawa, O, Hishikawa, Y (1996) Electrophysiological evidence suggesting that sensory stimuli of unknown origin induce spontaneous K-complexes. *Electroencephalogr Clin Neurophysiol* **98**(5)**:** 394-400.

Novak, CM, Nunez, AA (1998) Daily rhythms in Fos activity in the rat ventrolateral preoptic area and midline thalamic nuclei. *Am J Physiol* **275**(5 Pt 2)**:** R1620-1626.

Oke, AF, Carver, LA, Gouvion, CM, Adams, RN (1997) Three-dimensional mapping of norepinephrine and serotonin in human thalamus. *Brain Res* **763**(1)**:** 69-78.

Overton, E (1901) Studien uber die Narkose, zugleich ein Beitrag zur allgemeinen Pharmakologie.

Pang, DS, Robledo, CJ, Carr, DR, Gent, TC, Vyssotski, AL, Caley, A, Zecharia, AY, Wisden, W, Brickley, SG, Franks, NP (2009) An unexpected role for TASK-3 potassium channels in network oscillations with implications for sleep mechanisms and anesthetic action. *Proc Natl Acad Sci U S A* **106**(41)**:** 17546-17551.

Panula, P, Yang, HY, Costa, E (1984) Histamine-containing neurons in the rat hypothalamus. *Proc Natl Acad Sci U S A* **81**(8)**:** 2572-2576.

Pare, D, Smith, Y, Parent, A, Steriade, M (1988) Projections of brainstem core cholinergic and non-cholinergic neurons of cat to intralaminar and reticular thalamic nuclei. *Neuroscience* **25**(1)**:** 69-86.

Patel, AJ, Honore, E (2001) Properties and modulation of mammalian 2P domain K+ channels. *Trends Neurosci* **24**(6)**:** 339-346.

Paxinos, G, Watson, C (1986) *The Rat Brain in Stereotaxic Coordinates*. 2nd edn. London: Academic Press Inc.

Petersen, CC, Hahn, TT, Mehta, M, Grinvald, A, Sakmann, B (2003) Interaction of sensory responses with spontaneous depolarization in layer 2/3 barrel cortex. *Proc Natl Acad Sci U S A* **100**(23)**:** 13638-13643.

Plested, AJ, Wildman, SS, Lieb, WR, Franks, NP (2004) Determinants of the sensitivity of AMPA receptors to xenon. *Anesthesiology* **100**(2)**:** 347-358.

Raines, DE, Claycomb, RJ, Scheller, M, Forman, SA (2001) Nonhalogenated alkane anesthetics fail to potentiate agonist actions on two ligand-gated ion channels. *Anesthesiology* **95**(2)**:** 470-477.

Reichova, I, Sherman, SM (2004) Somatosensory corticothalamic projections: distinguishing drivers from modulators. *J Neurophysiol* **92**(4)**:** 2185-2197.

Renshaw, B, Forbes, A, Morison, B (1940) Activity of isocortex and hippocampus: electrical studies with microelectrodes. *J Neurophysiol* **3:** 74-105.

Rey, M, Bastuji, H, Garcia-Larrea, L, Guillemant, P, Mauguiere, F, Magnin, M (2007) Human thalamic and cortical activities assessed by dimension of activation and spectral edge frequency during sleep wake cycles. *Sleep* **30**(7)**:** 907-912.

Reynolds, DS, O'Meara, GF, Newman, RJ, Bromidge, FA, Atack, JR, Whiting, PJ, Rosahl, TW, Dawson, GR (2003) GABA(A) alpha 1 subunit knock-out mice do not show a hyperlocomotor response following amphetamine or cocaine treatment. *Neuropharmacology* **44**(2)**:** 190-198.

Rhoades, RW, Belford, GR, Killackey, HP (1987) Receptive-field properties of rat ventral posterior medial neurons before and after selective kainic acid lesions of the trigeminal brain stem complex. *J Neurophysiol* **57**(5)**:** 1577-1600.

Richter, JA, Holtman, JR, Jr. (1982) Barbiturates: their in vivo effects and potential biochemical mechanisms. *Prog Neurobiol* **18**(4)**:** 275-319.

Rigas, P, Castro-Alamancos, MA (2007) Thalamocortical Up states: differential effects of intrinsic and extrinsic cortical inputs on persistent activity. *J Neurosci* **27**(16)**:** 4261-4272.

Rudolph, M, Pospischil, M, Timofeev, I, Destexhe, A (2007) Inhibition determines membrane potential dynamics and controls action potential generation in awake and sleeping cat cortex. *J Neurosci* **27**(20)**:** 5280-5290.

Rudolph, U, Antkowiak, B (2004a) Molecular and neuronal substrates for general anaesthetics. *Nat Rev Neurosci* **5**(9)**:** 709-720.

Rudolph, U, Crestani, F, Benke, D, Brunig, I, Benson, JA, Fritschy, JM, Martin, JR, Bluethmann, H, Mohler, H (1999) Benzodiazepine actions mediated by specific gamma-aminobutyric acid(A) receptor subtypes. *Nature* **401**(6755)**:** 796-800.

Rudolph, U, Mohler, H (2004b) Analysis of GABAA receptor function and dissection of the pharmacology of benzodiazepines and general anesthetics through mouse genetics. *Annu Rev Pharmacol Toxicol* **44:** 475-498.

Ruffolo, RR, Jr., Hieble, JP (1994) Alpha-adrenoceptors. *Pharmacol Ther* **61**(1-2)**:** 1-64.

Ryder, S, Way, WL, Trevor, AJ (1978) Comparative pharmacology of the optical isomers of ketamine in mice. *Eur J Pharmacol* **49**(1)**:** 15-23.

Sainsbury, RS, Heynen, A, Montoya, CP (1987) Behavioral correlates of hippocampal type 2 theta in the rat. *Physiol Behav* **39**(4)**:** 513-519.

Sanchez-Vives, MV, McCormick, DA (2000) Cellular and network mechanisms of rhythmic recurrent activity in neocortex. *Nat Neurosci* **3**(10)**:** 1027-1034.

Saper, CB, Chou, TC, Scammell, TE (2001) The sleep switch: hypothalamic control of sleep and wakefulness. *Trends Neurosci* **24**(12)**:** 726-731.

Saper, CB, Fuller, PM, Pedersen, NP, Lu, J, Scammell, TE (2010) Sleep state switching. *Neuron* **68**(6)**:** 1023-1042.

Sato, Y, Seo, N, Kobayashi, E (2006) Genetic background differences between FVB and C57BL/6 mice affect hypnotic susceptibility to pentobarbital, ketamine and nitrous oxide, but not isoflurane. *Acta Anaesthesiol Scand* **50**(5)**:** 553-556.

Schiff, ND (2008) Central thalamic contributions to arousal regulation and neurological disorders of consciousness. *Ann N Y Acad Sci* **1129:** 105-118.

Schiff, ND, Giacino, JT, Kalmar, K, Victor, JD, Baker, K, Gerber, M, Fritz, B, Eisenberg, B, Biondi, T, O'Connor, J, Kobylarz, EJ, Farris, S, Machado, A, McCagg, C, Plum, F, Fins, JJ, Rezai, AR (2007) Behavioural improvements with thalamic stimulation after severe traumatic brain injury. *Nature* **448**(7153)**:** 600-603.

Schiff, ND, Rodriguez-Moreno, D, Kamal, A, Kim, KH, Giacino, JT, Plum, F, Hirsch, J (2005) fMRI reveals large-scale network activation in minimally conscious patients. *Neurology* **64**(3)**:** 514-523.

Sheeba, JH, Stefanovska, A, McClintock, PV (2008) Neuronal synchrony during anesthesia: a thalamocortical model. *Biophys J* **95**(6)**:** 2722-2727.

Sherman, SM, Guillery, RW (1998) On the actions that one nerve cell can have on another: distinguishing "drivers" from "modulators". *Proc Natl Acad Sci U S A* **95**(12)**:** 7121-7126.

Sirois, JE, Lei, Q, Talley, EM, Lynch, C, 3rd, Bayliss, DA (2000) The TASK-1 two-pore domain K+ channel is a molecular substrate for neuronal effects of inhalation anesthetics. *J Neurosci* **20**(17)**:** 6347-6354.

Slezia, A, Hangya, B, Ulbert, I, Acsady, L (2011) Phase advancement and nucleus-specific timing of thalamocortical activity during slow cortical oscillation. *J Neurosci* **31**(2)**:** 607-617.

Sonner, JM, Gong, D, Eger, EI, 2nd (2000) Naturally occurring variability in anesthetic potency among inbred mouse strains. *Anesth Analg* **91**(3)**:** 720-726.

Souter, MJ, Rozet, I, Ojemann, JG, Souter, KJ, Holmes, MD, Lee, L, Lam, AM (2007) Dexmedetomidine sedation during awake craniotomy for seizure resection: effects on electrocorticography. *J Neurosurg Anesthesiol* **19**(1)**:** 38-44.

Steriade, M (2005) Sleep, epilepsy and thalamic reticular inhibitory neurons. *Trends Neurosci* **28**(6)**:** 317-324.

Steriade, M (1997) Synchronized activities of coupled oscillators in the cerebral cortex and thalamus at different levels of vigilance. *Cereb Cortex* **7**(6)**:** 583-604.

Steriade, M (1995) Thalamic origin of sleep spindles: Morison and Bassett (1945). *J Neurophysiol* **73**(3)**:** 921-922.

Steriade, M, Amzica, F, Nunez, A (1993a) Cholinergic and noradrenergic modulation of the slow (approximately 0.3 Hz) oscillation in neocortical cells. *J Neurophysiol* **70**(4)**:** 1385-1400.

Steriade, M, Contreras, D, Curro Dossi, R, Nunez, A (1993b) The slow (< 1 Hz) oscillation in reticular thalamic and thalamocortical neurons: scenario of sleep rhythm generation in interacting thalamic and neocortical networks. *J Neurosci* **13**(8)**:** 3284-3299.

Steriade, M, Datta, S, Pare, D, Oakson, G, Curro Dossi, RC (1990) Neuronal activities in brain-stem cholinergic nuclei related to tonic activation processes in thalamocortical systems. *J Neurosci* **10**(8)**:** 2541-2559.

Steriade, M, Deschenes, M (1984a) The thalamus as a neuronal oscillator. *Brain Res* **320**(1)**:** 1-63.

Steriade, M, Deschenes, M, Domich, L, Mulle, C (1985) Abolition of spindle oscillations in thalamic neurons disconnected from nucleus reticularis thalami. *J Neurophysiol* **54**(6)**:** 1473-1497.

Steriade, M, Domich, L, Oakson, G, Deschenes, M (1987) The deafferented reticular thalamic nucleus generates spindle rhythmicity. *J Neurophysiol* **57**(1)**:** 260-273.

Steriade, M, Glenn, LL (1982a) Neocortical and caudate projections of intralaminar thalamic neurons and their synaptic excitation from midbrain reticular core. *J Neurophysiol* **48**(2)**:** 352-371.

Steriade, M, Llinas, RR (1988a) The functional states of the thalamus and the associated neuronal interplay. *Physiol Rev* **68**(3)**:** 649-742.

Steriade, M, McCormick, DA, Sejnowski, TJ (1993c) Thalamocortical oscillations in the sleeping and aroused brain. *Science* **262**(5134)**:** 679-685.

Steriade, M, Nunez, A, Amzica, F (1993d) Intracellular analysis of relations between the slow (< 1 Hz) neocortical oscillation and other sleep rhythms of the electroencephalogram. *J Neurosci* **13**(8)**:** 3266-3283.

Steriade, M, Nunez, A, Amzica, F (1993e) A novel slow (< 1 Hz) oscillation of neocortical neurons in vivo: depolarizing and hyperpolarizing components. *J Neurosci* **13**(8)**:** 3252-3265.

Steriade, M, Oakson, G, Ropert, N (1982b) Firing rates and patterns of midbrain reticular neurons during steady and transitional states of the sleep-waking cycle. *Exp Brain Res* **46**(1)**:** 37-51.

Steriade, M, Pare, D, Parent, A, Smith, Y (1988b) Projections of cholinergic and non-cholinergic neurons of the brainstem core to relay and associational thalamic nuclei in the cat and macaque monkey. *Neuroscience* **25**(1)**:** 47-67.

Steriade, M, Parent, A, Hada, J (1984b) Thalamic projections of nucleus reticularis thalami of cat: a study using retrograde transport of horseradish peroxidase and fluorescent tracers. *J Comp Neurol* **229**(4)**:** 531-547.

Sukhotinsky, I, Zalkind, V, Lu, J, Hopkins, DA, Saper, CB, Devor, M (2007) Neural pathways associated with loss of consciousness caused by intracerebral microinjection of GABA A-active anesthetics. *Eur J Neurosci* **25**(5)**:** 1417-1436.

Takahashi, K, Kayama, Y, Lin, JS, Sakai, K (2010) Locus coeruleus neuronal activity during the sleep-waking cycle in mice. *Neuroscience* **169**(3)**:** 1115-1126.

Tiesinga, PH, Sejnowski, TJ (2010) Mechanisms for Phase Shifting in Cortical Networks and their Role in Communication through Coherence. *Front Hum Neurosci* **4:** 196.

Timofeev, I, Grenier, F, Bazhenov, M, Sejnowski, TJ, Steriade, M (2000) Origin of slow cortical oscillations in deafferented cortical slabs. *Cereb Cortex* **10**(12)**:** 1185-1199.

Timofeev, I, Steriade, M (1996) Low-frequency rhythms in the thalamus of intact-cortex and decorticated cats. *J Neurophysiol* **76**(6)**:** 4152-4168.

Torrence, C, Compo, G (1998) A Practical Guide to Wavelet Analysis. *Bull Amer Meteor Soc* **79:** 61-78.

Van der Werf, YD, Witter, MP, Groenewegen, HJ (2002) The intralaminar and midline nuclei of the thalamus. Anatomical and functional evidence for participation in processes of arousal and awareness. *Brain Res Brain Res Rev* **39**(2-3)**:** 107-140.

Vanderwolf, CH (1969) Hippocampal electrical activity and voluntary movement in the rat. *Electroencephalogr Clin Neurophysiol* **26**(4)**:** 407-418.

Velly, LJ, Rey, MF, Bruder, NJ, Gouvitsos, FA, Witjas, T, Regis, JM, Peragut, JC, Gouin, FM (2007) Differential dynamic of action on cortical and subcortical structures of anesthetic agents during induction of anesthesia. *Anesthesiology* **107**(2)**:** 202-212.

Venn, RM, Bradshaw, CJ, Spencer, R, Brealey, D, Caudwell, E, Naughton, C, Vedio, A, Singer, M, Feneck, R, Treacher, D, Willatts, SM, Grounds, RM (1999) Preliminary UK experience of dexmedetomidine, a novel agent for postoperative sedation in the intensive care unit. *Anaesthesia* **54**(12)**:** 1136-1142.

Volgushev, M, Chauvette, S, Mukovski, M, Timofeev, I (2006) Precise long-range synchronization of activity and silence in neocortical neurons during slow-wave oscillations [corrected]. *J Neurosci* **26**(21)**:** 5665-5672.

von Krosigk, M, Bal, T, McCormick, DA (1993) Cellular mechanisms of a synchronized oscillation in the thalamus. *Science* **261**(5119)**:** 361-364.

Vyssotski, AL, Serkov, AN, Itskov, PM, Dell'Omo, G, Latanov, AV, Wolfer, DP, Lipp, HP (2006) Miniature neurologgers for flying pigeons: multichannel EEG and action and field potentials in combination with GPS recording. *J Neurophysiol* **95**(2)**:** 1263-1273.

Walker, WF, Homberger, DG (1997) *Anatomy and dissection of the rat*. 3rd edn. W. H. Freeman: New York.

White, PF, Schuttler, J, Shafer, A, Stanski, DR, Horai, Y, Trevor, AJ (1985) Comparative pharmacology of the ketamine isomers. Studies in volunteers. *Br J Anaesth* **57**(2)**:** 197-203.

Wolter, S, Friedel, C, Bohler, K, Hartmann, U, Kox, WJ, Hensel, M (2006) Presence of 14Hz spindle oscillations in the human EEG during deep anesthesia. *Clin Neurophysiol* **117**(1)**:** 157-168.

Wooltorton, JR, Moss, SJ, Smart, TG (1997) Pharmacological and physiological characterization of murine homomeric beta3 GABA(A) receptors. *Eur J Neurosci* **9**(11)**:** 2225-2235.

Wright, KP, Jr., Badia, P, Wauquier, A (1995) Topographical and temporal patterns of brain activity during the transition from wakefulness to sleep. *Sleep* **18**(10)**:** 880-889.

Yasui, Y, Masaki, E, Kato, F (2007) Sevoflurane directly excites locus coeruleus neurons of rats. *Anesthesiology* **107**(6)**:** 992-1002.

Ying, SW, Abbas, SY, Harrison, NL, Goldstein, PA (2006) Propofol block of I(h) contributes to the suppression of neuronal excitability and rhythmic burst firing in thalamocortical neurons. *Eur J Neurosci* **23**(2)**:** 465-480.

Young, CK, McNaughton, N (2009) Coupling of theta oscillations between anterior and posterior midline cortex and with the hippocampus in freely behaving rats. *Cereb Cortex* **19**(1)**:** 24-40.

Zecharia, AY, Nelson, LE, Gent, TC, Schumacher, M, Jurd, R, Rudolph, U, Brickley, SG, Maze, M, Franks, NP (2009) The involvement of hypothalamic sleep pathways in general anesthesia: testing the hypothesis using the GABAA receptor beta3N265M knock-in mouse. *J Neurosci* **29**(7)**:** 2177-2187.

Zhang, L, Jones, EG (2004) Corticothalamic inhibition in the thalamic reticular nucleus. *J Neurophysiol* **91**(2)**:** 759-766.